AD-A061 748 BIPHASE ENERGY SYSTEMS SANTA MONICA CA F/G 13/10.1
DESIGN STUDY OF A TWO-PHASE TURBINE ENGINE FOR SUBMARINE PROPUL--ETC(U)
AUG 78 E RITZI, L HAYS N00014-77-C-0545
UNCLASSIFIED 106-F NL

1 OF 2
ADA
061748

LEVEL II

(14) 12

Report No. 106-F

Biphase Energy Systems

Research-Cottrell

AD A061748

DDC FILE COPY

(15) FINAL REPORT.

N-00014-77-C-0545

(6) DESIGN STUDY OF A TWO-PHASE TURBINE ENGINE FOR SUBMARINE PROPULSION.

by

(10) Emil Ritzi & Lance Hays

BIPHASE ENERGY SYSTEMS,
SUBSIDIARY OF RESEARCH-COTTRELL, INC.
2907 Ocean Park Boulevard
Santa Monica, California 90405

(11) 18 August 1978

(9) Final Report for Period
1 July 1977-31 May 1978,

(12) 179 p.

Prepared for

OFFICE OF NAVAL RESEARCH
DEPARTMENT OF THE NAVY
800 N. Quincy Street
Arlington, Virginia 22217

Prepared for public release ; distribution unlimited. Reproduction in whole or in part is permitted for any purpose of the United States government. The research was sponsored by the Office of Naval Research, Contract No. N-00014-77-C-0545, Work Unit 097-422.

New 410 956

78 11 30 057 4B

ABSTRACT

A design study of the Biphase turbine engine for underwater propulsion was performed. The design output using steam and oil was 15,000 horsepower at 180 rpm. A single stage turbine with no gear reduction (direct drive) was designed. A single stage unit with a small turbine and moderate gear reduction was also designed.

In both cases significant performance advantages and weight and volume savings over the existing steam turbine engine were found using the same heat source. Thermal Efficiencies of the order of 22 to 24% were predicted at full power and 21% at cruise conditions. For the steam-oil unit with gears the total estimated weight including the 400 kW ship service turbine/generator set was 126 600 kg (278 000 lbs) and the volume 113 m^3 (3970 ft^3). The heavy gear reduction train (a large noise source) can be eliminated.

Another Biphase turbine engine which uses steam and water was analyzed. A five-stage unit provided similar performance advantages as the steam-oil systems, but with a larger gear reduction ratio when a reaction type liquid turbine is used. The estimated weight of the wet-steam engine was 101 800 kg (243 750 lb) and the box volume 86.4 m^3 (3046 ft^3), including the 400 kW ship service turbine/generator set.

On the basis of the results, a development program is recommended and the scope discussed.

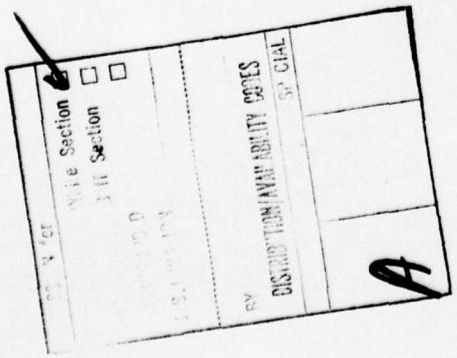

ACKNOWLEDGMENT

Many people have contributed to the result of the study; special thanks are due to Ron Morinishi, Ying M. Chen and Bill Baggenstoss for computational and graphical work; the engine design drawings were the work of Laurence Cooke and Brian O'Connor; the report was edited and produced by Hisa Olds. Much of the conceptions were developed in discussions with Dr. E. Quandt, Dr. H. Urbach and D. Knauss of the David Taylor Ship Research and Development Center in Annapolis, and W. R. Seng, R. Pariseau and K. Ellingsworth of the Office of Naval Research, Washington D.C., who were directing the program.

TABLE OF CONTENTS

TABLE OF CONTENTS (continued)

LIST OF FIGURES

LIST OF FIGURES (continued)

LIST OF FIGURES (continued)

LIST OF TABLES

I. INTRODUCTION

Present marine engines are highly developed versions of the diesel engine and the steam turbine. Very little margin for further improvement exists. Increased performance demands must be met by development of new prime movers. An example is the advent of the gas turbine, which has been successfully adapted for some marine applications. However, gas turbines and steam turbines both suffer from the same problem -- use of high specific speed turbomachinery for a relatively low speed propulsion application.

A further disadvantage of the gas turbine is the requirement for a high temperature heat source. For a submarine, this would mean a new reactor development program. If a new prime mover could be used with the existing nuclear heat source to increase performance a substantial savings in both cost and time would result.

The Biphase turbine is a machine having low specific speed and high torque. As such, it is ideally suited for marine propulsion. In many cases the Biphase turbine can drive the propellers directly with no gear reduction required. This feature leads to improvements in weight, volume and noise.

The two-phase thermodynamic cycle of the Biphase engine is more efficient than the Rankine cycle. A constant temperature expansion in the two-phase nozzle leads to a "Carnotized" engine. Thus the potential exists for added power output using the existing nuclear heat source.

The major objective of the present study is to assess the potential advantages of the Biphase turbine for underwater propulsion. The heat source chosen for the power plant is a nuclear reactor. Typical for that source is that the energy carrier or heat transfer fluid is saturated steam of relatively low temperature like

215°C (420°F). Compared to stationary fossil fuel burning power plants, the available enthalpy drop is less than half.

A thermodynamically efficient layout of the engine cycle is difficult: Referring to Figure 1, an isentropic expansion of saturated steam leads to a cycle with an efficiency considerably less than that of a Carnot cycle. With an inlet temperature of $T_1 = 505.2°K$ (232°C) and a condenser temperature of $T_2 = 337.2°K$ (64°C), the Carnot efficiency is $\eta_c = 1-T_2/T_1 = 0.333$.

A cycle that expands isentropically from a condition of saturated steam at the inlet results in an ideal efficiency of 0.291. At the exhaust the vapor quality is $x_2 = 0.75$, a value that is too low for a conventional turbine from the standpoint of impact losses and erosion. The drop in efficiency from 33% to 29% is solely due to the layout of the cycle and does not include irreversibilities due to friction losses and temperature drops in heat exchangers.

Carnotizing a thermodynamic cycle means to lay it out such that its efficiency approaches that of the Carnot cycle. What is typical in the Carnot cycle is that the work area in the temperature-entropy diagram (illustrated below) has the same width as the heat rejection area.

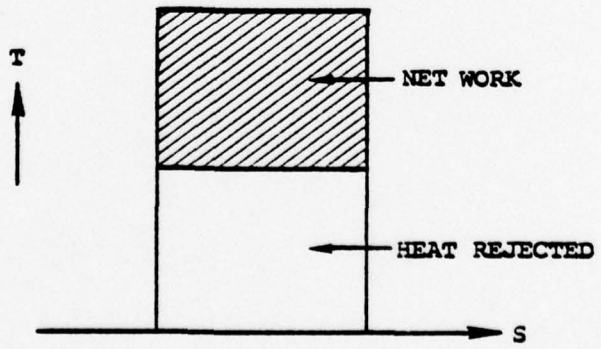

It is typical for the Carnot cycle that it does not matter what the width is of the cycle on the T-S diagram, at least as far as the thermal efficiency is concerned.

Two-Component Approach - One method to Carnotize a steam cycle is to add a second (liquid) component having a low vapor pressure. This component provides a source of heat for the expanding vapor producing a near-isothermal expansion. In Figure 1 it can be seen that the temperature at the end of the nozzle expansion is 218°C compared to 64°C which would occur in the Rankine cycle. This results in an isentropic cycle efficiency of 31% versus 29% for the Rankine cycle.

This cycle was invented by Elliott[1] for liquid metal MHD. It has been extensively analyzed[2] and tested[3] and forms the basis for the initial design approach.

Single Component Approach - Another method to Carnotize the basic steam cycle is the wet steam cycle shown in Figure 2. In this cycle the expansion process is ideally parallel to the saturated liquid line that outlines the left hand side of the dome.

In order to achieve that type of carnotizing, heat has to be removed during expansion. While it may be possible to do that through the walls of the nozzle, a more conventional way is to extract steam in steps. That means that a scheme of pressure staging is required, where after each expansion stage steam is extracted and used to preheat feed water by condensing all of the extracted steam.

To assess the potential of the Biphase Turbine for underwater propulsion, an engine was designed to operate with an existing heat source. The basic requirements were to "design a two phase turbine using as given maximum temperature and pressure inputs of of appropriate values. The design value for shaft horsepower will be a minimum of 15,000 HP. The net shaft power, weight and volume of the two-phase turbine engine, which will not require

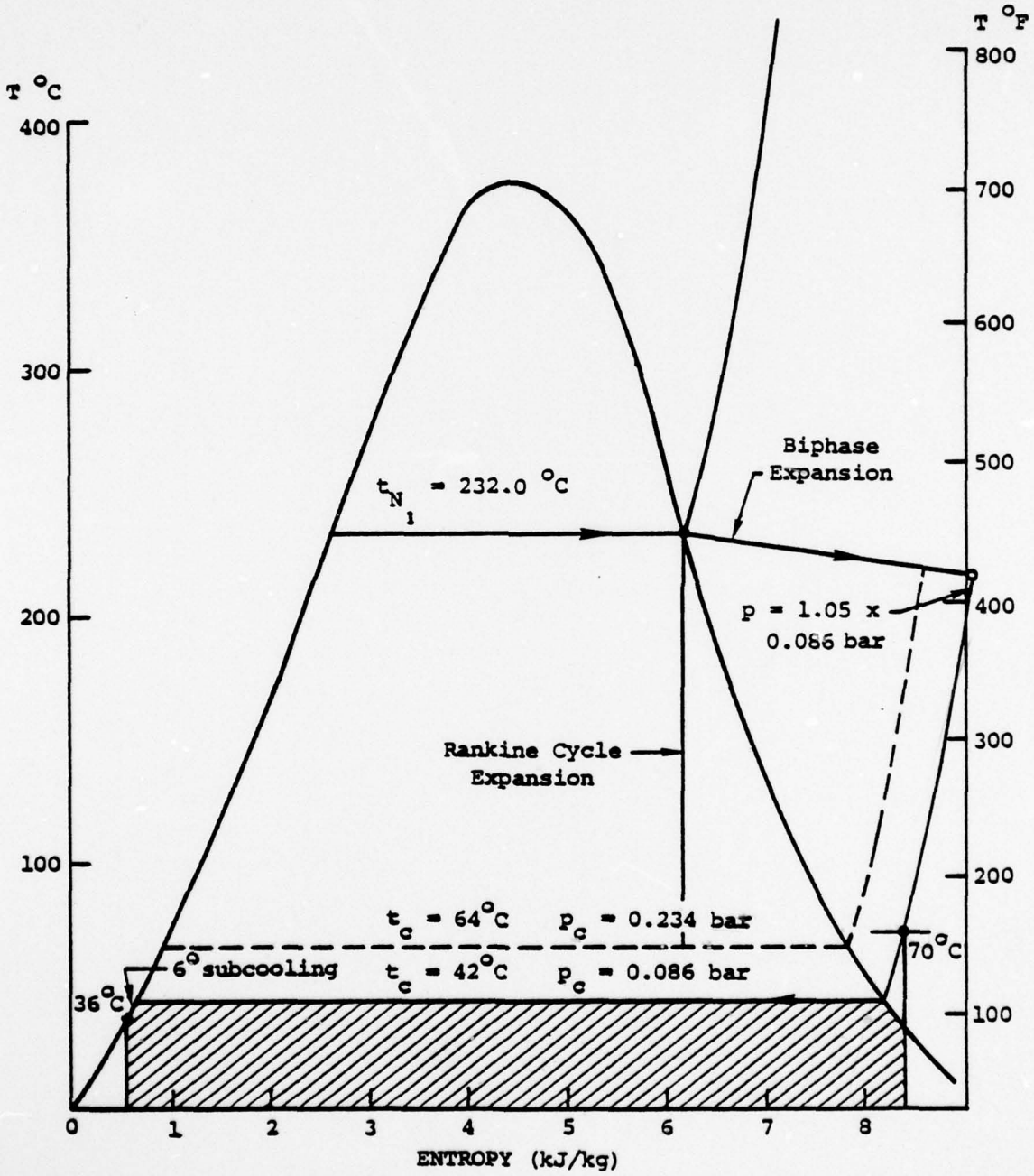

Figure 1. Comparison of Rankine Cycle and Two-Component Biphase Cycle

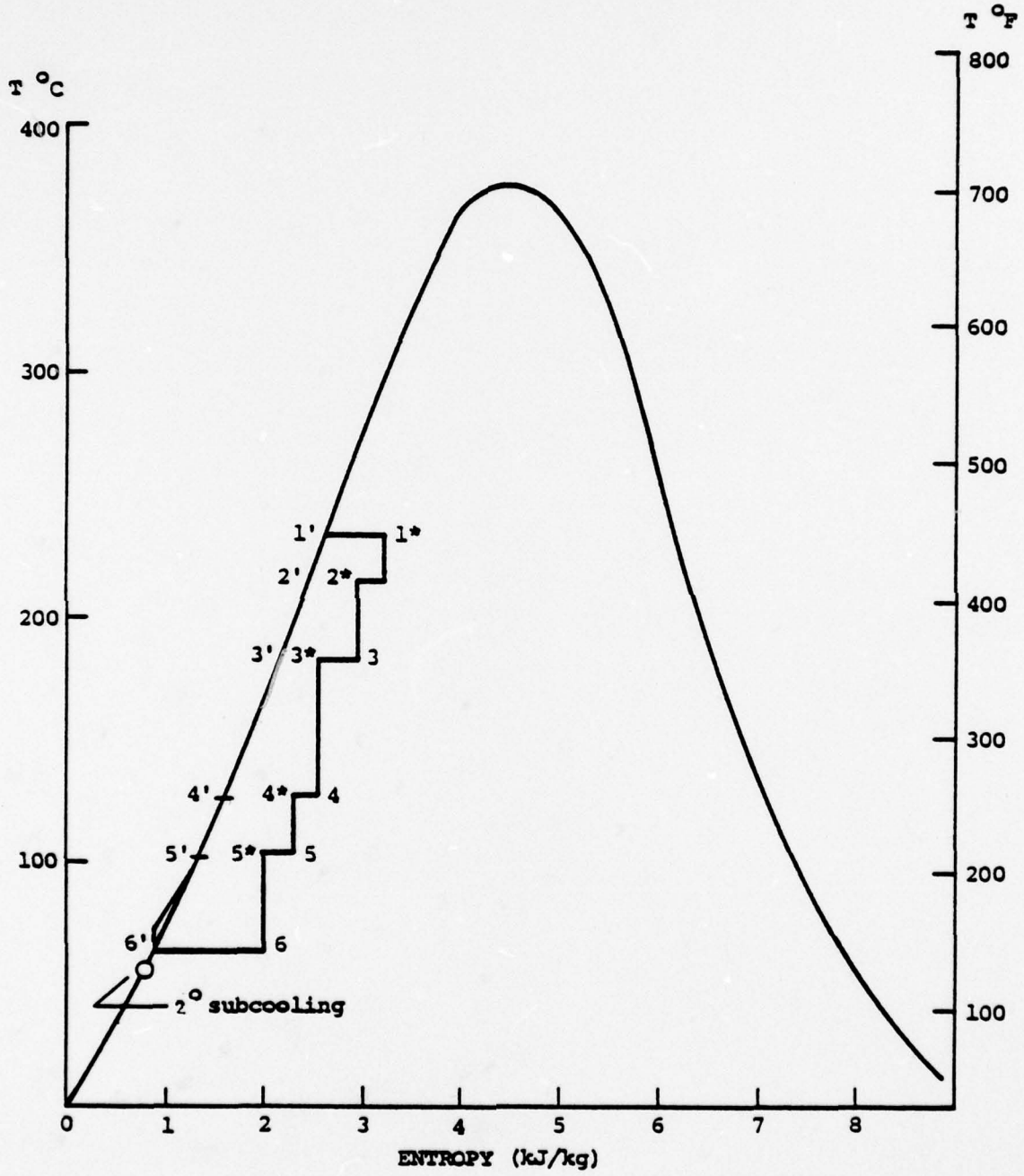

Figure 2. Single Component Biphase Cycle

a reduction gear will be determined and be available for comparison to existing steam turbine engines (including reduction gears) MHD and existing electric drives (SEGMAG and Super "C"). Development cost will be estimated. Preliminary engine layout drawings will be prepared and used as the basis for cost and dimensional characteristics. Lower temperature inputs will be discussed along with a detailed thermodynamic investigation of the system."[4]

A detailed cycle analysis was carried out on the two-component approach followed by engine design and layout. Weight and volume estimates were performed. Because of its promise, preliminary analysis and design of the one-component approach were also completed. Results were evaluated and a development program was formulated leading to a full-size underwater propulsion engine.

II. BIPHASE CYCLES

Several variations of the basic two-phase power cycle exist. The particular version chosen for an application will depend upon the power and speed requirements and the heat source temperature. In this section each of the cycle variations is discussed to provide the basis for later analysis and design.

TWO-COMPONENT

The two-component cycle uses a low vapor pressure liquid and a high vapor pressure liquid having different chemical makeup. Some fluid combinations which have been considered are steam-Krytox, steam-Caloria, steam-lead bismuth eutectic, and Dowtherm-Therminol. The basic advantages of a two-component engine are low rpm, high efficiency with no steam extraction and a more compact turbine. Disadvantages include larger heat exchangers and the complexity of handling two fluids.

1. U-Tube Turbine - Figure 3 is a schematic of a two-component cycle with a U-tube turbine. Steam is generated in a heat exchanger and flows to the two-phase nozzle and to a liquid heater. Low vapor pressure oil (such as Krytox) is heated and also flows to the nozzle. The two fluids mix and are expanded in the nozzle. The two-phase jet from the nozzle is used to drive a rotary separator and liquid turbine. The steam from the rotary separator flows through a recuperator to a condenser, where it is condensed. The condensate is pressurized and pumped back through the recuperator to the heat source. The liquid discharging from the "U-tube" liquid turbine is collected on a second rotary-separator where it flows through a diffuser back to the liquid heater.

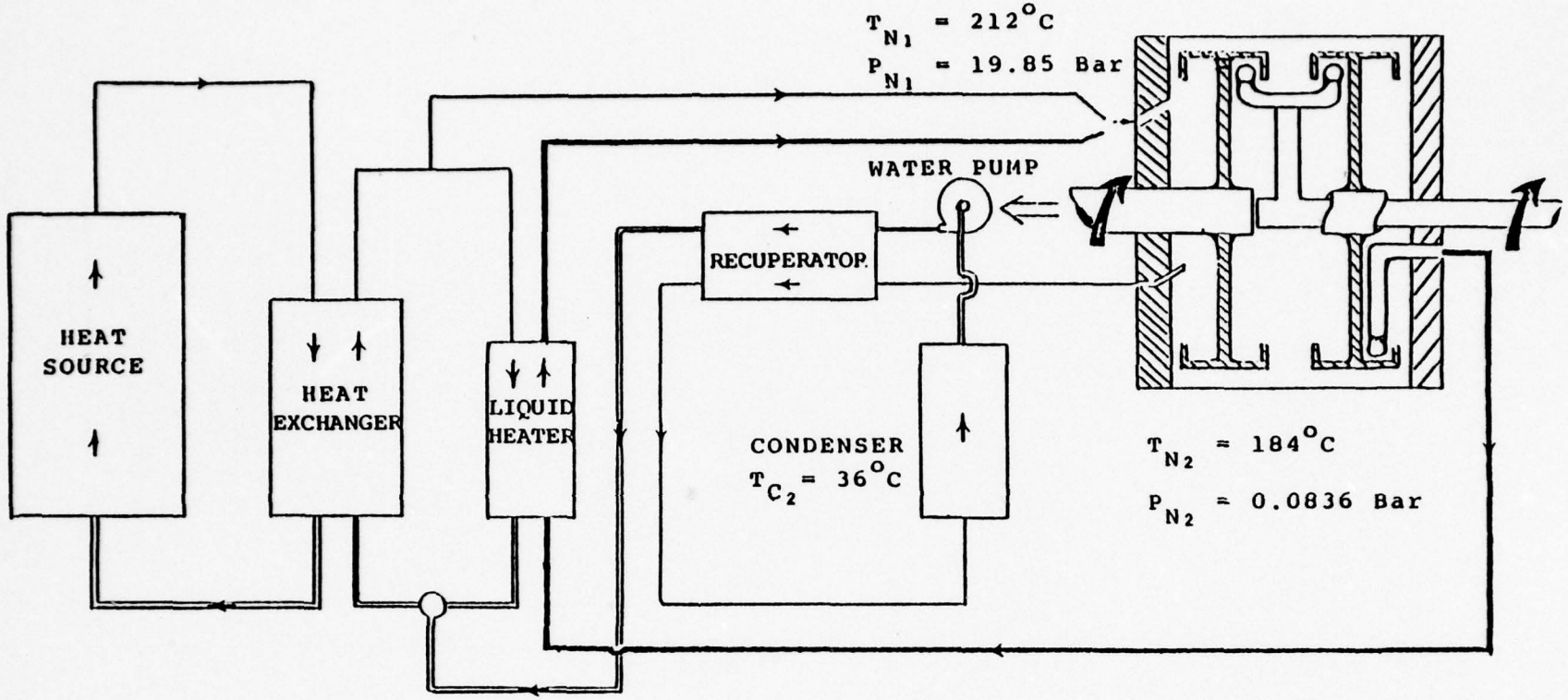

Figure 3. U-Tube Turbine Engine

2. Impulse Turbine - This cycle, shown in Figure 4, is very similar to the "U-tube" version. The major change is that the two-phase jet issuing from the nozzle impinges directly on impulse turbine blading. The turbine may be either radial outflow or axial flow. The liquid discharging from the turbine is collected on a rotary separator, pressurized in a diffuser, and flows back through the liquid heater.

SINGLE COMPONENT

The single component system has the advantage of eliminating oil or heat transfer fluid as the second component. The two-phase mixture in this case consists of steam and water. Typical ratios of water to steam are 10:1 or less so this cycle produces somewhat higher values of turbine speed.

In order to obtain high efficiency several expansion stages are used. The five stage system resulting in the temperature-entropy variation of Figure 2 is shown schematically in Figure 5. Steam from the heat exchanger flows to the first stage nozzle. A portion of the steam is also used to heat the water flowing to the first stage nozzle. The mixture of primary steam and water is expanded in the nozzle from an inlet vapor quality of 15% to an exit quality of 18%. The two-phase mixture drives a rotary separator turbine (which may be one of several types).

Part of the separated steam is extracted and flows to a feed water heater. The remainder of the steam is re-mixed with the water exiting the first stage turbine. This mixture is expanded in the second stage nozzle from an inlet vapor quality of 12% to an exit quality of 18%.

The two-phase mixture drives the second stage rotary separator turbine, where additional steam extraction occurs. In the final stage, steam exhausting from the turbine flows to the condenser.

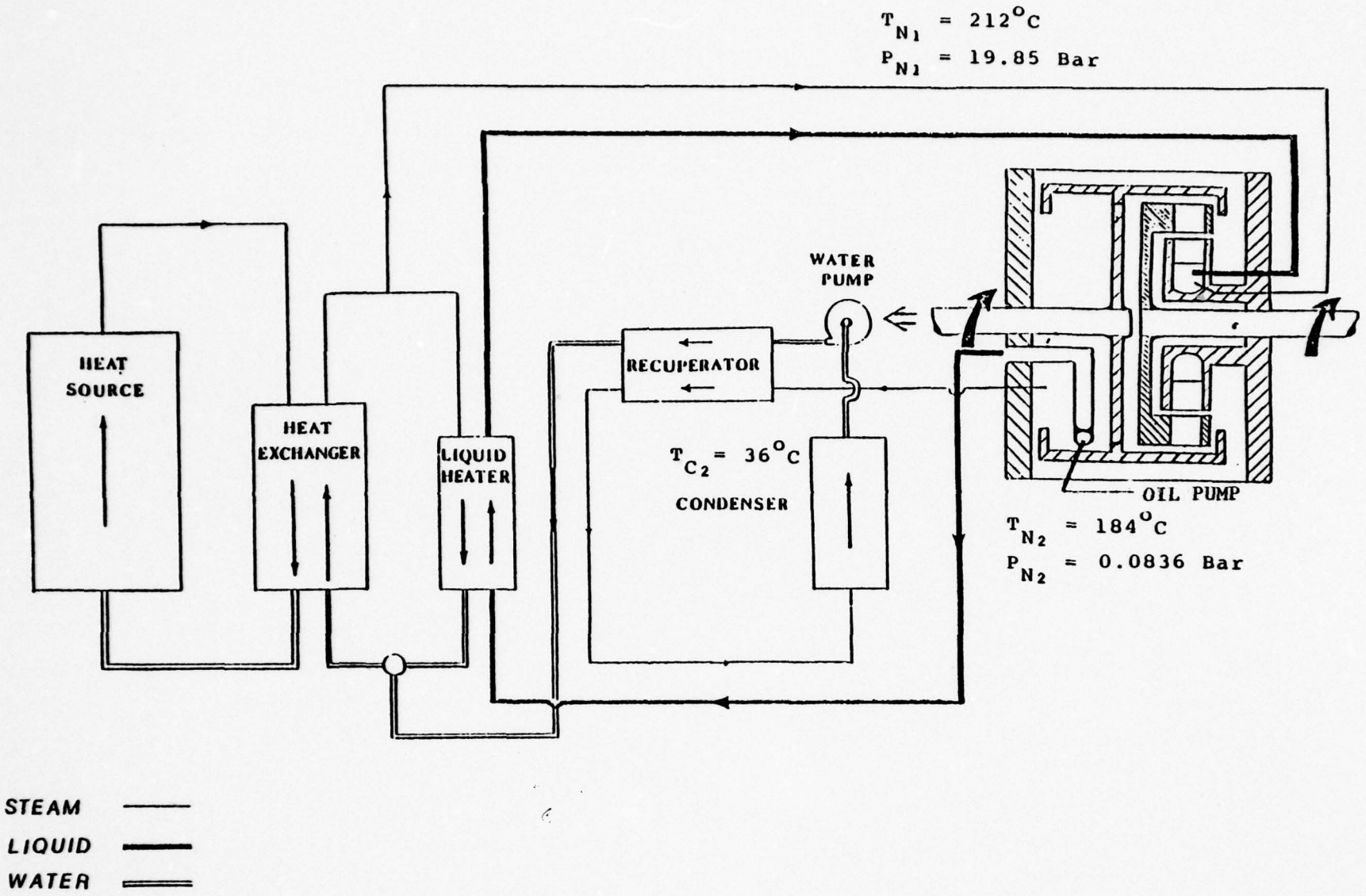

Figure 4. Impulse Turbine Engine

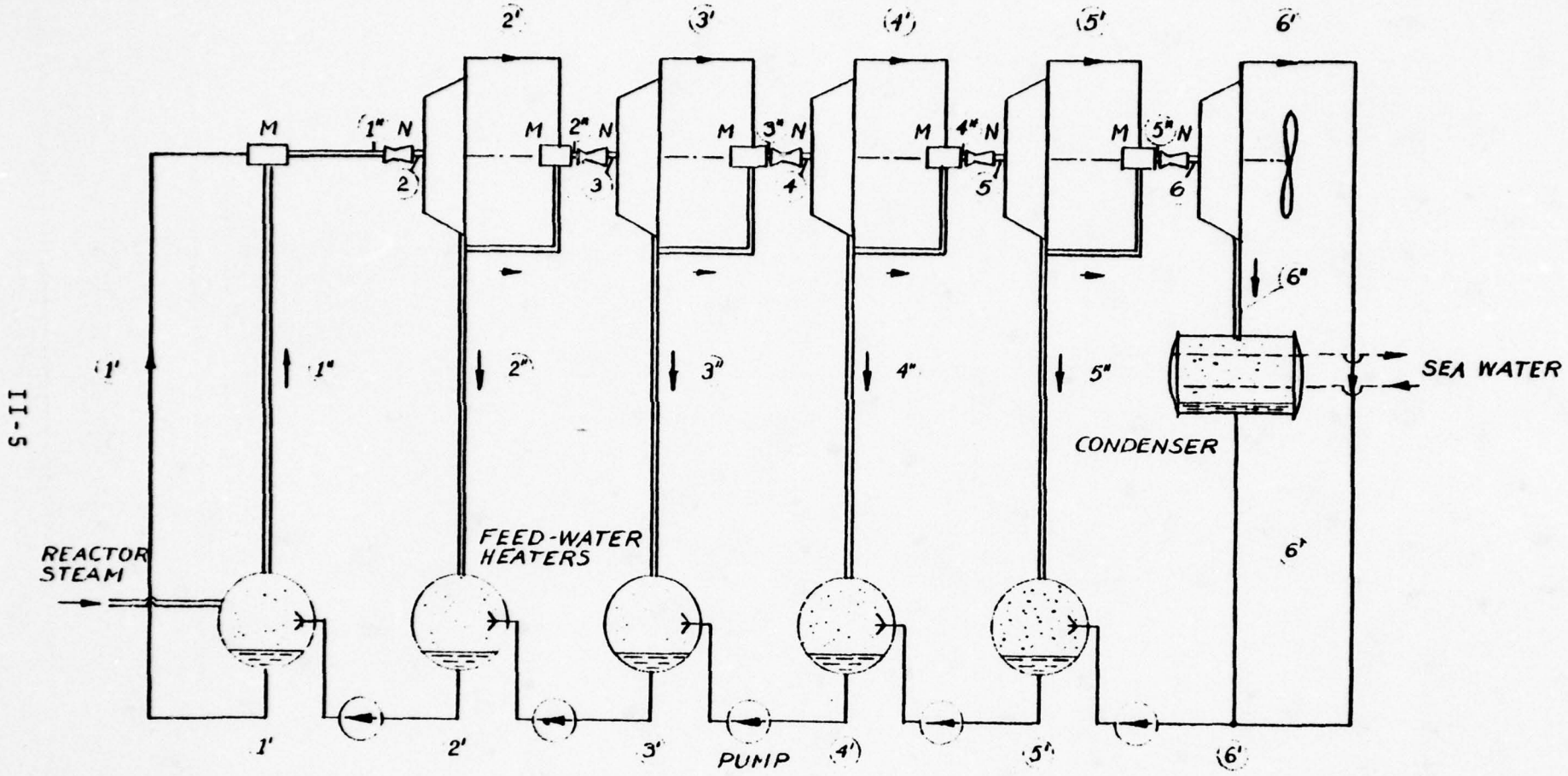

Figure 5. Wet-Steam Five Stage Regenerative Turbine Engine

The condensate is remixed with the liquid exiting the last stage turbine. The feed water flows through several stages of a feed water heater where the extraction steam is condensed on the feed water.

Five stages are shown in Figure 5. The actual number of stages will be determined by a tradeoff between efficiency and cost and complexity.

The cycles shown are the three considered for this design study. Many other variations exist which can possibly result in higher efficiency or other advantages. However, these three are the closest to the current stage of the art and provide more than adequate performance improvement.

III. COMPONENTS

The loss analysis of major components in the system have resulted in efficiency values used in cycle performance calculations. In the case of some components such as the nozzle, extensive test data have been used in combination with analysis to derive these values. Other components such as the turbine rely more heavily on analytical treatment. In every case the components have been demonstrated but at conditions somewhat different than the parameters of this engine. In this section some of the more important features of the component analysis and design will be discussed.

NOZZLE

The two-phase nozzle has been investigated extensively, both analytically and experimentally. Elliott[5] reported on the results of an analysis which accurately predicted performance for nitrogen-water, nitrogen-NaK and Freon-water mixtures. The same analysis accurately predicted the performance of steam-water nozzles[6] and cesium-lithium nozzles[7]. Figure 6 is a comparison of test results obtained for Freon and water with the performance predicted by Elliott's model. Excellent agreement is shown to exist.

The values of nozzle efficiency (85%) used in the cycle analysis are lower than the peak values reported by Elliott (88%) or Alger (90%). Moreover, preatomization of the liquid or improved nozzle contours postulated by Ritzi[2] should result in improved performance.

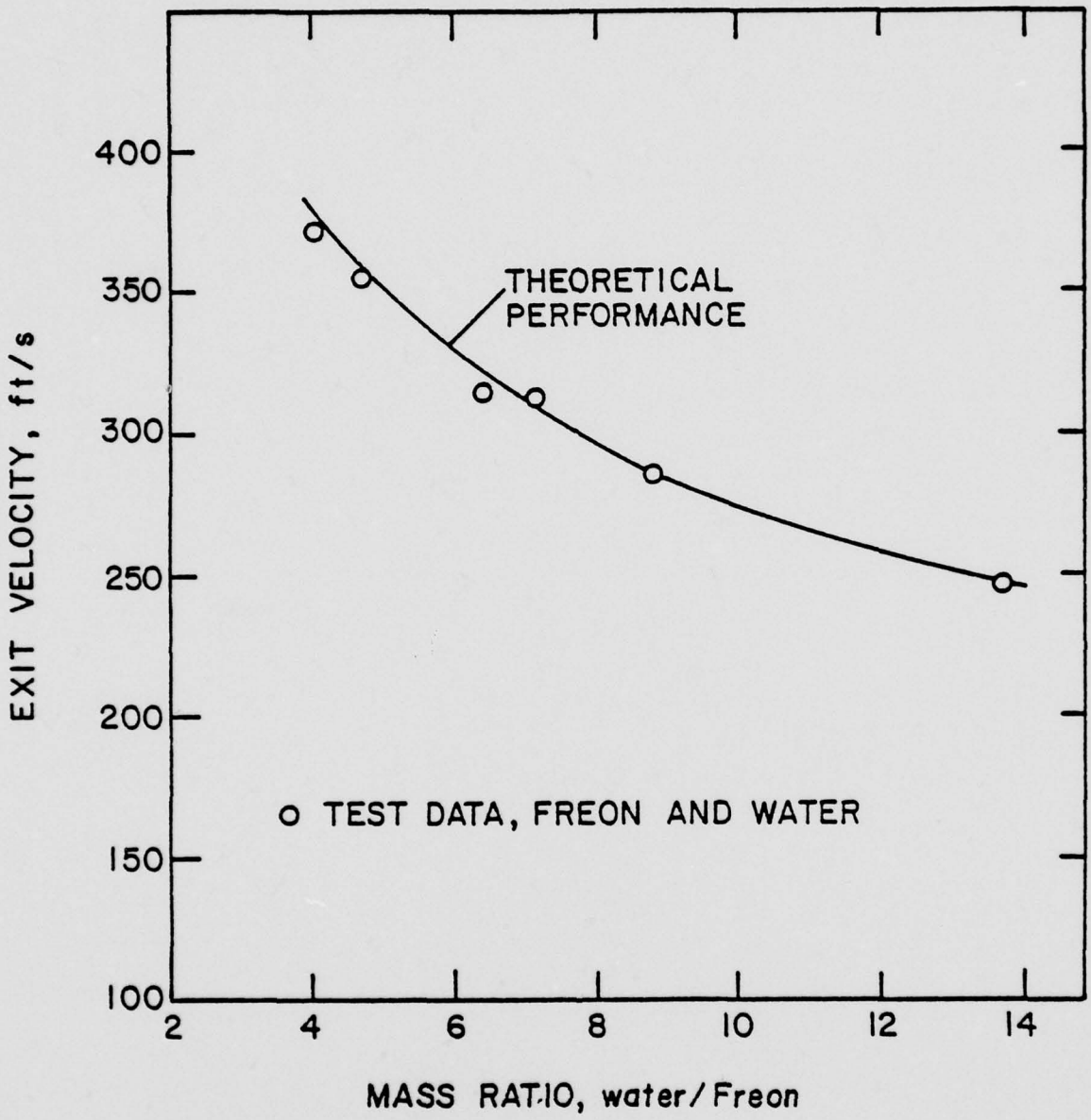

Figure 6. Measured Performance of Two-Phase Nozzle With Vaporizing Flow

TURBINE

Since good two-phase nozzle performance is tied to fine droplet sizes, it seemed logical to concentrate on obtaining fine atomization. If a droplet size of less than about 5 μm could be obtained an *impulse turbine* capable of handling the two phase flow efficiently is a distinct possibility. Since the sonic velocity of such a two-phase mixture is low, the impulse turbine will be operating in the supersonic regime. An analysis of the trajectories of droplets in the mixture that flows through large buckets indicated droplets with a few microns diameter will follow the vapor streamlines. Excellent performance possibilities exist, therefore, since the kinetic energy transition loss from nozzle to a separator, typical for a liquid turbine, is not typically present.

Supersonic turbines were studied in some detail as part of the present program (see Refs. 8, 9, 10, 11, 12, and 13). Also, component performance plots for impulse turbines were developed based first upon a set of relations as given in Table II, Eq. (8) and (10); since those equations did not include reaction across the buckets, the relations were generalized according to Table I. The same relations were incorporated in the cycle program. Separate performance graphs are given in Figures 7, 8, 9, and 10. However, since sufficient analytical and experimental results for droplet break-up were not yet obtained, it was considered important in our judgement to seek for alternate turbine designs with less performance sensitivity to droplet size. Since additional means have since become available as part of a contract extension for the study of nozzles and turbines, a further discussion of the impulse turbine is deferred to a later date.

Among the alternates are the liquid turbines which rely on a separation of liquid and vapor before the turbine. Among these, the U-tube turbine is of course in the foreground. Efficiency relationships are listed as part of the entire cycle program in

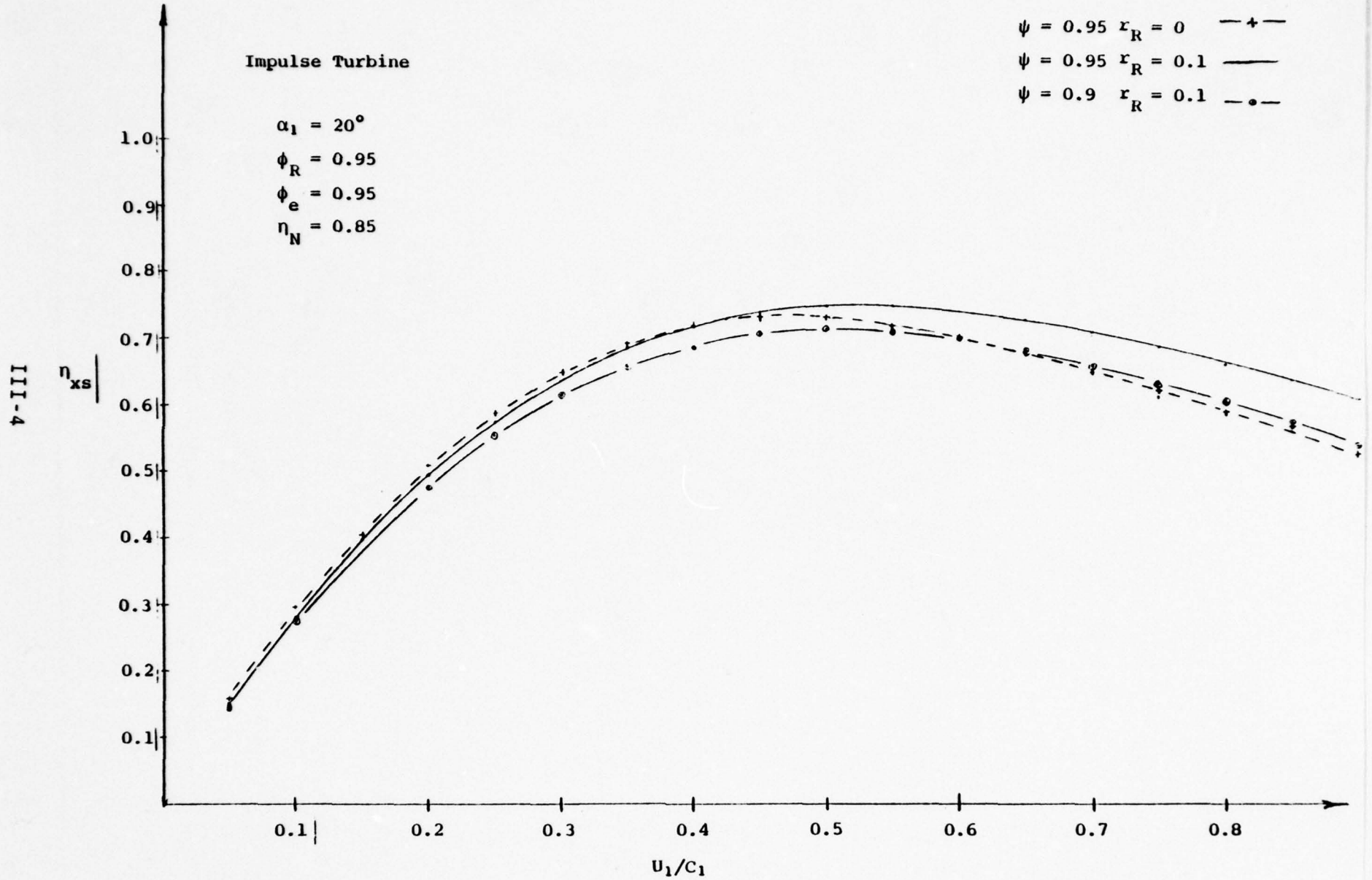

Figure 7. Estimated Turbine Performance – Static Efficiency vs Speed Ratio

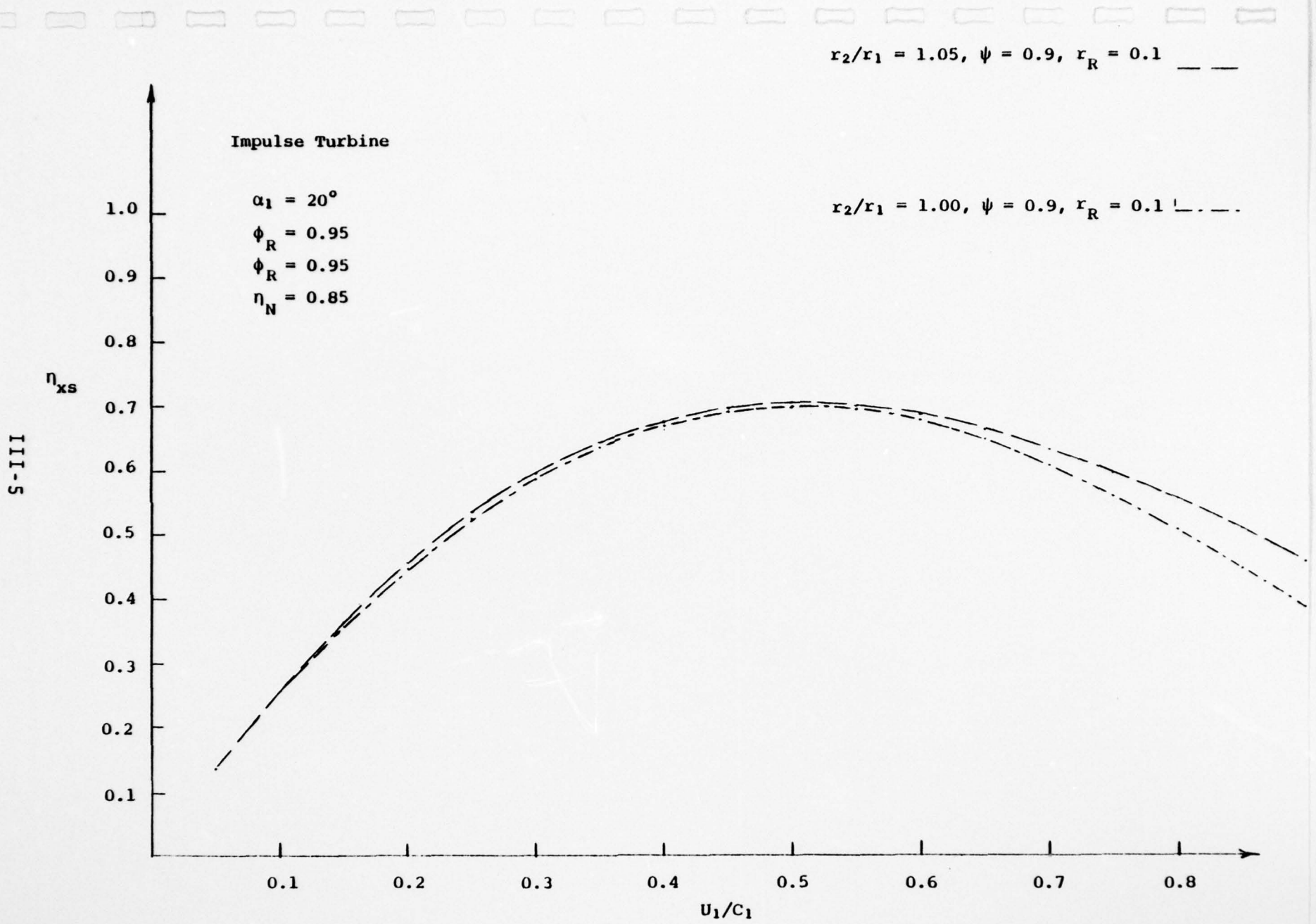

Figure 8. Estimated Turbine Performance – Static Efficiency vs Speed Ratio

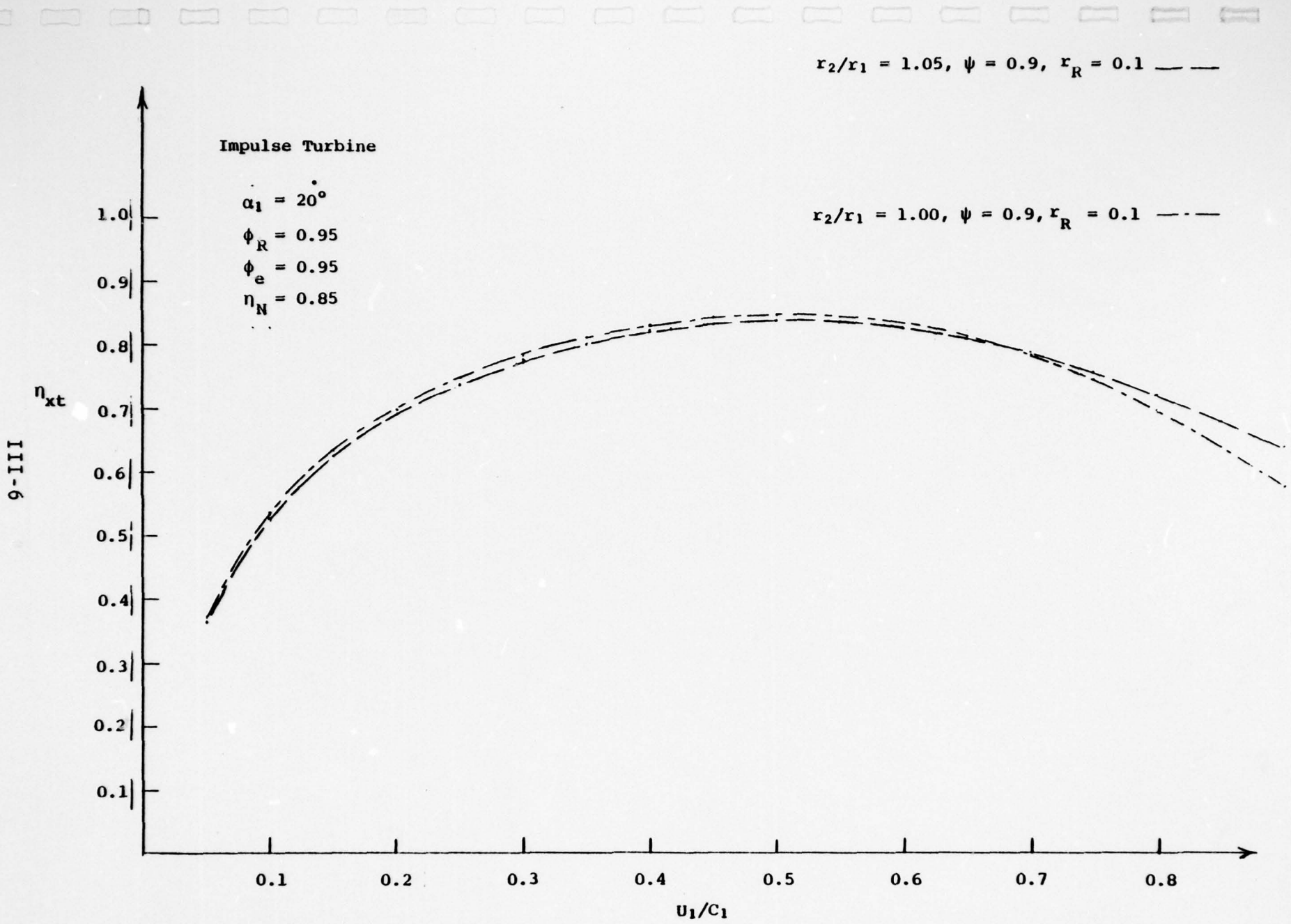

Figure 9. Estimated Turbine Performance – Total Efficiency vs Speed Ratio

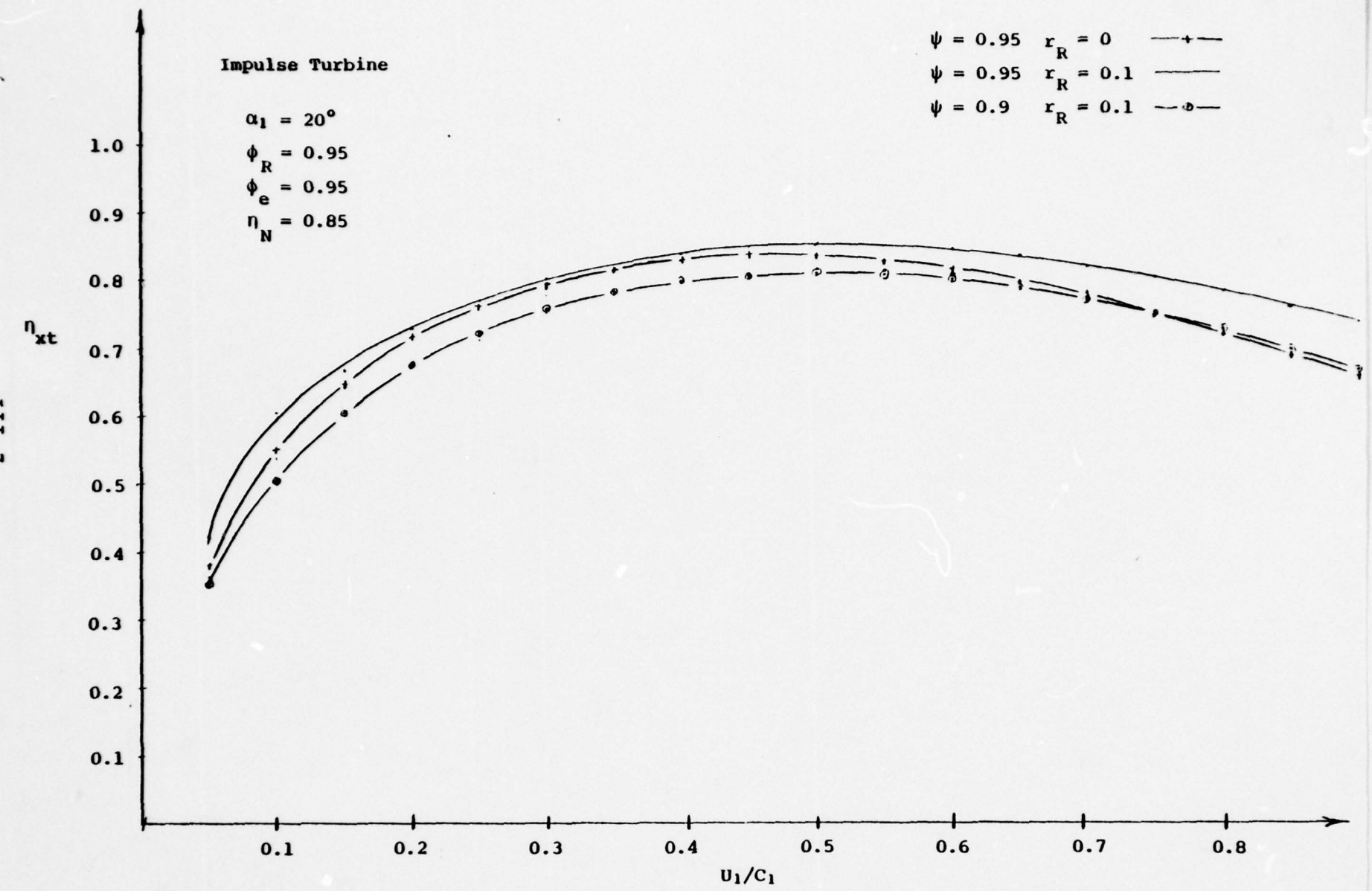

Figure 10. Estimated Turbine Performance – Total Efficiency vs Speed Ratio

Table IV. Note that the feed-water pump is considered part of the separator assembly; its power extraction from the separator shaft results in a hardly noticeable slowdown of the separator speed, as expressed by c_{s2}/c_{s1}. A realistic appraisal of the U-tube turbine must note – in addition to its many attractive features like low speed – certain characteristics that make it difficult at present to predict high performance levels with sufficient certainty.

These characteristics have to do with the fact that it is difficult to make the U-tube flow full for two reasons:

1. The present U-tube is an impulse device with mere turning of the flow.
2. Deep immersion of the probe inlet into the ring of liquid in the separator causes disturbances and drag losses in the liquid ring which still make the entrainment of vapor difficult to avoid.

At the present time the U-tube turbine, together with the impulse turbine are deemed to both require additional research.

An alternate solution with an anticipated high degree of performance predictability seems to be at present the Euler turbine.

While looking for as foolproof a liquid turbine design as possible, the thought occurred in January 1978 that it may be worth investigating a reaction version of a liquid turbine. Besides the possibility of having the back pressure of the nozzle at a value above the condenser pressure (which would require an efficient way of imparting kinetic energy to liquid by the action of expanding steam in the turbine rotor), the possibility exists of producing a pressure rise in a rotating ring of liquid constrained inside of a rotating drum (with solid-body rotation assumed). The pressure of the free surface of the liquid may equal the pressure surrounding the rotating drum. The pressure difference across the ring may then be used for the acceleration of liquid through a

nozzle opening in the drum that allows the liquid to discharge from the drum in a direction opposite to that of rotation, see Figure 11. In this fashion the absolute kinetic energy of the liquid leaving the turbine may be made small (by proper choice of the radius ratio across the liquid ring and the speed).

Even with a horizontal turbine axis the turbine is expected to clear itself of stray liquid outside of the ring; the point is to see to it that the turbine is accelerated rapidly enough by the steam and liquid to prevent initially discharged liquid from the nozzle to accumulate on the outside of the drum or between nozzle and drum. By placing initially radial vanes inside the drum the torque exerted by the steam may be increased and the solid-body rotation of the liquid assured. More sophisticated steam buckets may be located on the sides of the drum.

Further sophistication is possible by:

1. Addition of a second separator and stationary pick-up pitot for the conversion of residual kinetic energy into pressure rise,
2. Another velocity-staged turbine design would scoop up flow from a free-wheeling drum (outside the turbine drum) and re-introduce the residual kinetic energy into a smaller drum on the same turbine wheel, which also has an exit nozzle,
3. The arrangement of buckets inside of the drum that protrude inward beyond the liquid level so that residual kinetic energy of the steam discharging from the nozzle may be used for additional turbine driving action.

It became clear that the proposal for a turbine sketched by Euler in 1754 (see Figure 12) contains the essential ingredients of the arrangement described above; notable is the fact that in Euler's arrangement, which has no seal, the pressure at the nozzle discharge also has to equal the value at the rotor outlet. The Institute for

Aerodynamics at the Swiss Federal Institute of Technology directed by J. Ackeret, in cooperation with the firm Escher Wyss, built a model from Euler's sketches with a diameter ratio across the rotor of 1.5. A peak hydraulic efficiency of nozzle and turbine of 71.2% was measured. A report was published in 1944 in Ref. 14; a later account was given by Ackeret at a symposium in Zurich in 1955 (Ref. 15).

Performance

The anticipated flow losses can be divided into 1) transition losses encountered between nozzle discharge and the inside of the liquid film; 2) the friction losses encountered in the discharge nozzle of the drum and 3) the losses after the rotating drum. Without the benefit of Ref. 14 an independent analysis was made of the turbine performance.

In comparing later our approach with that of Euler and Ackeret the main differences were twofold: (1) In Euler's machine the tip speeds were so low that the possibility was utilized to increase the wheel relative spouting velocity by the action of a vertical gravity head in the runner as will be shown. 2) the nozzle discharge velocity component normal to the liquid ring at the inlet to the rotor is usually considered lost in Biphase turbines, however, since the Euler turbine has a steady radial outward flow (in contrast to the U-tube turbine) the assumption of some carry-over of energy seems justified. The carry-over coefficient will depend on the ratio of liquid volume flow to steam volume flow, see Appendix A. Still, all the kinetic energy of velocity components other than the one above and the one equal to the peripheral velocity of the liquid ring at the interface with the vapor may be considered as completely lost.

Perhaps the most critical of the losses is the friction loss (2) in the rotating nozzle, expressed by η'', see below. The magnitude of that loss will be affected by the relative size of the nozzle

opening. The specific speed concept is used below in correlating opening to diameter ratios. The derivation of the efficiency formula is given now in some detail. The application of Euler's momentum equation to the single-phase flow of the liquid from the free surface of the liquid ring in the Euler turbine drum to the exit of the rotating nozzle yields the relative discharge velocity as follows.

For steady flow the moment of momentum equation may be written to give the output per unit mass-flow in the form of the Euler equation

$$gH = c_{u_1} u_1 - c_{u_2} u_2 \tag{1}$$

where the c_u's are the peripheral components of the absolute velocities and the u's are the peripheral velocities of the wheel at inlet (subscript 1) and outlet (subscript 2). [The above equation may be given in the form of a Torque

$$T = \int_{(S_1)} \dot{m}_1 r_1 c_{u_1} - \int_{(S_2)} \dot{m}_2 r_2 c_{u_2} \tag{2}$$

where the integrals of the products are taken over the turbine inlet and outlet control surfaces S_1 and S_2 of rotational symmetry.] Application of the cosine-law to the velocity triangles at the inlet yields

$$c_{u_1} u = \frac{1}{2} \left(c_1^2 + u_1^2 - w_1^2 \right) \tag{3}$$

and, for the outlet

$$c_{u_2} u_2 = \frac{1}{2} \left(c_2^2 + u_2^2 - w_2^2 \right) \tag{4}$$

Substitution into the Euler equation gives

$$gH = \frac{1}{2}\left(c_1^2 - c_2^2 + w_2^2 - w_1^2 + u_1^2 - u_2^2\right), \qquad (5)$$

which is the "basic equation of turbines." Note that the static pressure head in the frictionless case is in a rotating system

$$v\left(p_1 - p_2\right) = \frac{w_2^2 - w_1^2}{2} - \frac{u_2^2 - u_1^2}{2} - g\Delta z \qquad (6)$$

where Δz is the height difference across the rotor. Therefore, after substitution of the last equation into the preceding equation we get

$$gH = \frac{1}{2}\left(c_1^2 - c_2^2\right) + v\left(p_1 - p_2\right) + g\Delta z \quad . \qquad (7)$$

In other words, the net output is derived from a change in the absolute kinetic energy and the pressure head (Bernoulli).

If no seal is used at the transition from the stationary nozzle to the rotor the pressure difference $p_1 - p_2$ is zero and

$$\frac{w_2^2}{2} = \frac{w_1^2}{2} + \frac{u_2^2 - u_1^2}{2} + g\Delta z \quad . \qquad (8)$$

The last equation and the Euler equation are now modified into a form that allows the efficiency to be expressed as a function of such basic parameters as r_1/r_2, the radius ratio across the liquid ring, α_1 the stationary nozzle discharge angle, the rotating nozzle discharge angle, β_2,u_1/c_1, the speed ratio, and the rotor and transition efficiencies η'' and ϕ_R. The equation for the normalized output becomes

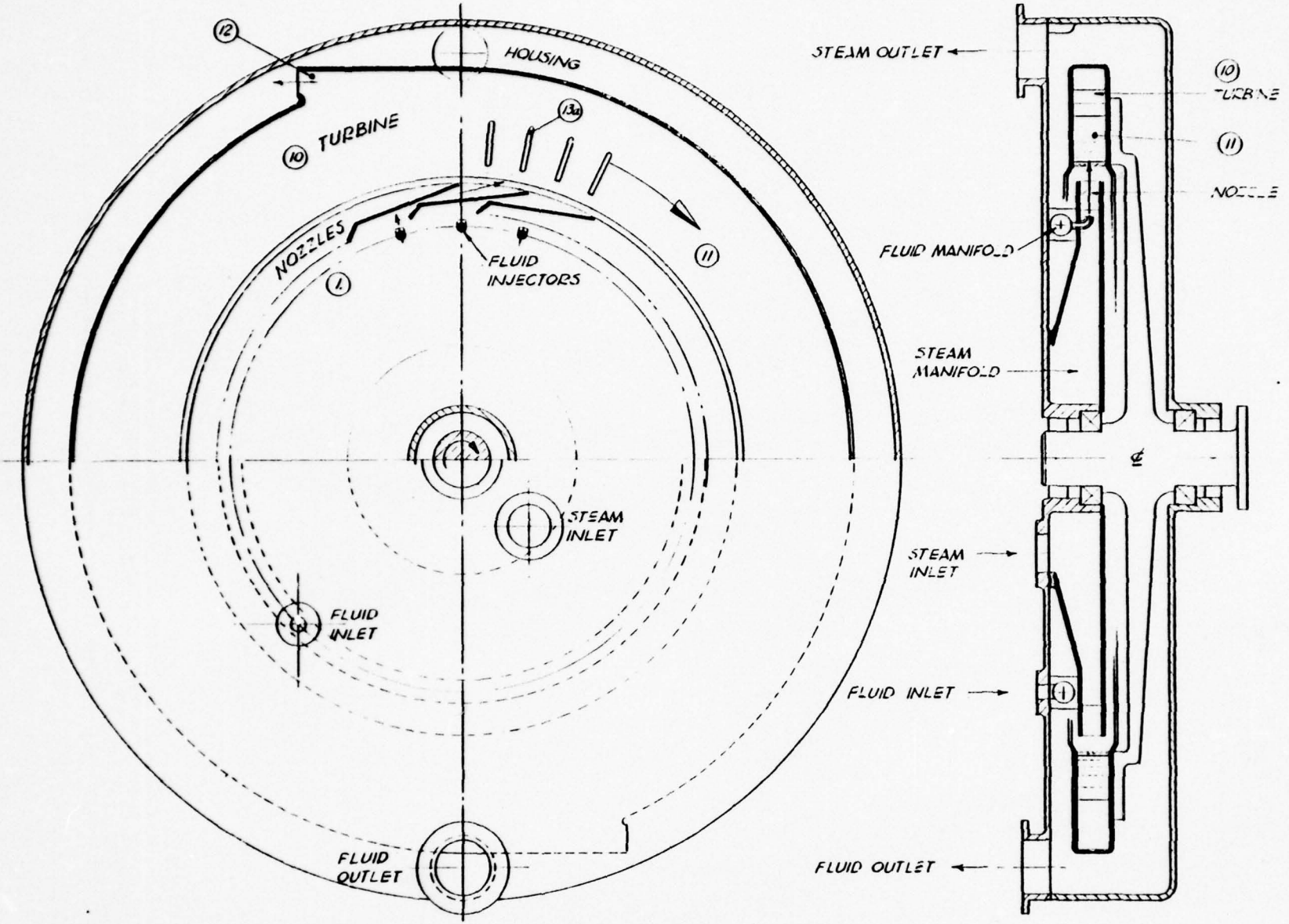

Figure 11. Euler Liquid Turbine

Die Eulerturbine.

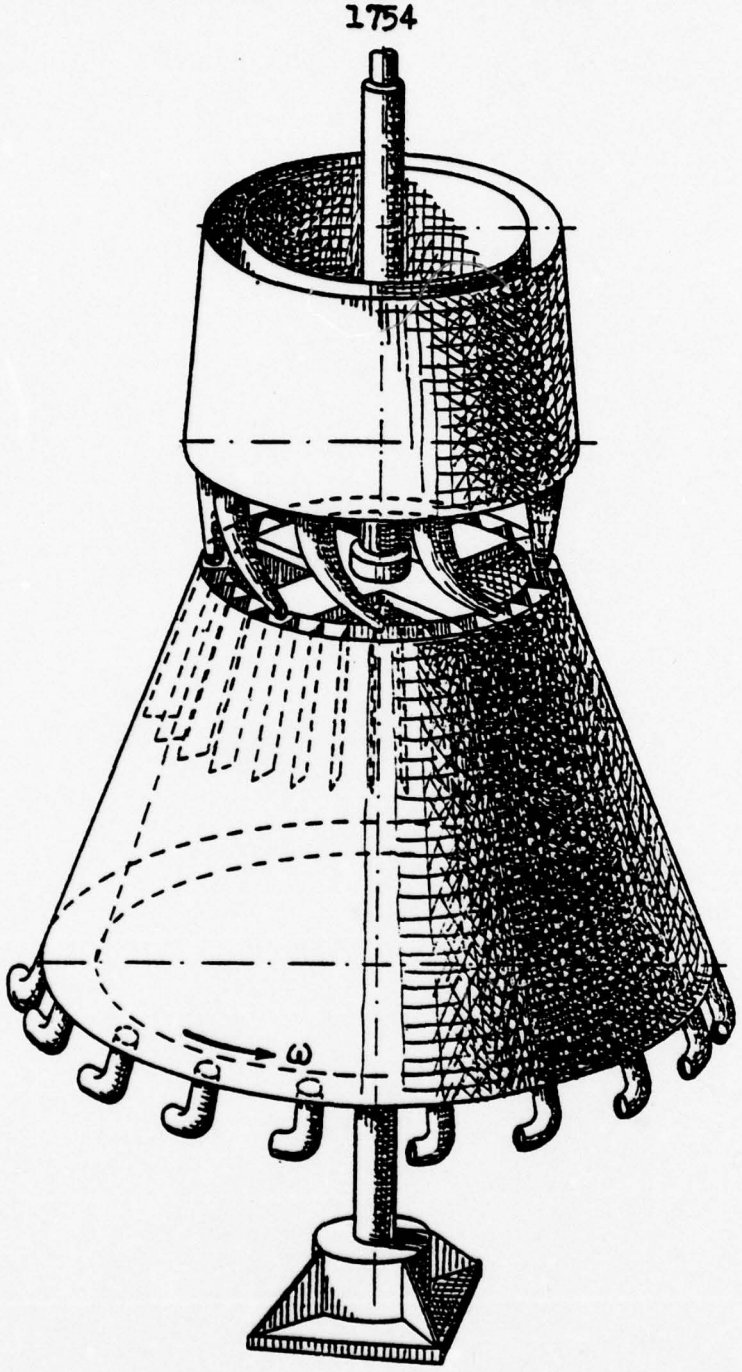

Zch. 22.6.44. R.Lt.

Figure 12. Die Eulerturbine

$$\frac{gH}{u_2^2} = \frac{c_{u_1} u_1 - c_{u_2} u_2}{u_2^2} \qquad (9)$$

The peripheral components of the absolute velocities are $c_{u_1} = c_{u_1}/u_1 * u_1$ at the inlet and $c_{u_2} = u_2 - w_{u_2}$ at the outlet. Therefore

$$\frac{gH}{u_2^2} = \frac{c_{u_1}}{u_1}\left(\frac{r_1}{r_2}\right)^2 - 1 + \frac{w_{u_2}}{u_2} \; . \qquad (10)$$

As explained, initial calculations were performed with the assumption that all of $w_1^2/2$ is lost in the transition from nozzle to rotor. If we introduce a carry-over coefficient ϕ_R, w_{u_2}/u_2 may be expressed as follows:

Normalizing the equation for $w_2^2/2$ gives without friction losses in the runner

$$\left(\frac{w_2}{u_2}\right)^2_{th} = \phi_R\left(\frac{w_1}{u_2}\right)^2 + 1 - \left(\frac{r_1}{r_2}\right)^2 + \frac{2g\Delta z}{u_2^2} \; . \qquad (11)$$

With friction losses and a discharge angle β_2 relative to the rotor: $w_2^2 = \eta'' w_{2_{th}}$, $w_{u_2} = w_2 \cos\beta_2$. Finally,

$$\frac{w_{u_2}}{u_2} = \sqrt{\eta''}\cos\beta_2 \sqrt{1 - \left(\frac{r_1}{r_2}\right)^2 \left[1 - \phi_R\left(\frac{c_{u_1}}{u_1}\right)^2\left(\tan\alpha_1\right)^2 - \frac{2g\Delta z}{u_1^2}\right]} \; . \qquad (12)$$

Substituted we get when $\phi_R = 0$, $\Delta z = 0$

$$\frac{gH_{th}}{u_2^2} = \left(\frac{c_1}{u_1}\right)\cos\alpha_1\left(\frac{r_1}{r_2}\right)^2 - 1 + \sqrt{\eta''}\sqrt{1-\left(\frac{r_1}{r_2}\right)^2}\cos\beta_2 = f\left(\frac{u_1}{c_1}, \eta'', \frac{r_1}{r_2}, \beta_2\right) . \quad (13)$$

In Euler's original concept he assumed according to Ref 14 $\tan\alpha_1 = 0.5$ and $2g\Delta z/u_1^2 = 3/4$ $\left[\Delta z = 3/8\ H\right]$. With $\phi_R = c_{u_1}/u_1 = 1$, the expression in brackets would become zero and $w_{u_2}/u_2 = 1$ and therefore $c_{u_2} = 0$ as desired.

In a Biphase application, where the tip speeds are preferably pushed to allowable top values from the standpoint of stress levels, the term $2g\Delta z/u_1^2$ is negligible and a zero absolute leaving velocity is more difficult to achieve.

The "static" efficiency, which assumes the leaving kinetic energy as lost, follows with gravity now neglected.

$$\frac{gH_{th}}{c_1^2/2} = 2\left(\frac{u_1}{c_1}\right)^2 \frac{gH_{th}}{u_2^2}\cdot\left(\frac{r_2}{r_1}\right)^2 = f\left(\frac{u_1}{c_1}, \eta'', \frac{r_1}{r_2}, \beta_2\right) . \quad (14)$$

A "total" efficiency, which considers recovery of the kinetic energy of the peripheral velocity component in a diffuser of efficiency, η_D, may be defined as:

$$\eta_{xT} = \frac{gH + \frac{c_{u_2}^2}{2}\cdot\eta_D}{\left(\frac{c_1^2}{2}\right)} = \frac{\left[2\frac{gH}{u_2^2} + \eta_D\left(\frac{c_{u_2}}{u_2}\right)^2\right]}{\left(\frac{r_1}{r_2}\right)^2}\cdot\left(\frac{u_1}{c_1}\right)^2 . \quad (15)$$

The static and total efficiencies for various radius ratios across the liquid ring, and for a turbine peripheral speed at the free liquid surface that matches the peripheral component

of the nozzle leaving velocity, are shown in Figure 14. Various friction losses were taken as parameter; they are expressed as an efficiency:

$$\eta'' = 1 - \frac{v\Delta p}{(u_2^2 - u_1^2)/2} \qquad (16)$$

where Δp is the pressure loss encountered in the exit turbine nozzle; it may be estimated in a first approximation by using the pipe-friction formula. Since the flow is accelerated, the loss is reduced compared to fully developed flow; the friction coefficient is that pertaining to entrance flow with a developing boundary layer. Also, the Reynolds' number is high. A sample calculation shows that for a 2000 kW turbine high nozzle expansion efficiencies of the order of 0.995 seem possible.

A comparison of total and static efficiency versus the speed ratio, u_1/c_1, where c_1 is the stationary nozzle exit velocity, is shown in Figure 15 for different radius ratios. In the given efficiency formula and the corresponding plots it was assumed that the kinetic energy pertaining to the velocity relative to the free liquid surface was entirely lost. (This kind of loss explains why the peak efficiency for η'' approaches the value $\cos^2\alpha_1 = 0.883$ in Figure 14.) Nevertheless, the peak efficiency according to Figure 15, occurs at a value of $u_1/c_1 = u_1 \cos\alpha_1/c_{u_1}$ which is lower than $\cos\alpha_1 = 0.940$ and is more nearly equal to 0.8 when the static efficiency, η_{xs}, peaks and equal to 0.866 for a peak η_{xT} when $r_1/r_2 = 0.6$.

Figures 16 and 17 give similar performance for higher carry-over (diffuser efficiencies $\eta_\eta = 0.95$) which is applicable to multi-stage arrangements.

Discussing the performance the assumption is initially being made that the turbine rotates at a speed that matches the discharge velocity from the nozzle.

In the idealized case of no friction loss in the spouting turbine nozzle, and $\phi_R = 0$, the analysis shows that zero kinetic energy loss at the exit occurs only when the drum is full of liquid, $r_1 = 0$ (which can be proven mathematically by differentiation of the efficiency formula with respect to the ratio r_1/r_2).

On the other hand, the normalized output power per unit mass-flow (referred to as $u_2^2/2$) has a maximum at a radius ratio of $r_1/r_2 = \sqrt{3/2} = 0.866$. With a full drum ($r_1 = 0$) the output becomes zero in the idealized case of no nozzle friction.

A design tool for determining the ratio of nozzle diameter, d, to the outer diameter, D, of the liquid ring is given by the specific speed, σ_b, of the liquid turbine. The grouping, $\sigma_b D/d$, is shown in Figure 13 as a function of the radius ratio, r_1/r_2, across the liquid ring for $\eta'' = 0.95$ and $\beta_2 = 0$ according to the formula:

$$\sigma_b = \frac{\frac{d}{D}\left[1 - \left(\frac{r_1}{r_2}\right)^2\right]^{1/4} (\eta'')^{1/4}}{2^{3/4}\left\{\left(\frac{r_1}{r_2}\right)^2 - 1 + \sqrt{\eta''}\sqrt{1-\left(\frac{r_1}{r_2}\right)^2}\right\}^{3/4}} \qquad (17)$$

For a required power output, $\dot{P}$, available steam kinetic energy, Δh_a (per unit mass), given speed, n (rps), given liquid kinetic energy per unit mass, Δh_b, and mass-flow ratio, r (liquid to vapor), liquid specific volume, v_b, and estimated turbine efficiency, η_x, the required specific speed σ_b, follows from:

$$\sigma_b = \frac{2^{1/4}\sqrt{\pi}\, n \sqrt{v_b}\sqrt{\dot{P}/\eta}\left[\sqrt{r}(1+r)^{3/4}\right]}{(\Delta h_a)^{5/4}\left[1+r(\Delta h_b/\Delta h_a)\right]^{5/4}} \; . \qquad (18)$$

RM 3/1/72

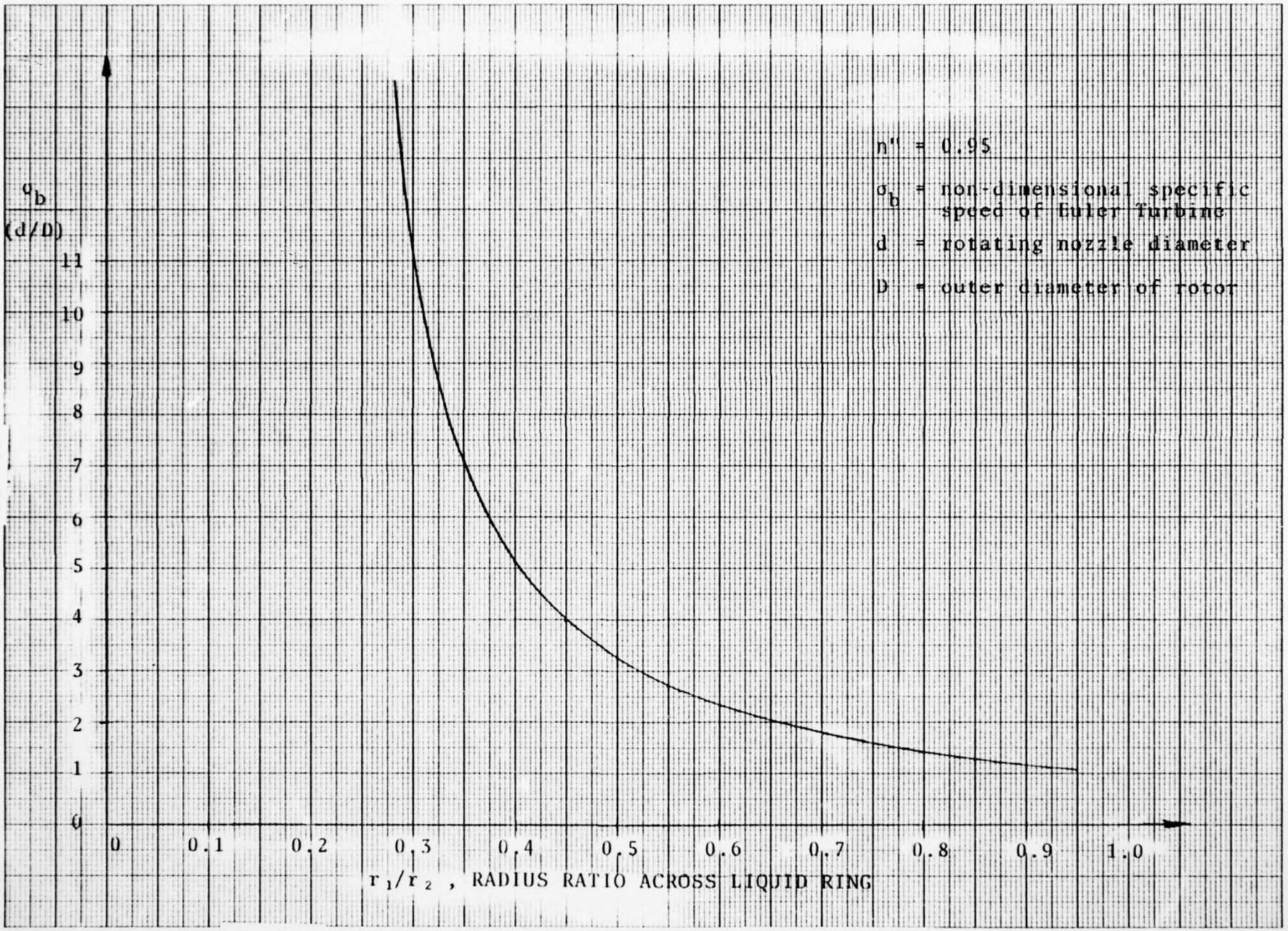

III-19

Figure 13. Specific Speed of Euler Turbine

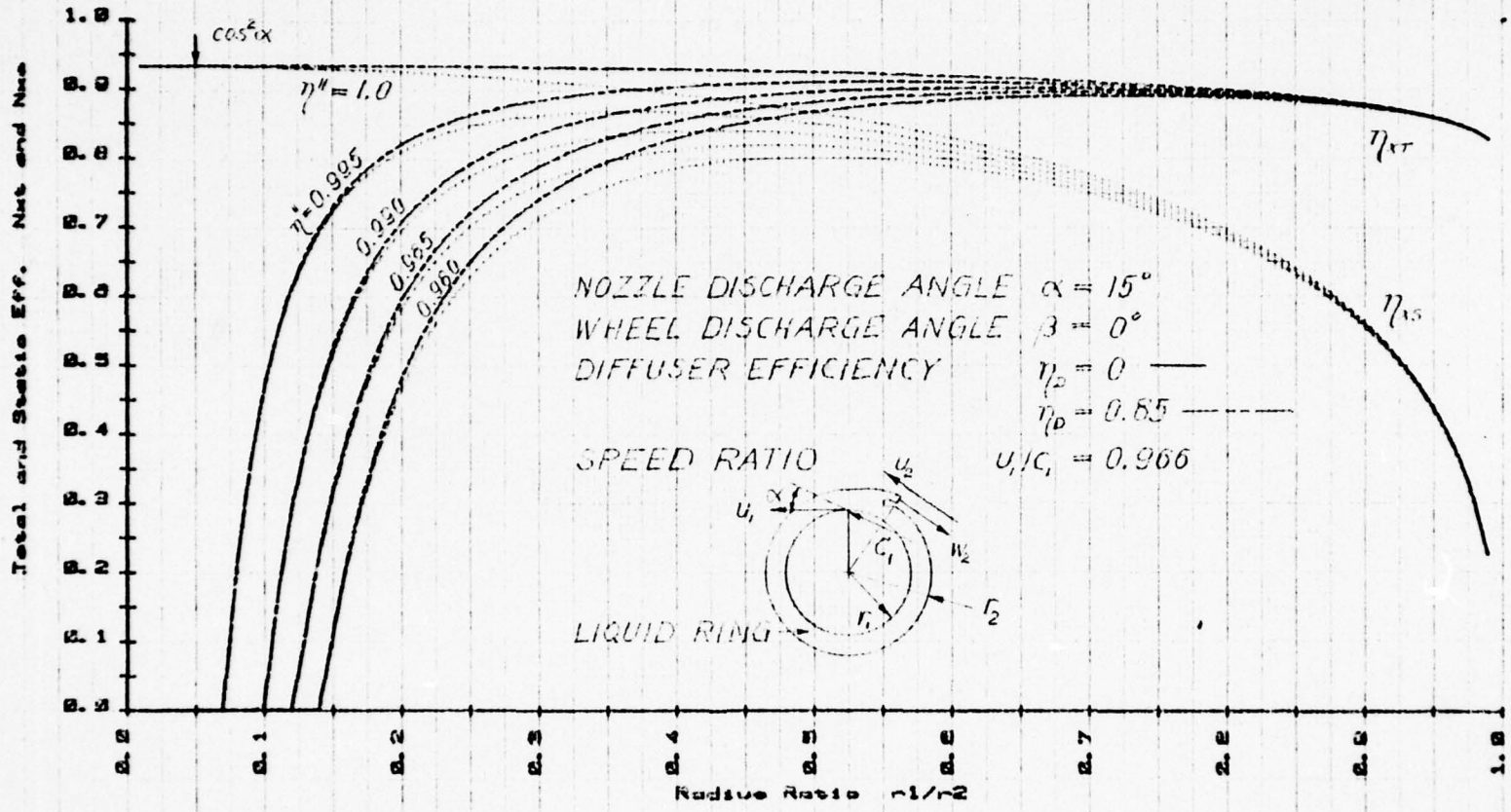

Figure 14. Euler Turbine Predicted Performance

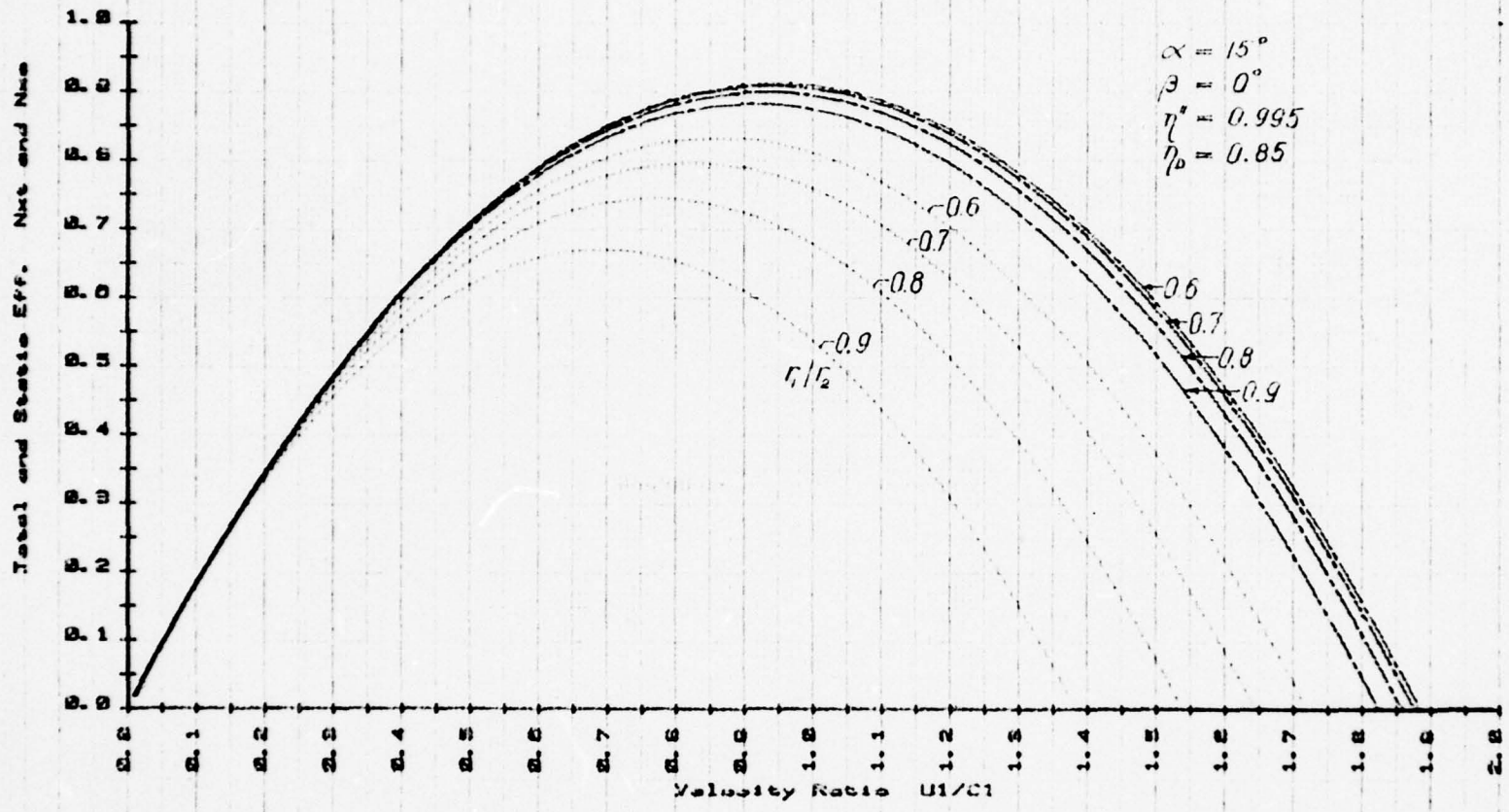

Figure 15. Euler Turbine Predicted Performance

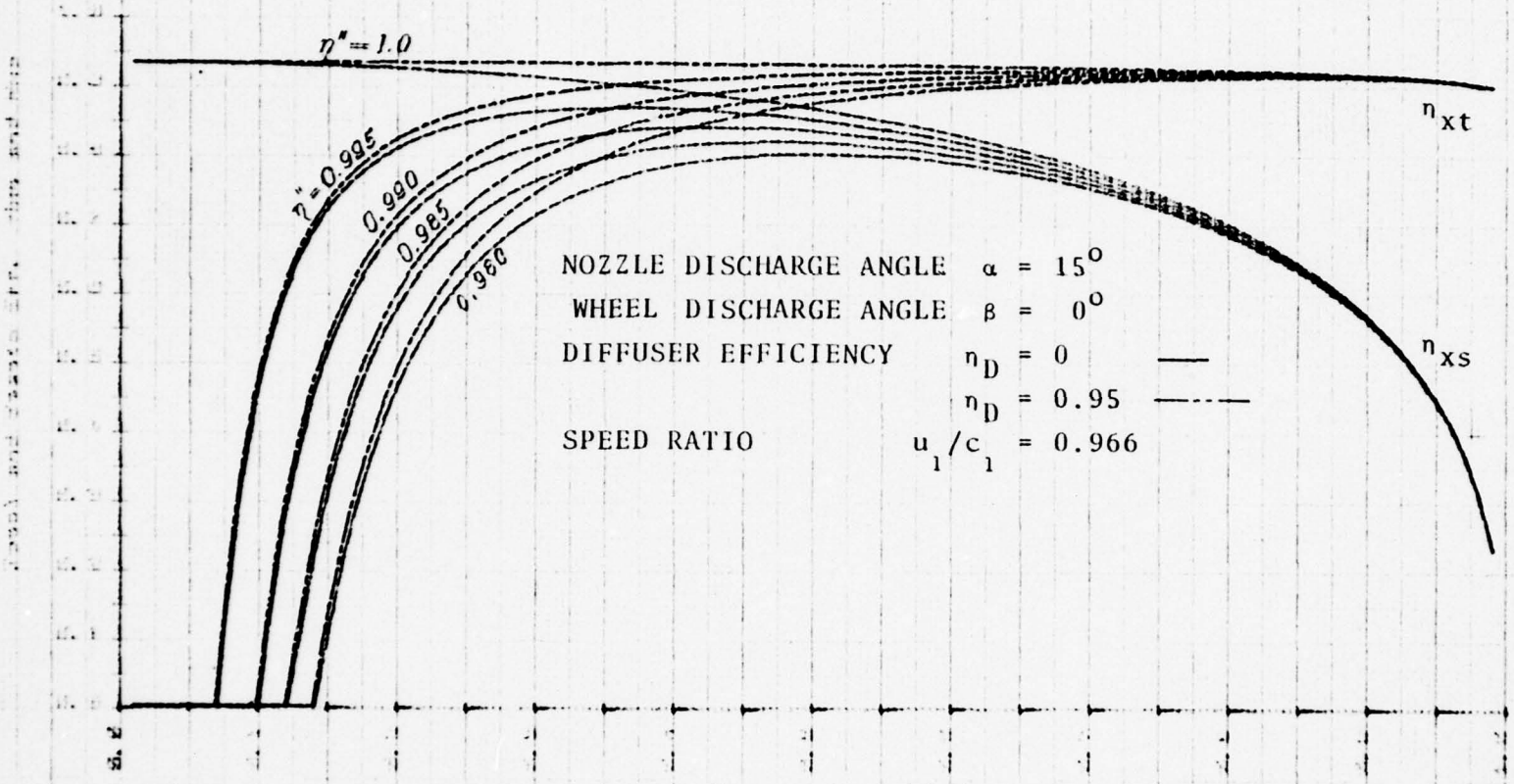

Figure 16. Euler Turbine Predicted Performance

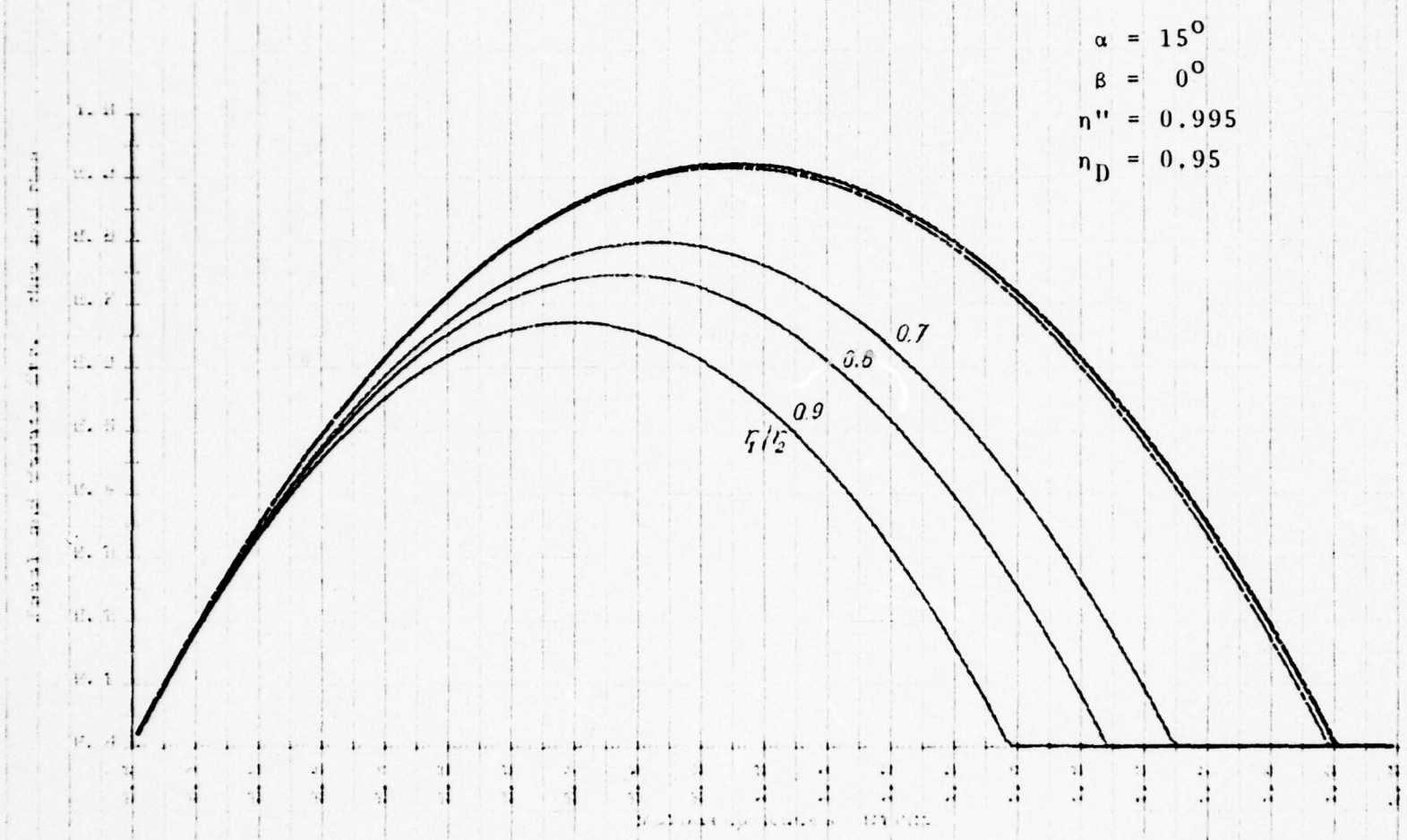

Figure 17. Euler Turbine Predicted Performance

The value, σ_b, is a non-dimensional value, defined as:

$$\sigma_b = \frac{2^{1/4}\sqrt{\pi}\, n \sqrt{V_b}}{(\Delta h_m)^{3/4}} = \frac{\phi_\sigma^{1/2}}{\psi^{3/4}} \quad . \tag{19}$$

In Appendix A the Euler turbine was applied to a five stage wet-steam turbine design. Table XI gives the sizes of the rotating nozzles and their number. The latter was influenced by the stationary nozzle width in the succeeding stage, required for a full admission nozzle with some blockage factor. At this point zero blockage was assumed.

To summarize, three distinctly different types of liquid turbine have been analyzed: the impulse turbine, the U-tube turbine and the Euler turbine. The impulse and U-tube turbines have been reduced to practice with small scale units by Biphase. The Euler turbine while simpler has yet to be tested with two-phase flow.

HEAT EXCHANGERS

It was decided to concentrate on all heat exchangers other than the condenser, since the latter may be a conventional design common to all engine systems, a design for which size and weight data are readily available for a standard condensing pressure condition. A nonconventional approach could be considered at a later date.

The primary heater and the regenerative feed-water preheater, however, are typical for the Biphase system. The distinction should be noted that all the heat exchangers for the single component wet-steam system -- namely, primary heater, feed-water heater and condenser -- have condensing saturated steam and liquid water as their heat transfer media. With exception of the condenser, the two media may be exposed directly to each other at the same pressure.

In the two-component system (using for example Krytox), the heater and condenser involve saturated steam to either heat Krytox in the heater or to heat cooling water in the condenser. The recuperator involves superheated steam and feed-water inherently at different pressures. Krytox may be used as intermediary fluid in direct contact with the superheated steam. The heated Krytox would then give up its heat to the feed-water in a tubular heat exchanger.

Among the designs considered were (1) the tubular heat exchangers with a conventional shell and tube design and with a counterflow design, and (2) the direct contact heat exchangers.

TUBULAR HEAT EXCHANGERS

Conventional Shell and Tube Design

The David W. Taylor Naval Ship Research and Development Center (DTNSRDC) has sized the heater and recuperator for the two-component system using finned tubing. The fins are made of copper. The recuperator uses straight tubing but has three passes in crossflow on the steam side.

The sizes obtained reportedly are acceptable and can be packaged in the allotted space.

Counterflow Design with Straight Liquid Tubing and Axial Copper Fins or Spirally Wound Copper Fins

A computer program was developed for the HP 9825 that determines the geometric characteristics, the fin effectiveness and other heat transfer characteristics and core pressure drop.

For flow inside straight tubing, a computer program was developed for the heat transfer and pressure drop characteristics in the laminar and turbulent range.

DIRECT CONTACT HEAT EXCHANGERS

A direct contact heat exchanger is a promising possibility when liquid and vapor phases of equal pressure can be exposed to each other directly. The advantages are based on the realization that small dimensions (small droplet or bubble sizes) lead to high heat transfer coefficients and also that the surface area A_h of a given volume V_c of liquid increases inversely proportional to the diameter d of n uniformly sized droplets of the same total liquid volume.

$$\frac{A_h}{V_b} = \frac{6}{d} \tag{20}$$

or

$$\frac{A_h}{V_b^{2/3}} = 6^{2/3}\ \pi^{1/3}\ n^{1/3} \tag{21}$$

Additional advantages beyond the savings in volume and the elimination of wall resistance are of course the economic benefits in (1) saving capital for material and labor, for tubing and headers and (2) the expected reduced maintenance because there is much less surface area subject to fouling.

Two basic categories were considered, stationary versions and rotating versions.

The stationary versions are either of the spray or the bubble type. Time limitations made it necessary to concentrate on the spray type since that arrangement lends itself also to rotating versions. Ref. 16 gives a description, theory and test results

---

[16] Kotelewskij, G.P., "Bubble Contact Heaters for Power Plants", *Industrial and Engineering Chemistry*, Vol. 48, No. 1, January 1956, 20-25.

for bubble contact heaters for power plants; Ref. 17 has additional test results.

The conceivable rotating versions are either of the spray type mentioned above or of the rotating disk type where at least portions of the heat transfer may be across a number of pairs of disks with liquid between them and steam condensing in a thin film on the other side of the disk.

Using published literature (for example, Refs. 18, 19, 20) on condensation on rotating disks, the film thickness, condensate flow rate and heat flux density has been calculated. High compactness could be realized, since excellent heat transfer characteristics are also obtained on the liquid side which can be engineered based on extensive data on flow and heat transfer in TESLA pumps (Refs. 21 and 22).

Since the rotating disk type is somewhat more demanding in the ducting of liquid and vapor to alternate spaces between consecutive disks, the spray type was considered for the primary and feed-water heating applications.

---

[17] Böhm, J., "Vergleichsversuche über das Anwärmen von Wasser mit Dampf", *Z. VDI, Beih. Verfahrenstechn.*, 1937, 197-201.

[18] Sparrow, E.M. and Gregg, J.L., "A Theory of Rotating Condensation", *Journal of Heat Transfer*, May 1959, 113-120.

[19] Nandapurkar, S.S., and Beatty, K.O., Jr., "Condensation on a Horizontal Rotating Disk", *Am. Inst. of Chem. Engrs., Progress Symposium Series No. 30*, Vol. 56, 1960, 129-137.

[20] Ginwala, K., *Engineering Study of Vapor Cycle Cooling Equipment for Zero-Gravity Environment*, WADD Technical Report No. TR60-776, Wright Air Development Division, U.S. Air Force, January 1961.

[21] Rice, W., and Crawford, M.E., "Calculated Design Data for the Multiple-Disk Pump Using Incompressible Fluid", *Trans. of the ASME*, July 1974, 274-282.

[22] Millsaps, K. and Pohlhausen, K., "Heat Transfer by Laminar Flow from a Rotating Plate", *Journal of the Aeronautical Sciences*, February 1952, 120-126.

An analysis of the spray-type exchanger has to consider in more detail:

1. The obtainable heat transfer flux density per unit droplet surface and the dwell-time required for the heating of droplets,
2. The required chamber volume for a required total heat transfer area.

Time Average of the Heat Transfer Flux Density – Dwell Time Required

In a paper "Heat Transmission by Condensation of Steam on a Spray of Water Drops", G. Brown (Ref. 23) considered the main resistance to heat flux into the droplets to be the liquid conduction in the droplets themselves. The resistance at the interface of droplets and steam was found to be negligibly small and thus the droplet surface temperature was assumed to be equal to the steam saturation temperature. Convection effects in the droplet were neglected.

The conduction problem is characterized by transient, non-steady heat flow with constant surface temperature, which is treated in Ref. 24 (Carslaw and Jaeger), Chpt. IX, p. 233. While the initial temperature of the droplet was constant over the sphere at time t=0, sudden exposure of the surface to a temperature θ_o above the uniform initial temperature raises the inside temperature with time according to Figure 17a, with the Fourier Number $Fo = at/r^2$ as parameter. It is seen that the temperature gradient at the interface with the steam is varying with time. An average temperature $\bar{\theta}$ may be defined at each moment so that the average heat flux $\bar{q}$ per unit spherical droplet surface area from time zero to t is represented by the heat stored in the droplet.

---

[23] Brown, G., "Heat Transmission by Condensation of Steam on a Spray of Water Drops", *Proceedings of the General Discussion on Heat transfer,* London, 1951.

[24] Carslaw, H.S. and Jaeger, J.C., *Conduction of Heat in Solids,* 1st Edition, Clarendon Press, Oxford, 1947.

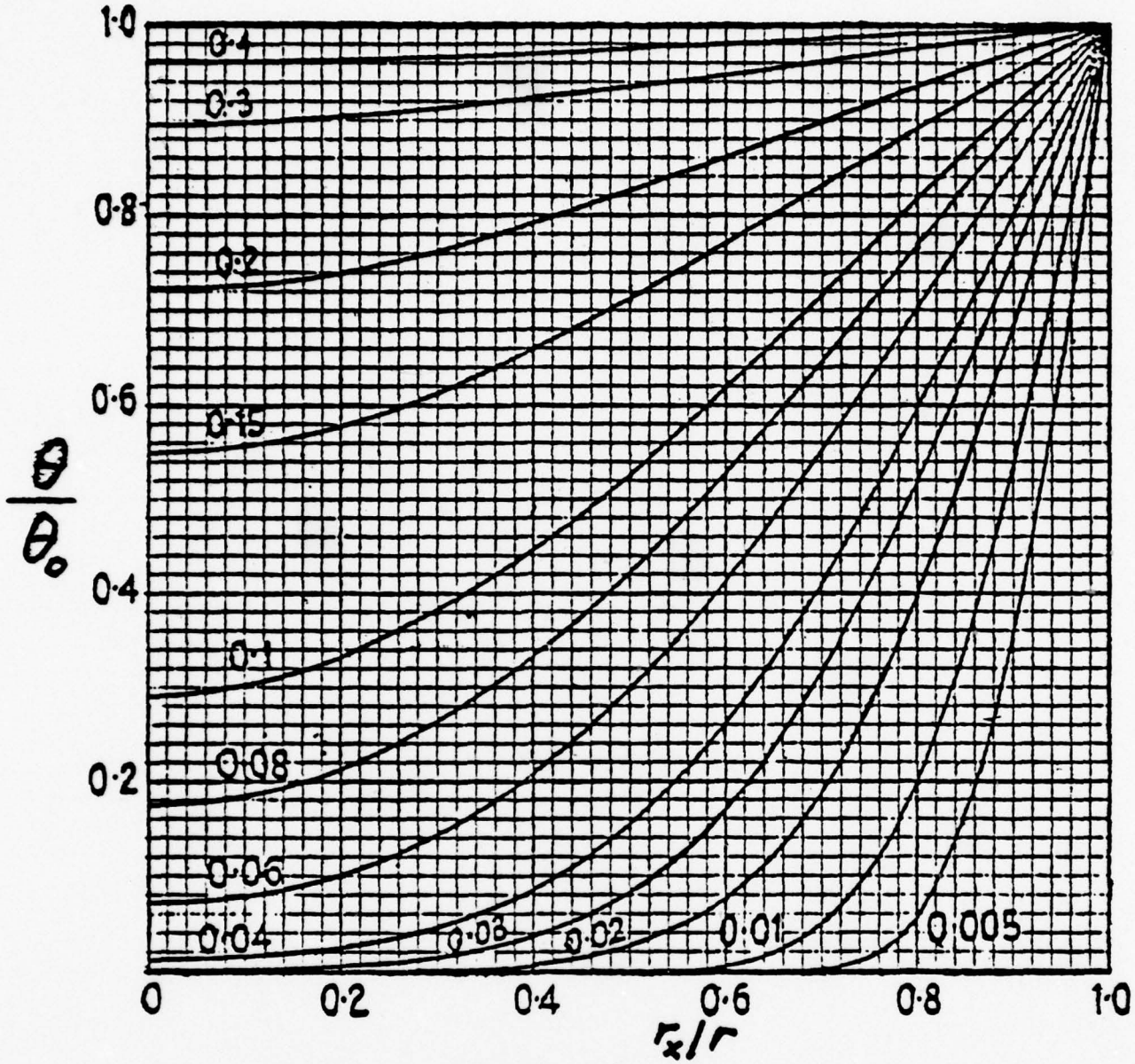

Figure 17a. Temperature Distribution at Various Times in a Sphere of Radius r with Zero Initial Temperature θ and Surface Temperature θ_o. The numbers on the Curves are the Values of $at/r^2 = Fo$

$$\bar{q}\,\pi d^2\,t = \frac{\pi d^3}{6}\,\rho_b\,c_{pb}\,\theta \tag{22}$$

The formula for $\bar{\theta}/\theta_o$ is given in Refs. 23 and 24 as follows:

$$\frac{\bar{\theta}}{\theta_o} = 1 - \frac{6}{\pi^2}\sum_{n=1}^{n=\infty}\frac{1}{n^2}\,e^{\frac{-4n^2\,\pi^2\,a_b t}{d^2}} \tag{23}$$

where a_b is the thermal diffusivity of the liquid

$$a_b = \frac{v_b\,k_b}{c_{p_b}} \quad \text{and} \quad Fo = \frac{4a_b t}{d^2} \quad \text{is the Fourier Number.}$$

The relation is plotted in Figure 18 as $\bar{\theta}/\theta_o = f(Fo)$.

Equation (22) may be rearranged as follows:

$$Nu = \frac{\bar{q}\,d}{k_b\theta_o} = \frac{2}{3}\,\frac{d^2}{4at}\,\frac{\bar{\theta}}{\theta_o} = \frac{2}{3}\,\frac{1}{Fo}\,\frac{\bar{\theta}}{\theta_o} \tag{24}$$

If Eq. (23) is used to eliminate Fo, the Nusselt Number Nu becomes a function of $\bar{\theta}/\theta_o$ only. That function has been programmed and is plotted in Figure 19. It is in agreement with the dashed lines of Figure 11 of Ref. 23. Corresponding numerical values are also given in Table XII at the end of the report.

The Heat Exchanger Volume Required

In the beginning of the section on direct contact heat exchangers, it was shown that for a given liquid volume V_b the ratio of droplet surface A_h to that total liquid volume is inversely proportional to droplet diameter

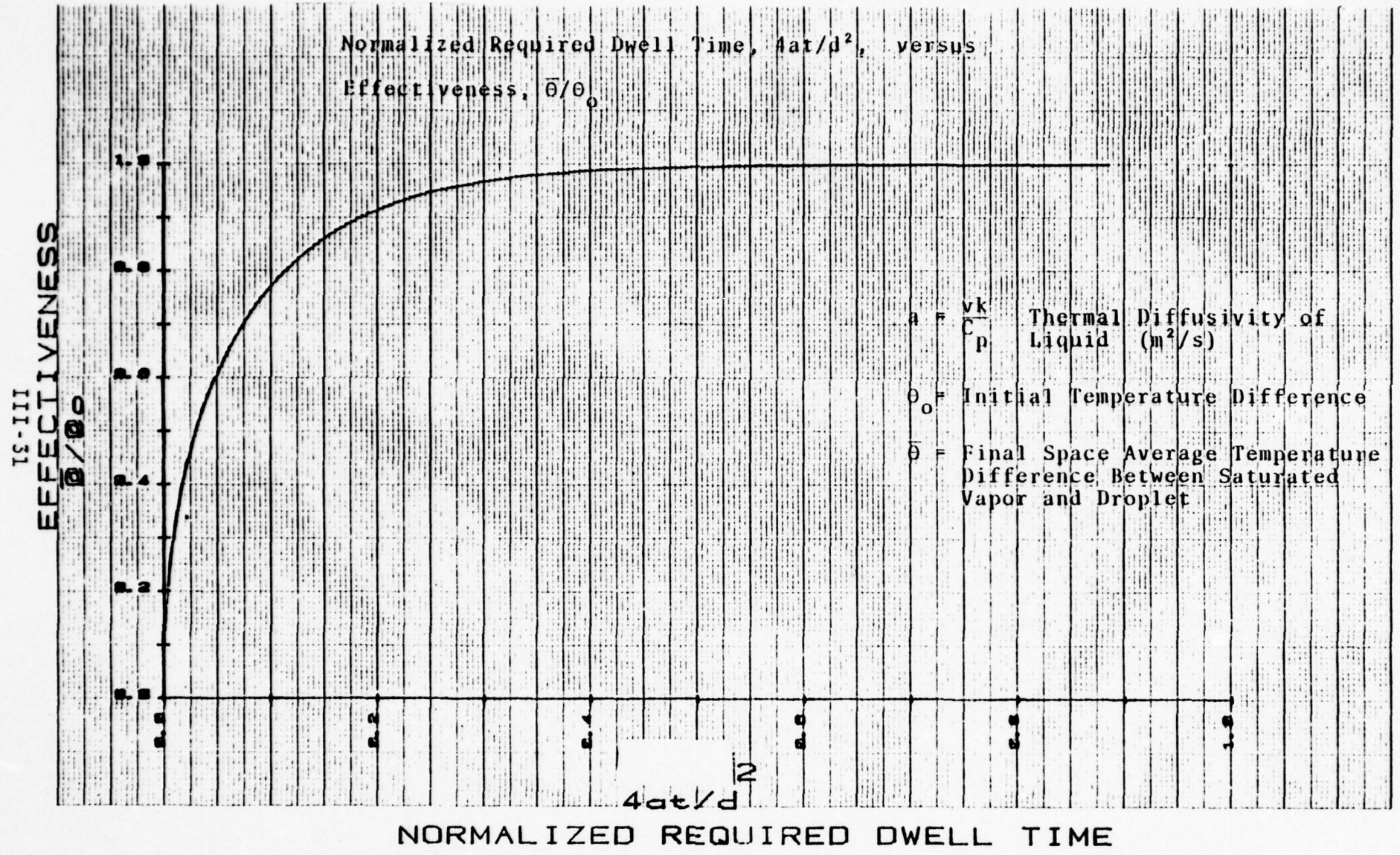

Figure 18. Transient Heat Conduction Into a Spherical Droplet

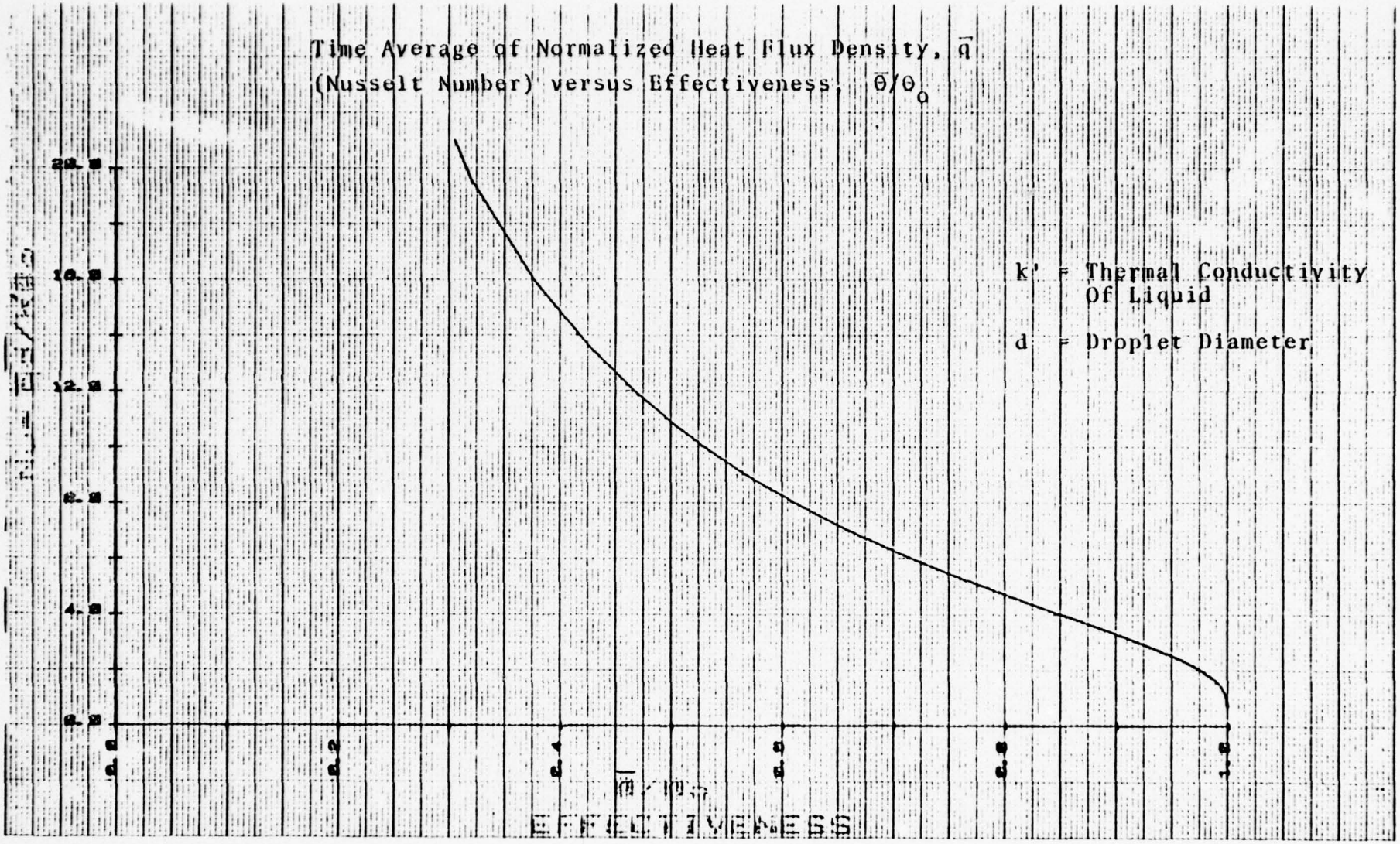

Figure 19. Transient Heat Conduction Into a Spherical Droplet

$$\frac{A_h}{V_b} = \frac{6}{d} \quad . \tag{25}$$

It remains to be shown how the chamber volume V_c is related to the liquid volume, V_b, and how the continuity equations for flow of steam and liquid into the chamber are formulated.

Dividing the heat exchanger volume V_c into equally sized cubes of size s, which each contains a spherical liquid droplet of radius r (see figure below), the volume ratio of liquid volume, V_b, to vapor volume, V_a, is

$$\frac{V_b}{V_a} = \frac{\frac{4}{3}\pi r^3}{s^3 - \frac{4}{3}\pi r^3} = \frac{1}{\frac{3}{4\pi}\left(\frac{s}{r}\right)^3 - 1} \quad . \tag{26}$$

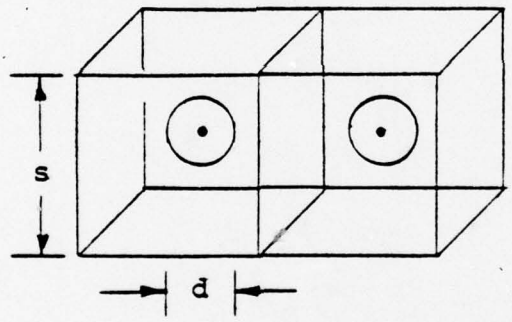

The mass flow ratio of the two streams follows from continuity

$$r_m = \frac{\dot{m}_b}{\dot{m}_a} = \frac{w_b A_b}{w_a A_a} \frac{v_a^*}{v_b^*} \tag{27}$$

where the w's are the respective true velocities and the A's are the respective cross-sectional areas.

The specific volumes v_a^* and v_b^* are fictitious values obtained by dividing the chamber volume $V_c = V_a + V_b$ by the total liquid mass contained in it;

for example, $$v_b^* = \frac{V_a + V_b}{\frac{V_b}{v_b}}$$

$$\frac{v_b^*}{v_b} = \frac{V_a + V_b}{V_b} = \frac{V_a}{V_b} + 1 \equiv \phi \qquad (28)$$

where ϕ equals the ratio of total volume to liquid volume.

With Eq. (26) substituted

$$\frac{v_b^*}{v_b} = \frac{3}{4\pi} \left(\frac{s}{r}\right)^3 \quad . \qquad (29)$$

The ratio s/r may be replaced as follows by the ratio of total surface of all the spheres, A_h, and the total volume, V_c, of the direct contact heat exchanger:

$$\frac{A_h}{V_c} = \frac{n\ 4\pi r^2}{n\ s^3} = 4\pi \left(\frac{r}{s}\right)^3 \frac{1}{r} \quad . \qquad (30)$$

An alternate derivation considers that the ratio of total spherical droplet surface, A_h, to total liquid volume, V_b, is according to Eq. (25) equal to

$$\frac{A_h}{V_b} = \frac{6}{d} \quad .$$

On the other hand, according to Eqs. (28) and (29), the ratio of total volume V_a+V_b to liquid volume equals

$$\phi = \frac{V_c}{V_b} = 1 + \frac{V_a}{V_b} = \frac{v_b^*}{v_b} = \frac{3}{4\pi}\left(\frac{s}{r}\right)^3 .$$

Accordingly,

$$\frac{A_h}{V_c} = \frac{A_h}{V_b} \cdot \frac{V_b}{V_c} = 4\pi\left(\frac{r}{s}\right)^3 \frac{1}{r} . \qquad (31)$$

Eliminating s/r from Eq. (29) and (31) gives

$$\frac{v_b^*}{v_b} = \frac{3V_c}{rA_h} \equiv \phi . \qquad (32)$$

Correspondingly, the fictitious specific volume, v_a^*, for the vapor follows

$$\frac{v_a^*}{v_a} = \frac{\frac{3}{4\pi}\left(\frac{s}{r}\right)^3}{\left[\frac{3}{4\pi}\left(\frac{s}{r}\right)^3 - 1\right]} = \frac{1}{1-\frac{1}{\phi}} \qquad (33)$$

The mass flow ratio $m_b/m_a=r_m$ finally becomes

$$r_m = \frac{w_b}{w_a}\frac{A_b}{A_a}\frac{v_a}{v_b}\frac{1}{(\phi-1)} . \qquad (34)$$

Rearranged, we get with the droplet diameter $d=2r$

$$\boxed{\frac{1}{\phi} = \frac{dA_h}{6V_c} = \frac{1}{1+\frac{A_b}{A_a}\frac{w_b}{w_a}\frac{v_a}{v_b}\frac{1}{r_m}}} \qquad (35)$$

That resulting relation expresses the fact that a high vapor specific volume, v_a , leads to large heat exchanger volumes for a required direct contact heat transfer area, A_h ; a high percentage of liquid mass flow and a high vapor velocity will alleviate the volume requirement. The assumption of constant droplet diameter, spherical droplet shape and uniform distribution has to be kept in mind when applying the equation.

While the combined Eq. (35) has to be fulfilled, the continuity equations for each phase also have to be observed:

for the steam
$$\frac{\dot{m}_a}{A_a} = (1-\frac{1}{\phi}) \frac{w_a}{v_a} \tag{36}$$

for the liquid
$$\frac{\dot{m}_b}{A_b} = \frac{1}{\phi} \frac{w_b}{v_b} \quad . \tag{37}$$

and again, for the combination

$$\frac{A_b}{A_a} \frac{w_b}{w_a} \frac{v_a}{v_b} \frac{1}{r_m} = \phi-1 \quad . \tag{38}$$

When two of the three previous equations are met, the third is of course also fulfilled.

For design work, Eq. (36) may be useful because it recognizes that a limit is imposed on the actual steam velocity allowable from the standpoint of pressure losses.

In Eq. (36), the value of $1-\frac{1}{\phi}$ may vary between 0.476 and unity

$$0.476 < 1-\frac{1}{\phi} < 1 \quad .$$

A criterion for w_a is found when one considers that for one degree centigrade the allowable relative pressure drop for saturated steam varies between

$$\frac{\Delta p}{p} = 0.0452 \quad \text{at} \quad 64^{\circ}C$$

and

$$\frac{\Delta p}{p} = 0.0213 \quad \text{at} \quad 198^{\circ}C \quad .$$

Selecting $$\frac{\Delta p}{p} < 0.02$$

gives $$\frac{w}{\sqrt{p\ v_a}} = \sqrt{2\ \frac{\Delta p}{p}} \leq 0.20 \qquad (39)$$

We may now write Eq. (36) as follows:

$$\frac{m_a}{A_a} \leq 0.2\left(1-\frac{1}{\phi}\right) \sqrt{\frac{p}{v_a}} \quad . \qquad (40)$$

Verification for a Stationary Cylindrical Direct Contact Heat Exchanger

One possible arrangement of a direct contact heat exchanger is a vertical cylinder with liquid injection at the top with spray nozzles; the steam may likewise be entered at the top. The mixture of condensate and heated liquid may be drawn off at the bottom.

Such a device was tested by G. Brown, Ref. 23. While only ranges of the tested variables are given, a set of data at one end of the quoted range may be correlated as follows:

t_a = 120°C steam inlet temperature

p_a = 1.986 bar steam inlet saturation pressure

$e = \sqrt{p_a v_a} = 420.7$ m/s reference velocity

$t_{b1} = 20^{\circ}C$ water inlet temperature

$t_{b2} = 119^{\circ}C$ water outlet temperature

Therefore

$\theta_o = 100^{\circ}C = t_a - t_{b1}$

$\frac{\bar{\theta}}{\theta_o} = 0.990$; $Nu = \frac{\bar{q}d}{k_b \theta_o} = 1.586$ (theoretical Nusselt Number from Table XII)

$\bar{q} = 870.7 \frac{kW}{m^2}$ time average of heat flux density

$d = 125$ μm measured droplet diameter

$\left.\begin{aligned} \dot{m}_a &= 0.0329 \frac{kg}{s} \\ \dot{m}_b &= 0.1744 \frac{kg}{s} \end{aligned}\right\} r_m = 5.30$

$\dot{Q} = 73.0$ kW heat flux $= \dot{m}_a r_c = \dot{m}_b c_{p_b} \bar{\theta}$

$A_h = \frac{\dot{Q}}{\bar{q}} = 0.0838 \text{ m}^2$ (Calculated from transient conduction theory)

$V_c = 0.0506 \times 0.2096$ from geometry (D = 10 in., H = 8.25 in.)
$= 0.0106 \text{ m}^3$.

A theoretically calculated ϕ would follow from

$$\phi = \frac{6 V_c}{d A_h} = \frac{6 V_c k_b \theta_o Nu}{d^2 \dot{Q}}$$

Note that the value of ϕ is affected by the inverse square of the droplet diameter; if d is 125 μm (microns), $\phi = 6069$. On the other hand, using velocities and areas, etc., we would get another ϕ value from Eq. (35).

$$\phi = \frac{A_b}{A_a} \frac{w_b}{w_a} \frac{v_a}{v_b} \frac{1}{r_m} + 1 \qquad (35)$$

However, since the actual steam volume flow rate V_a is primarily known and the actual average velocity w_a would have to be calculated from Eq. (36).

$$w_a = \frac{\dot{V}_a}{A_a} \frac{1}{(1-\frac{1}{\phi})} \quad .$$

If that expression is substituted into Eq. (35), it is seen that the combination reduces of course to Eq. (37).

In the example of Brown's test, we obtain thus for w_b from Eq. (37):

$$w_b = \phi \frac{\dot{m}_b v_b}{A_b} = 6069 \frac{0.1744 \times 10^{-3}}{0.0506} = 20.92 \text{ m/s}$$

which affords a check on the value of ϕ based on the above continuity equation, because w_b thus calculated should be related to the velocity calculated from the injection pressure $\Delta p = 200$ psi. Assuming a nozzle efficiency of 0.90, the initial spray velocity would be 49.8 m/s. Considering that the spray velocity will gradually decrease toward the bottom of the chamber where the liquid is collected, the fair agreement between the two independently arrived velocity values is evidence for the consistency of the relations used.

A check on the dwell time required is based on the desired effectiveness $\bar{\theta}/\theta_o = 0.990$, the corresponding Fourier Number $Fo = 4\, a_b t/d^2 = 0.416$ from Table XII or Figure 18, and the thermal diffusivity

$$a_b = \frac{v_b k_b}{c_{pb}} = 1.639 \times 10^{-7} \frac{m^2}{s} .$$

Those values yield a dwell time $t = 9.92$ microseconds. With a droplet velocity $w_b = 20.9$ m/s calculated before, the required tank height is

$$H = w_b t = 0.207 \text{ m} = 8.16 \text{ in.}$$

The tank height in the experiment was 8¼ inches.

Summary

The measured flow rates of steam and liquid at a measured condition resulted first in a check of the heat balance; the latent heat of the steam released agrees within 1.1% with the heat required for heating the liquid drops from a temperature initially 100°C lower to within 1°C of the steam temperature.

The calculated Nusselt Number $Nu = \bar{q}d/k_b\bar{\theta}_o$ yielded a time average heat flux density $\bar{q}$ based upon a measured droplet diameter d, which, when combined with the measured heat flux would give a required heat transfer area or droplet surface area A_h. The entire liquid volume of the droplets in the chamber did then follow from the relation (25) $V_b = A_h d/6$; the ratio of that volume to the known total chamber volume did then give the ϕ-value. A fictitious average specific volume v_b^*, when considering the mass of liquid spread uniformly over the chamber was then given: $v_b^* = \phi v_b$. Finally, the average liquid velocity would follow from the cross-sectional area A_b and the measured mass-flow rate $\dot{m}_b$.

IV. ENGINE PERFORMANCE AND DESIGN STUDIES

In this section it is shown how a balanced design was developed by due consideration of thermodynamic, fluid flow and mechanical criteria in an effort to meet the performance, volume and weight targets.

In the torpedo study, which preceded the present work, extensive cycle performance studies were performed for two-component (steam and Krytox) systems with constant diameter turbines at a given speed. The inlet steam conditions and the condenser pressure were varied. Initially a recuperator was considered. The estimated cycle performance without recuperator for a single stage turbine using a U-tube turbine is given in Figure 20.

In the present study, single stage U-tube turbines and impulse turbines were used in a *two-component (steam/oil) system.*

A schematic of an oil/steam system that uses the impulse turbine is shown in Figure 4. A corresponding system that uses the alternate U-tube turbine is shown in Figure 3. The figures show how the oil (the low vapor pressure component) is mixed with the steam at the nozzle inlet; after passing the turbine its pressure is raised back to the nozzle pressure in a stationary scoop/diffuser. It is then reheated and returned to the nozzle.

The steam cycle is that of a conventional thermodynamic working fluid: After the nozzle expansion and turbine the superheated, low pressure steam is cooled in the recuperator and finally condensed. The liquid is then pressurized in the feed pump, which is mounted on a free-wheeling separator shaft. The feedwater is preheated in the recuperator by the superheated exhaust steam and, after further heating is returned to the nozzle. The

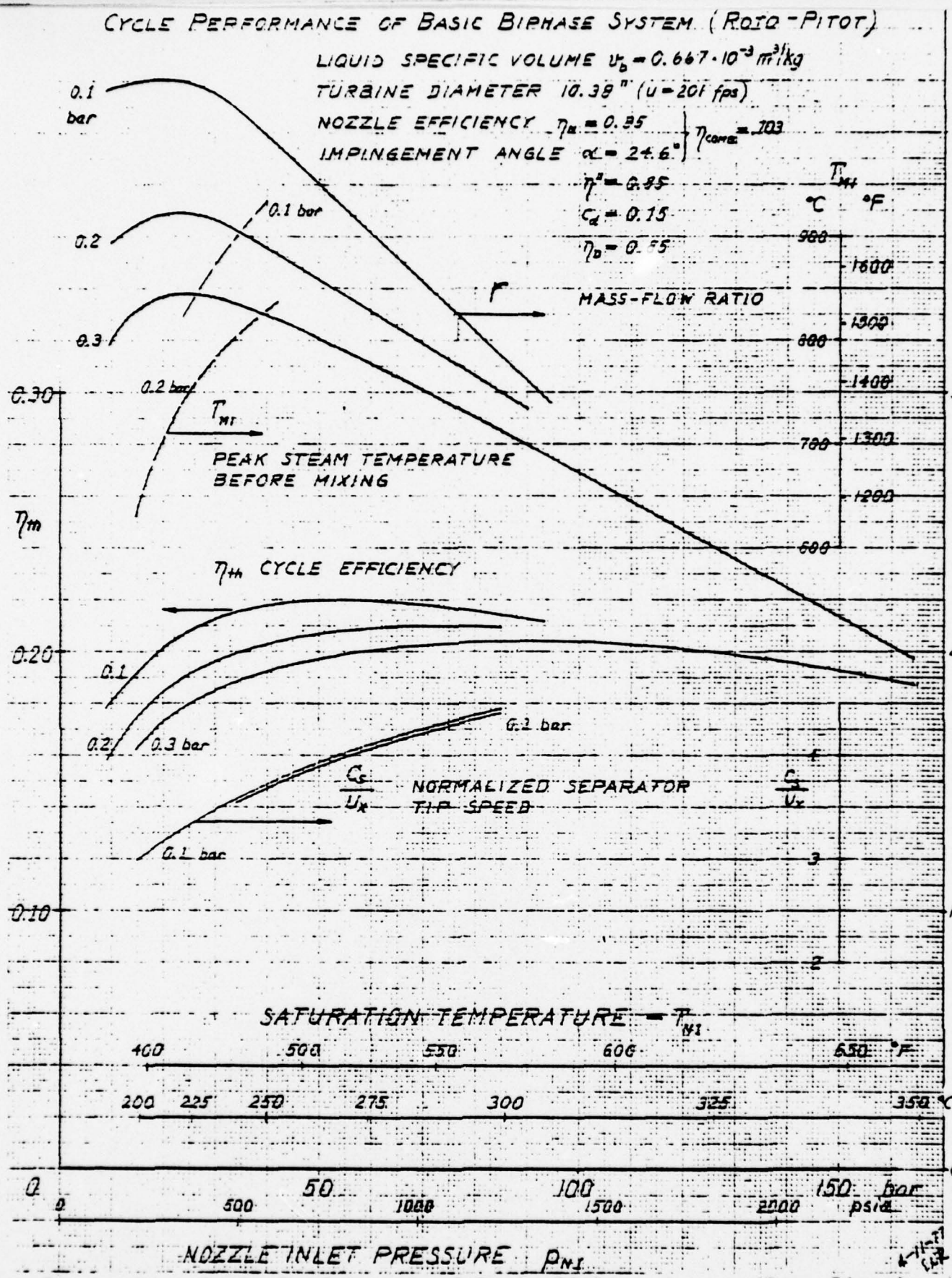

Figure 20. Cycle Performance of Basic Biphase System (Roto-Pitot)

thermodynamic cyle is shown in Figure 1 where an alternate path with higher discharge (condenser) pressure is also shown.

A *single-component* system using wet steam uses a multistage arrangement of the Euler turbine type or possibly the impulse turbine type or the U-tube turbine. The details will be given after the discussion of the steam/oil systems.

In contrast to the Torpedo study the present study investigated the characteristics of Biphase engines for nearly fixed steam inlet conditions. At first only gearless, direct drive machines were considered; the main variables were therefore the turbine diameter and the mass-flow ratio as will be explained below.

While finalizing the design, it seemed advantageous to consider the use of *gearing* since it allowed further performance gains and size advantages. Once gearing is considered for use, it seemed advisable to strive for gear ratios from five to ten. The deviation from the gearless approach, which is spelled out in the original work statement, was taken with due consultation with cognizant Navy personnel. *Either approach leads to a high performance engine relative to the existing steam-turbine engine.*

TWO-COMPONENT (STEAM-KRYTOX) SYSTEM

The Turbine

For two turbine types, the U-tube turbine, and the impulse turbine, the leaving kinetic energy at the turbine discharge was considered collected in a freely rotating drum (a second drum in case of the U-tube) where it would be scooped up in a stationary scoop/diffuser. The pressure developed in the stationary diffuser of efficiency η_D was used to pump the liquid component back to the nozzle inlet. Since no additional power source for assistance in pumping the oil back was considered at the design point, a constraint was imposed on the systems insolar as the turbine was

required to operate at a sufficiently low tip-speed ratio u/c to leave sufficient residual kinetic energy at the turbine discharge in order to meet the pressure balance in the recovery process.

The advantage of the approach is that low tip speed ratios for the turbine still lead to good overall performance; therefore, lower gear reduction is required. Indeed it became possible to consider a direct drive system without gear reduction at all.

The first task was therefore to explore possible solutions for a single stage direct drive turbine of the U-tube or impulse turbine type.

Figure 21 presents performance results and nozzle discharge diameters required for the *impulse turbine* of the radial-outflow type. Also shown are the nozzle widths b required for a full admission nozzle ring that is confined between two planes normal to the turbine axis.

The calculation of the above results involved an iteration procedure which started out by assuming a mass-flow ratio. A calculation of the required nozzle inlet pressure would indicate whether the assumption of the initial mass-flow ratio would have to be adjusted and the process repeated.

The analytical tools needed for the cycle analysis of the oil/steam system have been described in Ref. 2. Basically, relations are required to formulate the expansion of a two-component, two-phase nozzle flow under adiabatic conditions for the mixture. The expanding steam itself receives heat from the liquid in a very compact, intense transfer so that the steam almost follows an isothermal expansion; see the temperature-entropy diagram for water/steam, Figure 1. Analytically, a polytropic steam expansion with an exponent n determined from the relation

$$\frac{n}{n-1} = \frac{k}{k-1} + \frac{r_m \, c_{pb}}{R_a} \qquad (41)$$

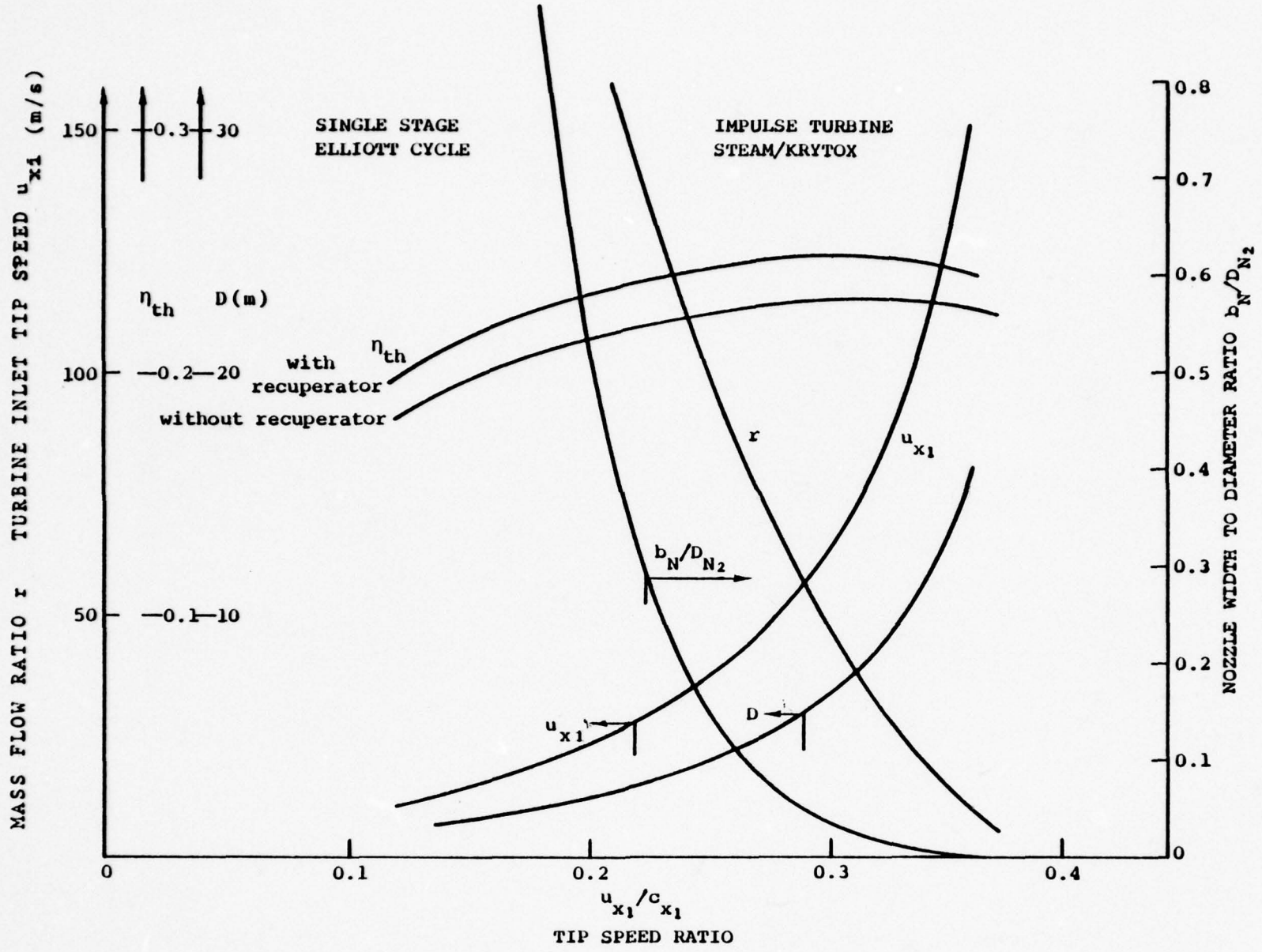

Figure 21. Performance of Two-Component System With Impulse Turbine

is needed. (Here r_m is the mass-flow ratio, liquid to steam, c_b is the specific heat of the liquid and $R_a = c_{pa}/ (k/ (k-1))$ is the gas constant of steam. The above simple approach was checked against results from the elaborate step by step program by Elliott-Weinberg, Ref. 5. A further check is provided by the work of Dr. H. Urbach at DTNSRDC.

A nomenclature is given preceding Table I, which goes together with Tables II, III, IV and V that lists all the relations needed for the cycle analysis. A sample input is shown in Tables III and V as it was needed for the HP 97 calculator program. Figures 22, 23, 24, and 25 show the influence of condenser back pressure and turbine bucket efficiency on performance and size required for the single stage direct drive system with an *impulse turbine*. Figures 22 and 23 pertain to the low nozzle back pressure of 0.086 bar whereas Figures 24 and 25 apply to the back pressure of 0.234 bar (= 3.4 psia) which is spelled out in the "ground rules" Reference (4a). *It is seen that thermal efficiencies of 24 to 25% are possible with a gearless turbine of about 3m diameter* at the nozzle discharge. Reference speed on the abscissa is the actual nozzle discharge velocity c_1. The peripheral speed u, is the value at the turbine inlet. Note that the turbine inlet temperature is 505°K = 450°F. According to DTNSRDC, it is possible to raise the value to around 460°F because of feed water pre-heating.

Figure 26 shows results similar to Figure 21, for the *U-tube turbine*. Here the flow handling for the exhaust steam presented a problem since the steam has to be turned axially (preferably to both sides) in order for it to be ducted out between the two cylinders formed by the separated drum and the nozzle discharge opening. That radial clearance space causes a transition loss for the droplet kinetic energy in its transfer from the nozzle discharge to the first separator drum.

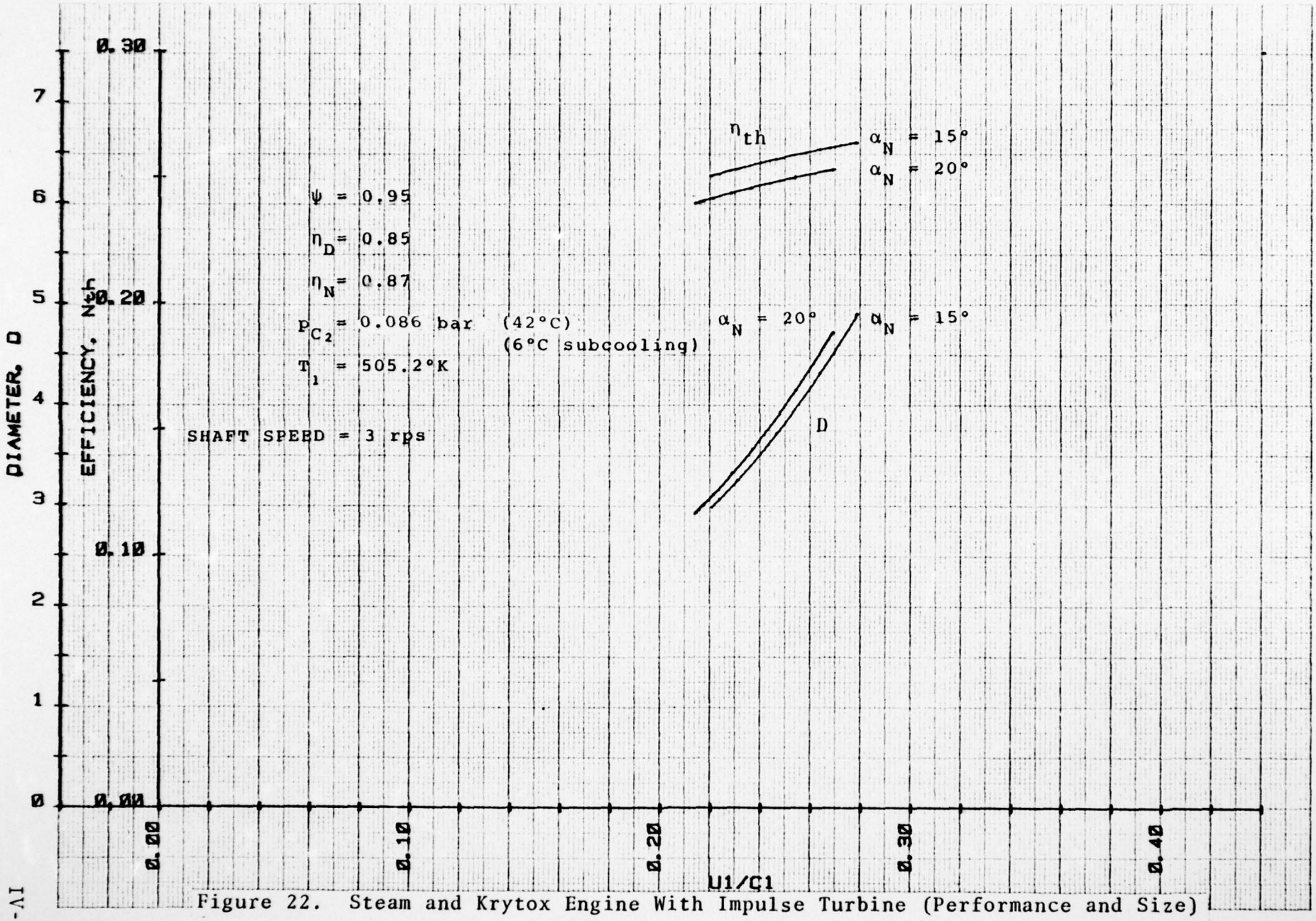

Figure 22. Steam and Krytox Engine With Impulse Turbine (Performance and Size)

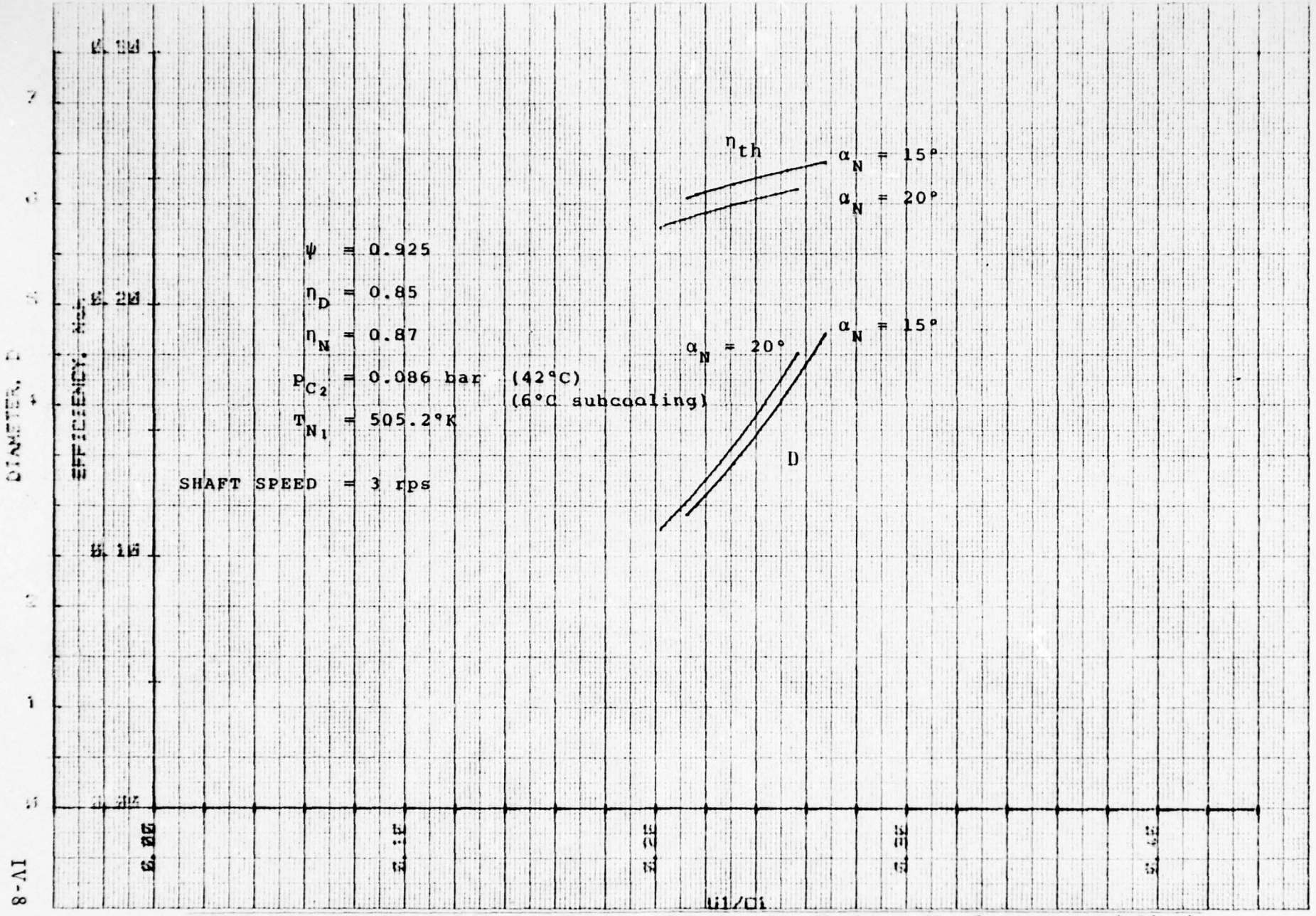

Figure 23. Steam and Krytox Engine With Impulse Turbine (Performance and Size)

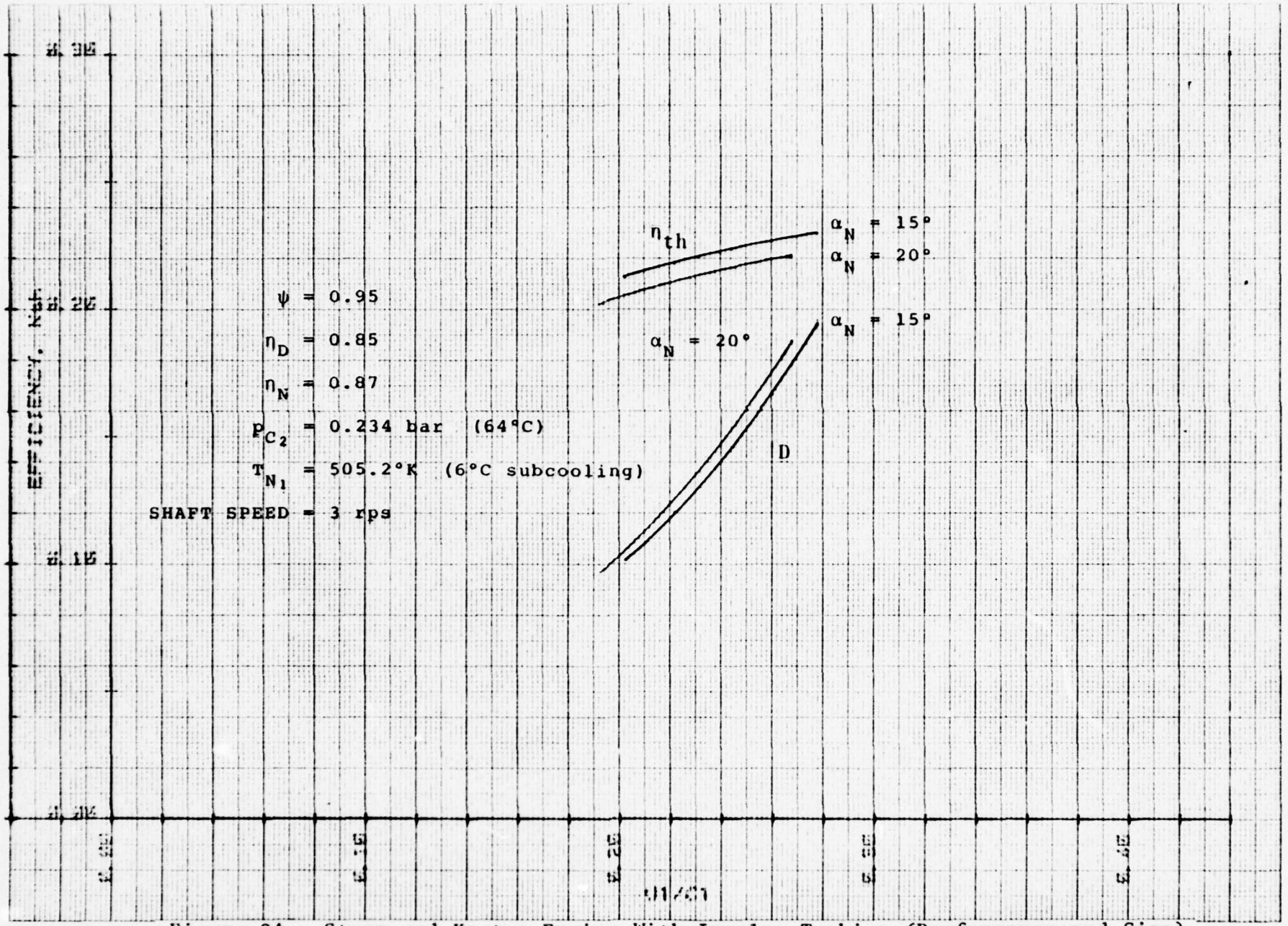

Figure 24. Steam and Krytox Engine With Impulse Turbine (Performance and Size)

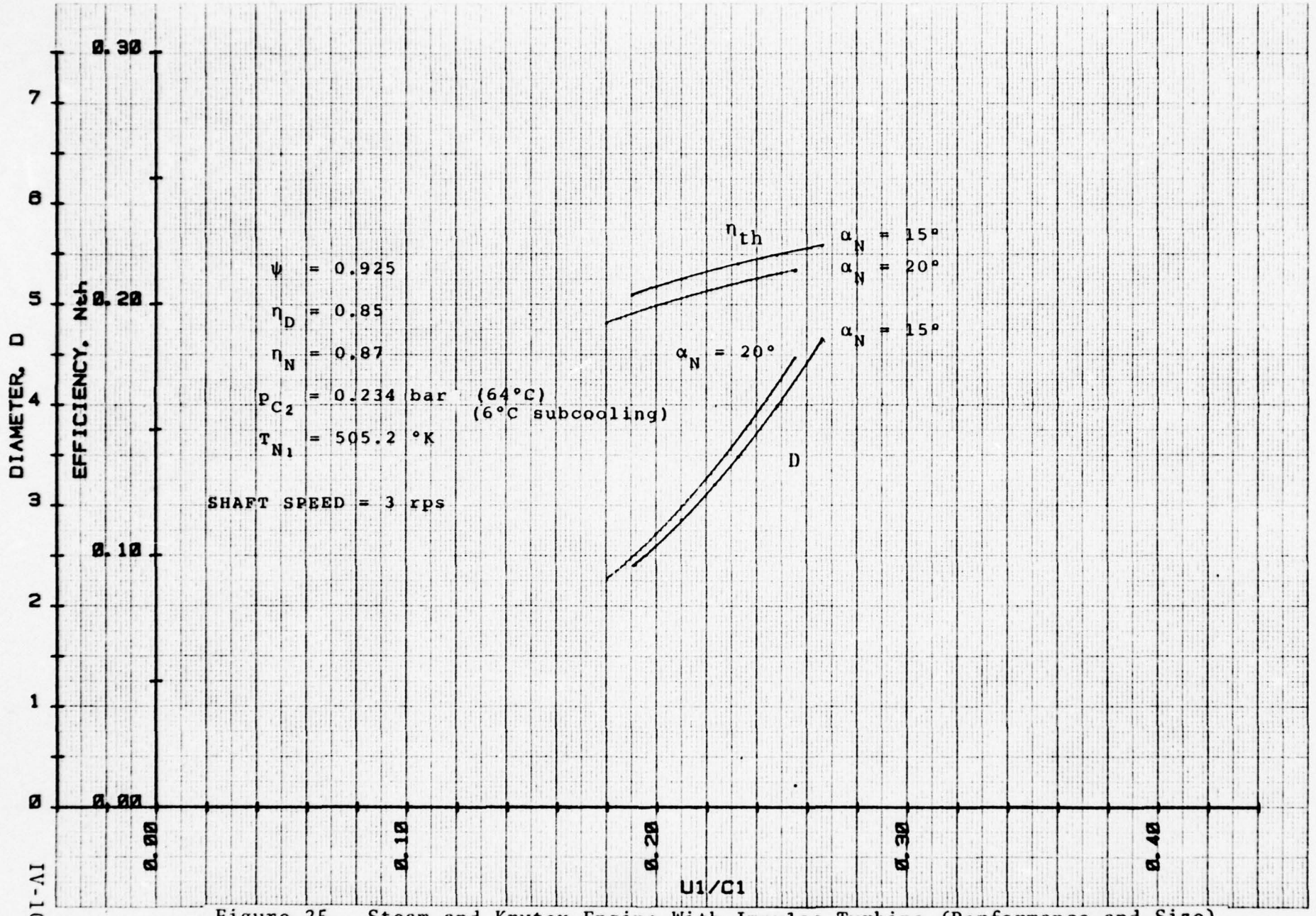

Figure 25. Steam and Krytox Engine With Impulse Turbine (Performance and Size)

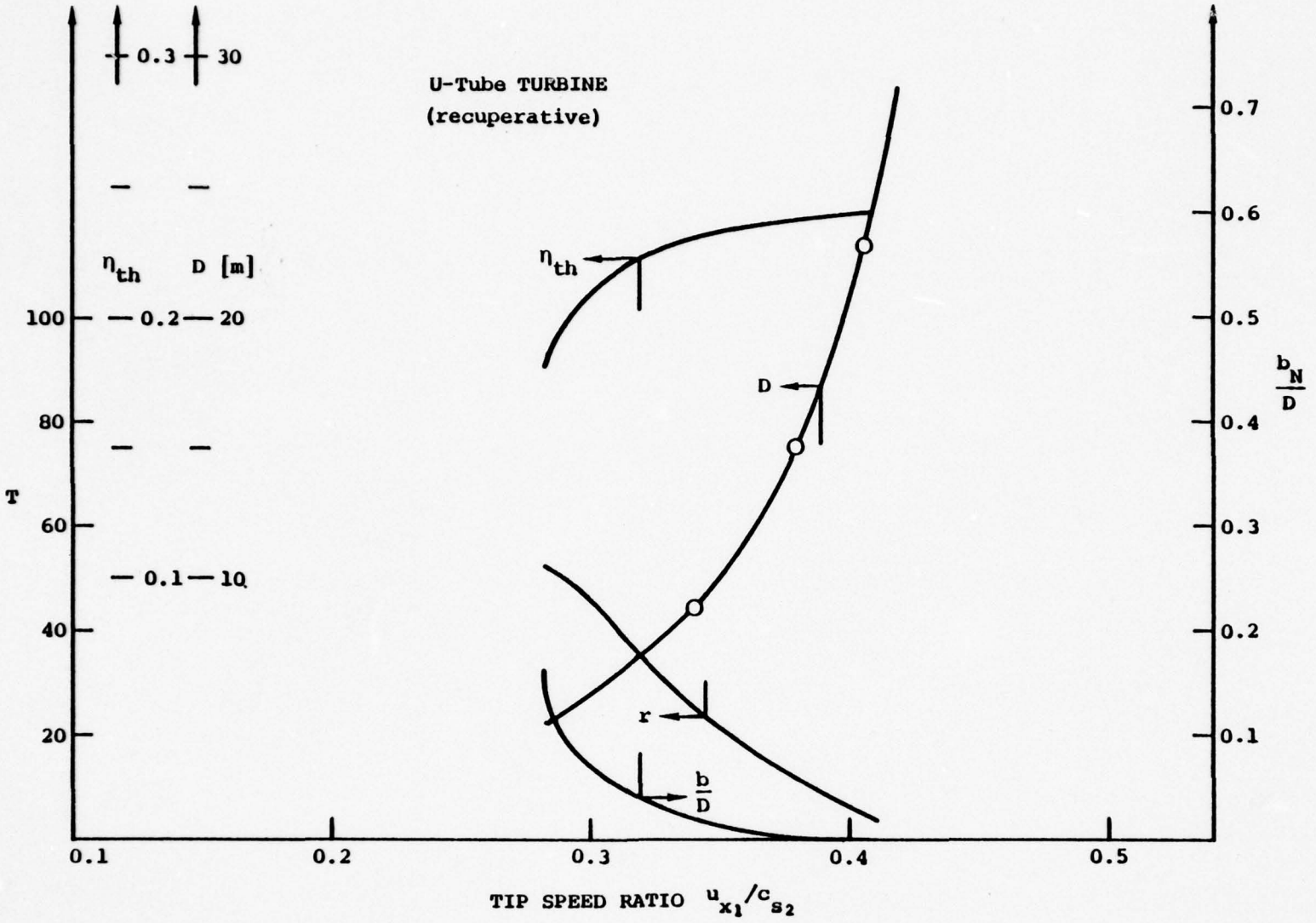

Figure 26. U-Tube Turbine Performance

In the analysis of the U-tube system, a double iteration procedure was required, one was aiming at the pressure balance by adjusting the mass-flow ratio, the other required an adjustment of the clearance between nozzle and separator drum according to the volume-handling characteristics. Changes in that clearance meant changes in the transition efficiency.

A performance and size comparison of single stage designs for full 15,000 hp in one "pancake" with either the impulse turbine or the U-tube turbine solution is shown in Figure 27. The performance penalties due to excessive nozzle/separator clearance requirements are apparent. An incorporation of an Euler turbine into the same scheme of pressure matching in a closed computer program was not completed.

A solution to the steam venting problem (which is also present for the Euler turbine) is provided by a dividing up of the stage into a series of parallel units or "pancakes", which are spaced apart from each other sufficiently so as to allow the steam to be vented radially outward in between them. Such a scheme offers at the same time a convenient geometry for varying the nozzle area for part load operation, by shutting off individual "pancakes".

The design of such a separator which incorporates reaction turbine buckets between the liquid collector rings has been considered in detail. In order to eliminate stationary scoop (pitot) diffusers at each pancake collection drum, the liquid may be ducted axially through the bucket cores and collected on one side of the turbine engine as shown in Figure 28 for a full 15,000 hp propulsion unit turning at 180 rpm. An astern turbine for reverse operation is included in the assembly. Table VI shows a compilation of performance data for such a system--consisting of six "pancakes" in parallel--with different condenser pressures and different mass-flow ratios.

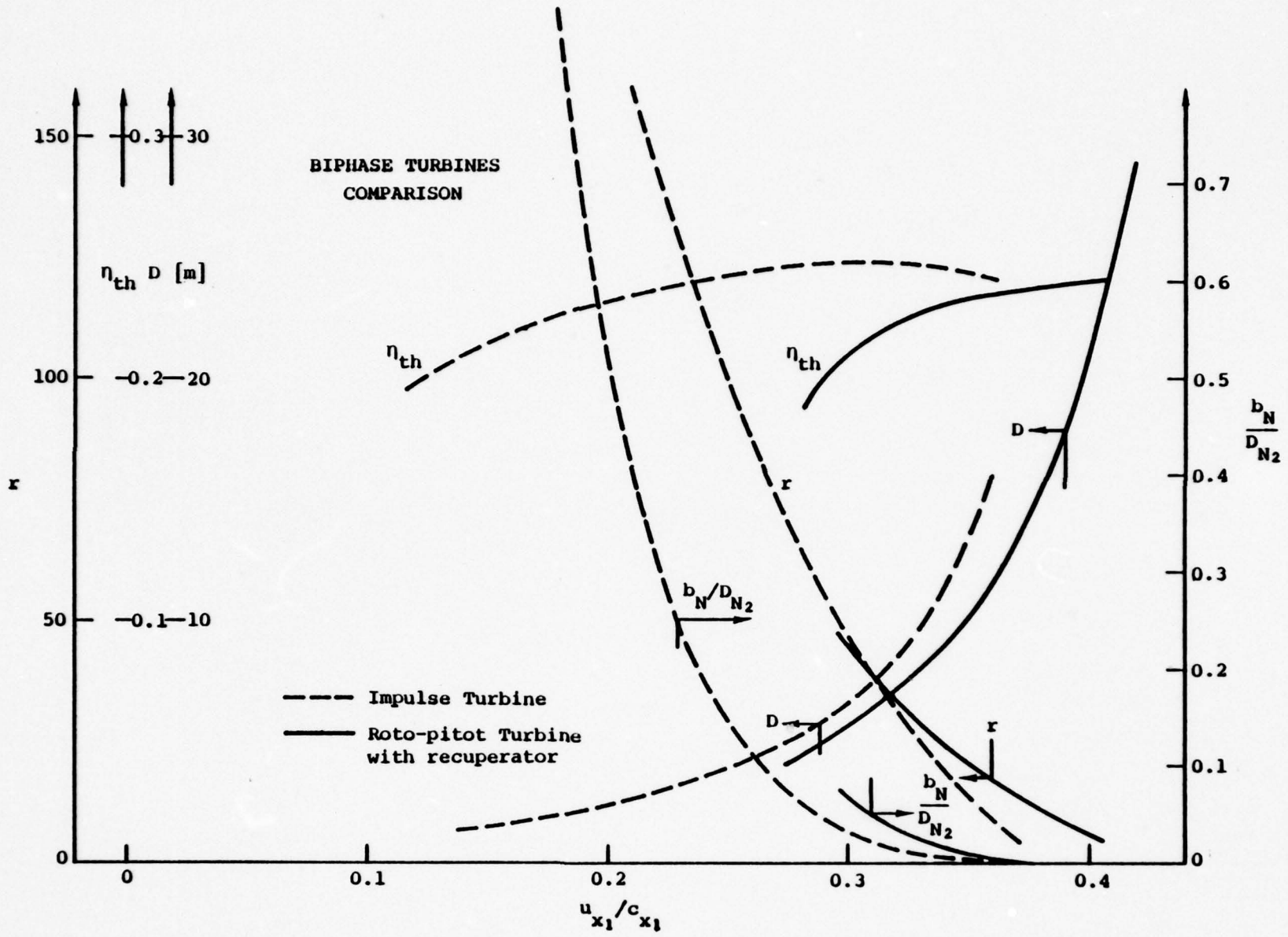

Figure 27. Biphase Turbine Engine Comparison

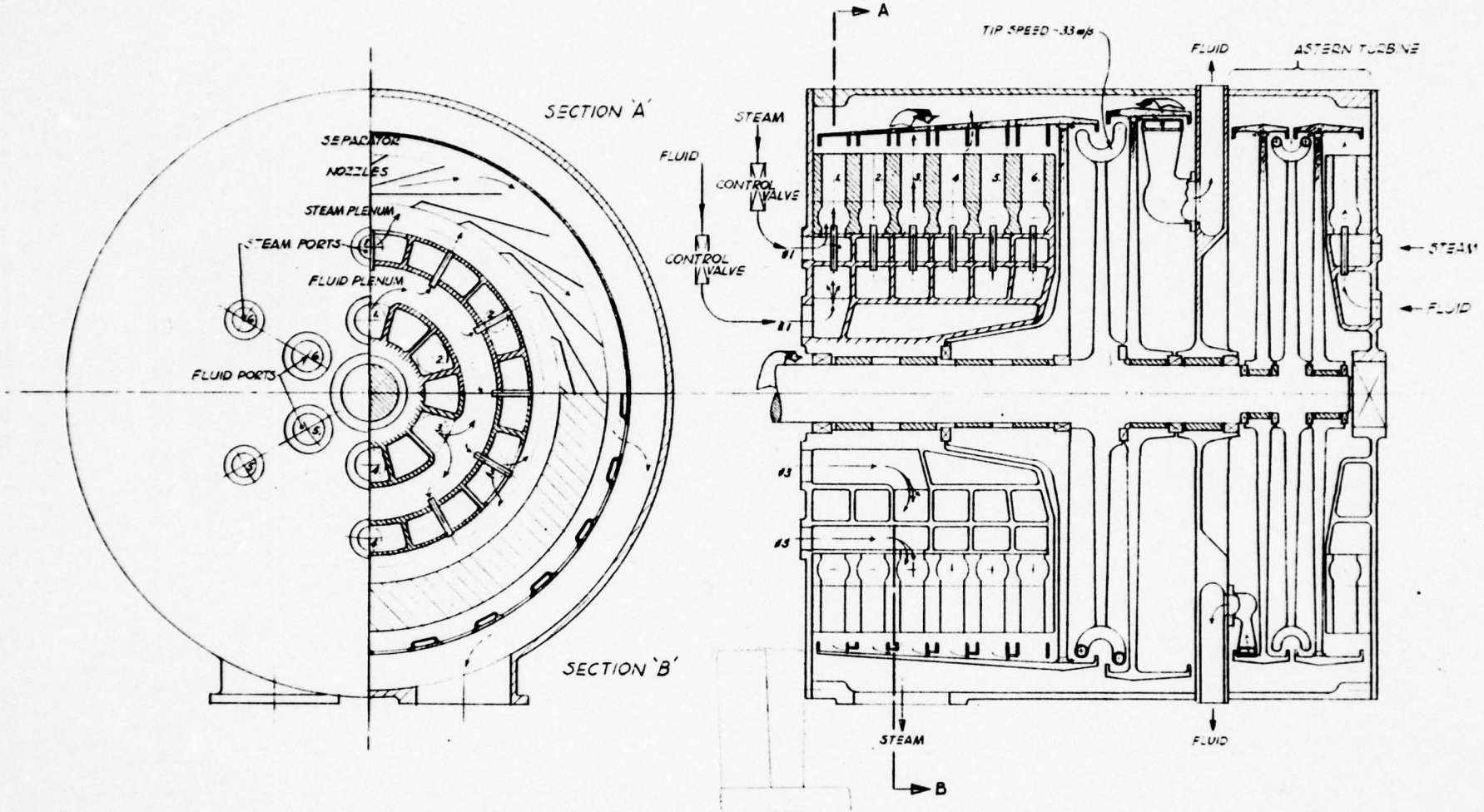

Figure 28. Submarine Engine
Main Propulsion Unit

A reduction of separator overhang is possible by dividing the entire turbine engine into two units, each in its own separate housing. The output per unit of three pancakes each is now 7500 hp. The advantage of a certain redundancy is thereby gained and conformance achieved with the "ground rules", Ref. 4a, which call for a dual prime mover.

A layout of one of the 7500 hp units, together with an astern turbine is shown in Figures 29 and 30. The speed selected is 1000 rpm.

A set of output performance data is given in Table VII (tape). An installation drawing is shown in Figure 31. A list of projected weights is given in Table VIII. A similar design using an Euler turbine is possible at a speed of 2000 rpm which requires a gear ratio of ten.

The performance variation with mass flow ratio and three different shaft speeds is shown in Figure 32.

The influence of different U-tube relative flow efficiencies $\eta'' = 0.85$ and 0.90 and different nozzle angles $\alpha_n = 15°$ and 20° on performance and size required is shown in Figures 33 and 34 as a function of the tip speed ratio (the reference value c_{s2} is the corrected separator tip speed) with shaft speed as a parameter.

THE ONE-COMPONENT (WET-STEAM) SYSTEM

The basic thermodynamic approach towards a carnotized cycle was already described in the previous section, namely how it may be realized with feed-water heating by extracted-steam and by the use of a liquid turbine that allows the expansion to take place deep in the wet region. At the same time by increasing the liquid to vapor ratio, r_m, the discharge velocity of the wet mixture from the nozzle is slowed down.

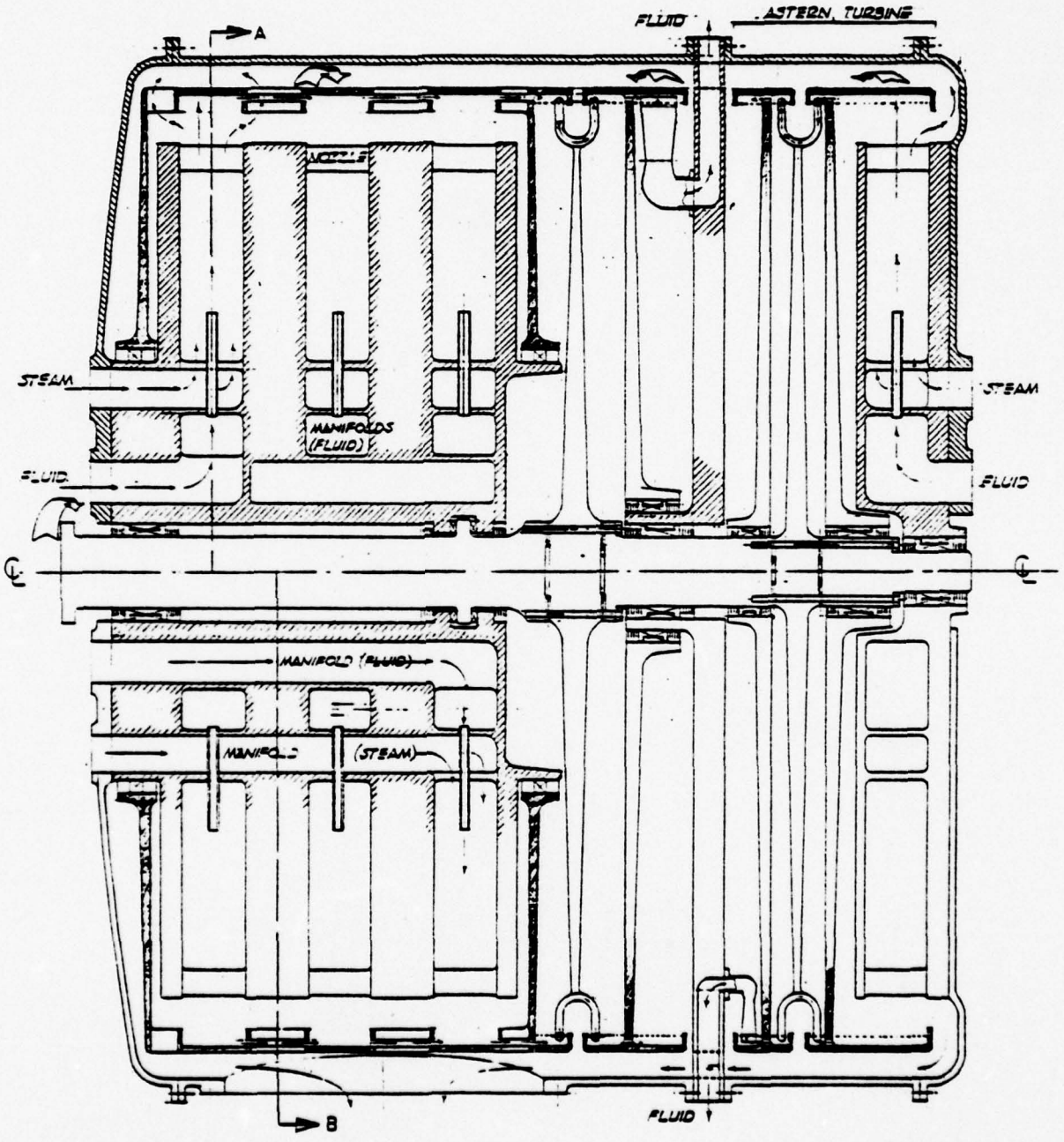

Figure 29. Main Propulsion Unit

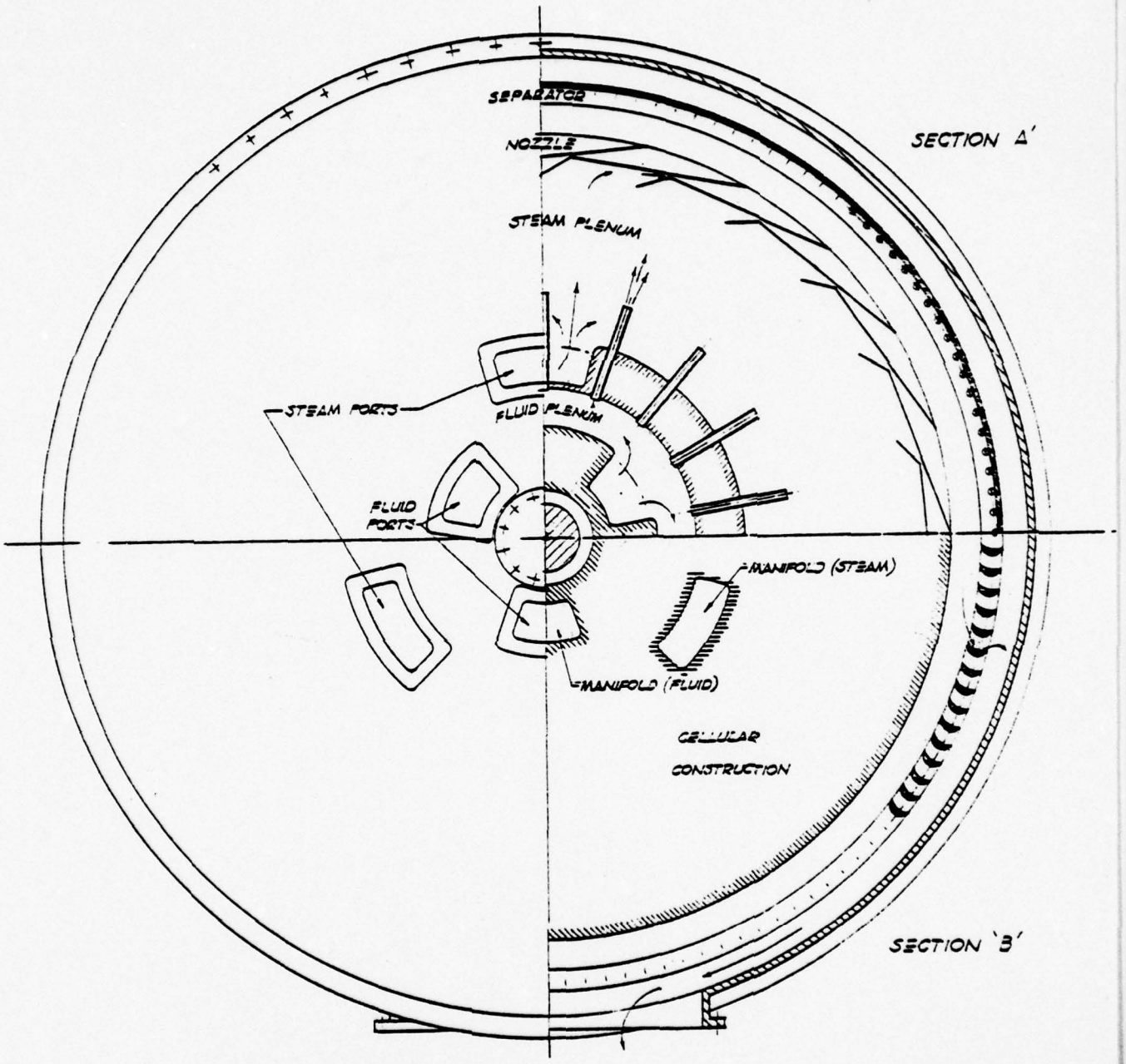

Figure 30. Main Propulsion Unit – End View & Sections

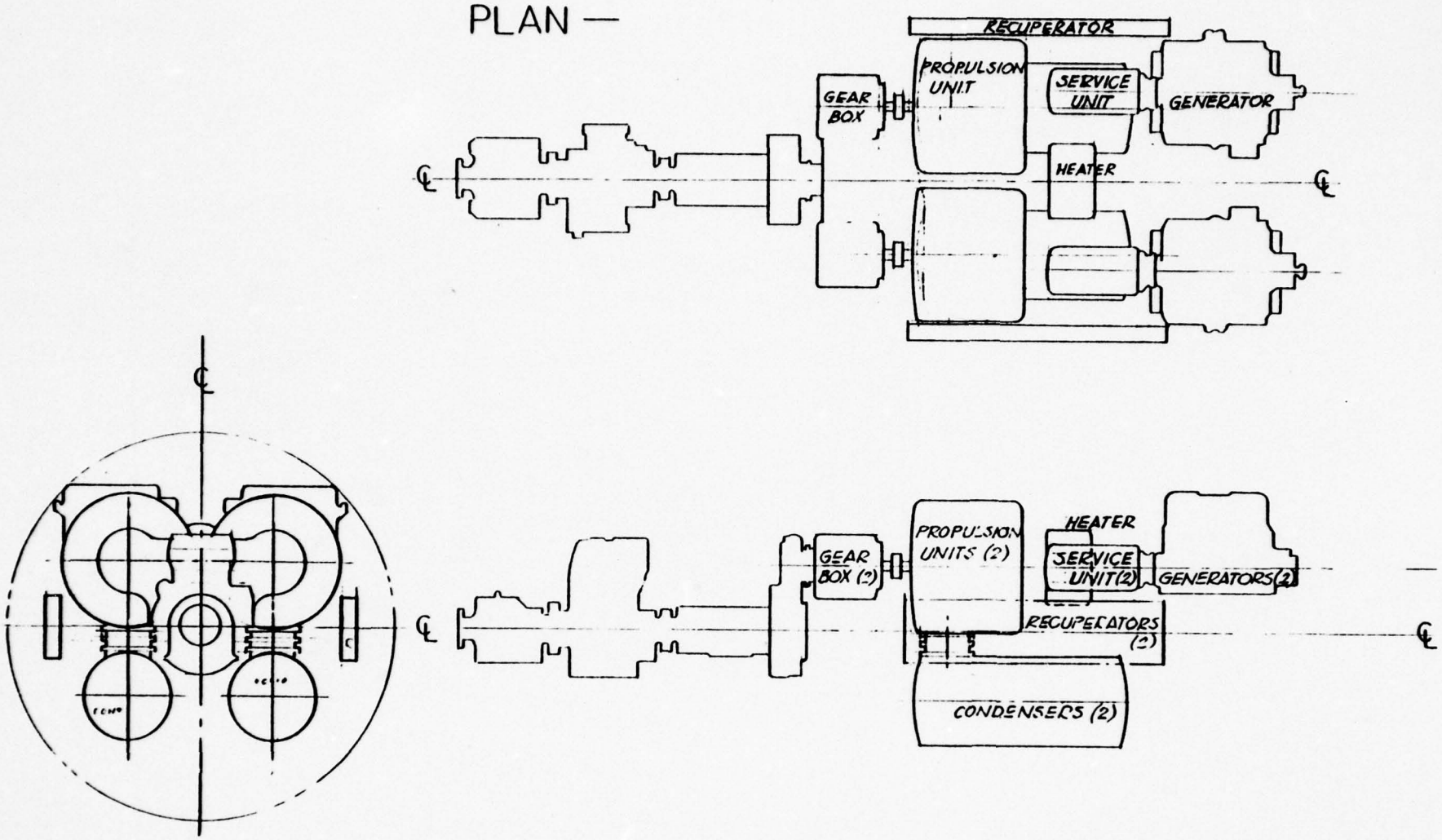

Figure 31. Component Installation

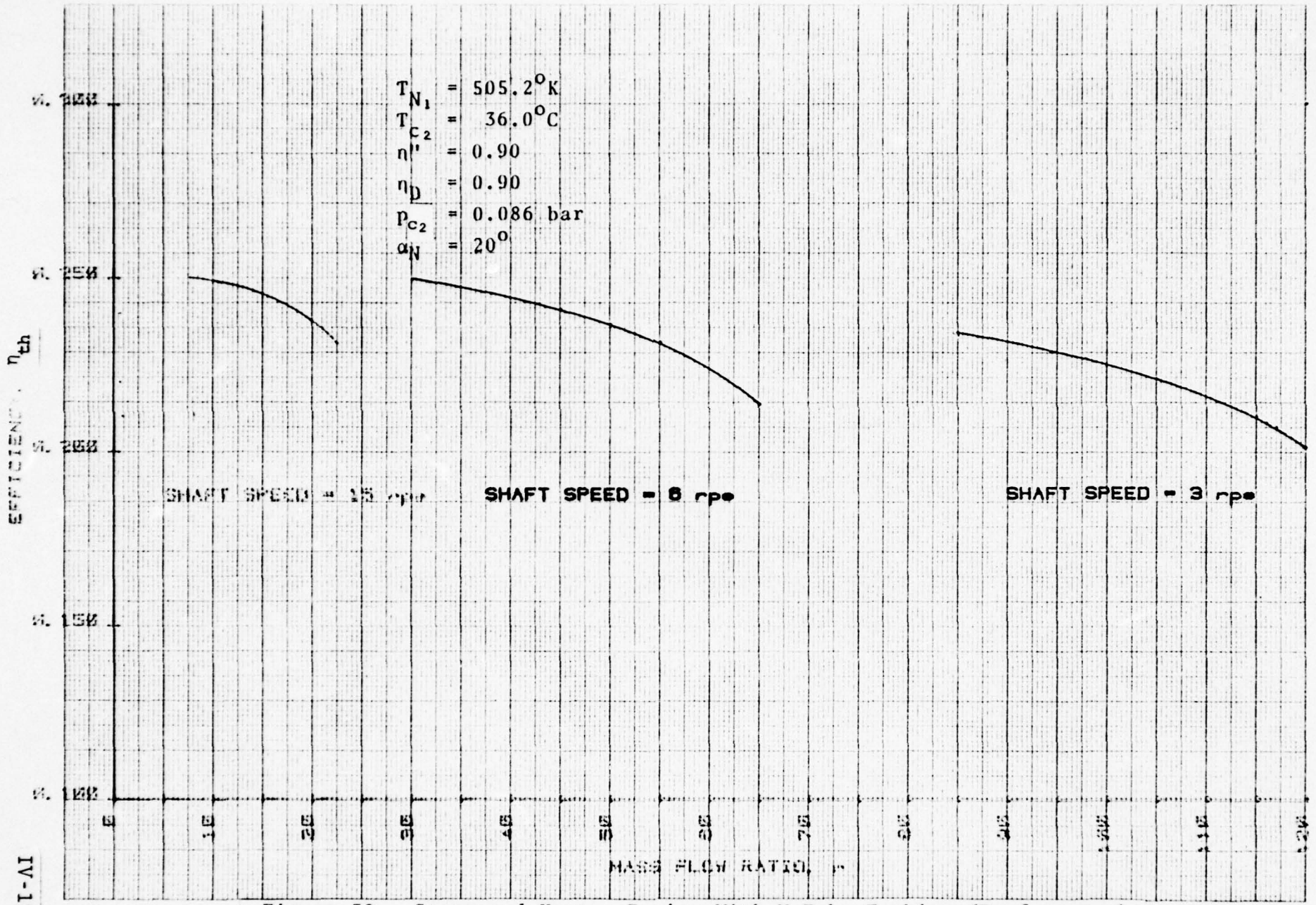

Figure 32. Steam and Krytox Engine With U-Tube Turbine (Performance)

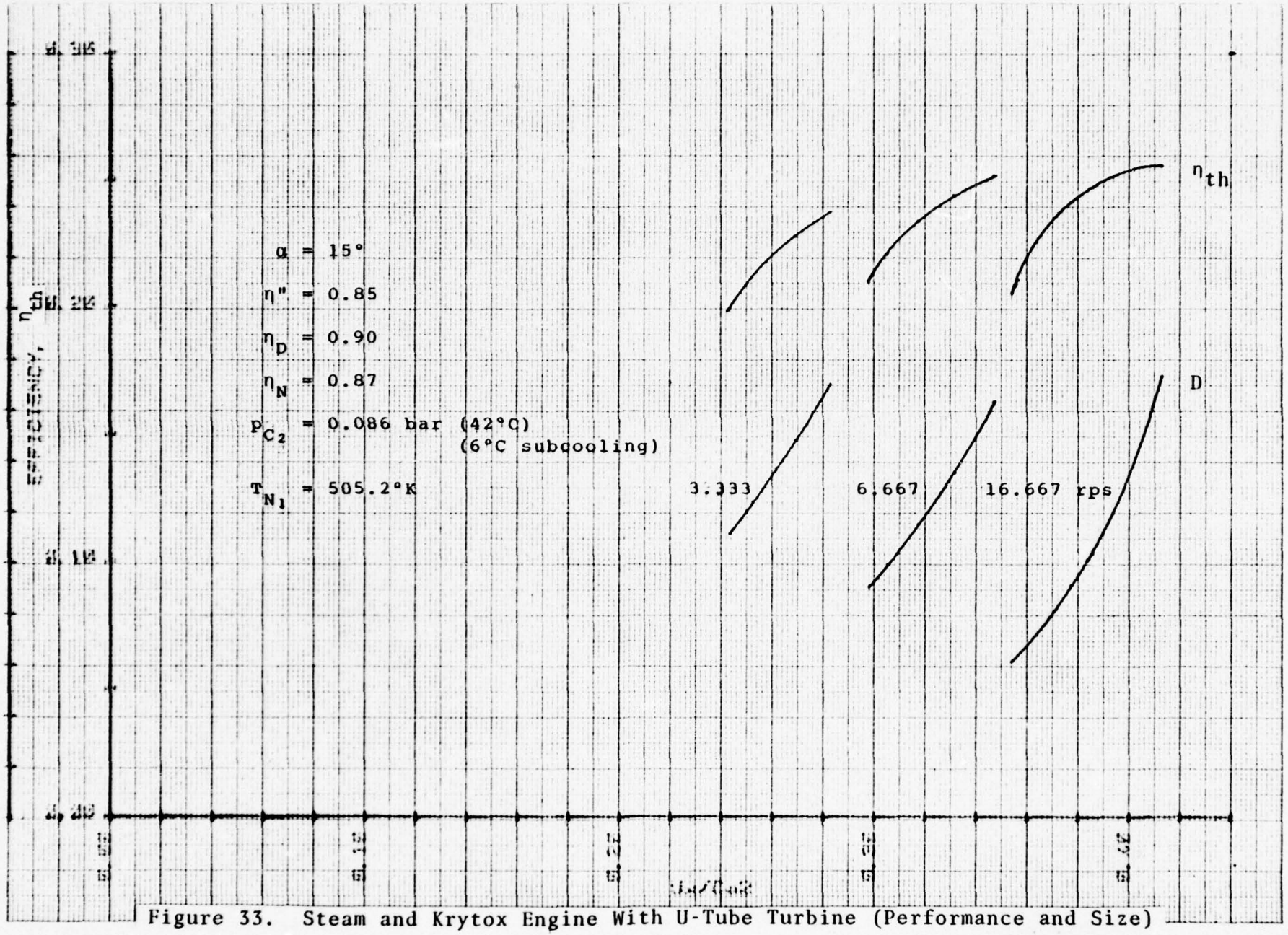

Figure 33. Steam and Krytox Engine With U-Tube Turbine (Performance and Size)

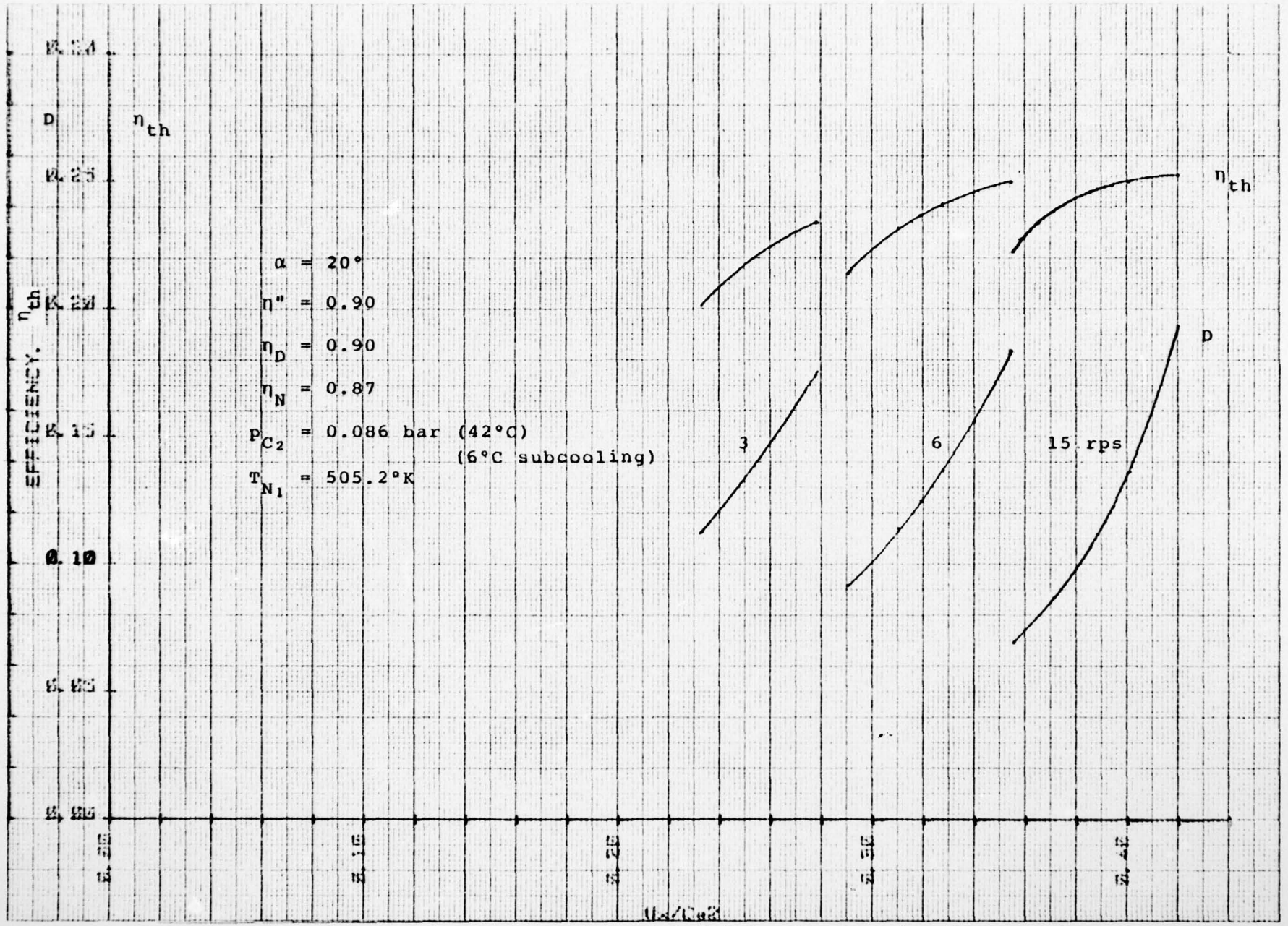

Figure 34. Steam and Krytox Engine With U-Tube Turbine (Performance and Size)

Instead of applying the analysis that was used for the two component case and which was applied to the Krytox-steam system, use is made of the fact that in an adiabatic nozzle expansion without friction losses the entropy must remain constant. Therefore the vdp or kinetic energy increase of a wet steam mixture must become equal to the enthalpy change of the mixture during expansion

$$\frac{c^2}{2} = i_1 - i_2 \quad .$$

In contrast to the oil system, where the masses of steam and of liquid each remain constant during expansion (neglecting possible oil evaporation) the wet steam mixture experiences an increase in steam quality if the expansion takes place from initially small steam qualities (left hand side of vapor dome). On the right hand side of the dome the opposite is true: During expansion of initially saturated steam the moisture content steadily increases, to the detriment of conventional turbines.

Note also that in contrast to the Oil system which uses superheated steam that expands nearly isothermally, the wet-steam system with its saturated steam experiences of necessity a lowering of temperature during expansion according to the vapor pressure-temperature relationship.

The magnitude of the ideal discharge velocity for a *single stage* obtained for $t_1 = 232°C$ and $t_2 = 64°C$ is shown in Figure 35 as a function of initial vapor quality x_o. Figure 36 shows the quality x_2 at the discharge of an isentropic expansion in a single stage. The ideal thermal efficiency is given in Figure 37. (No friction, no subcooling.)

The relations used for obtaining the velocities of Figure 35 are as follows.

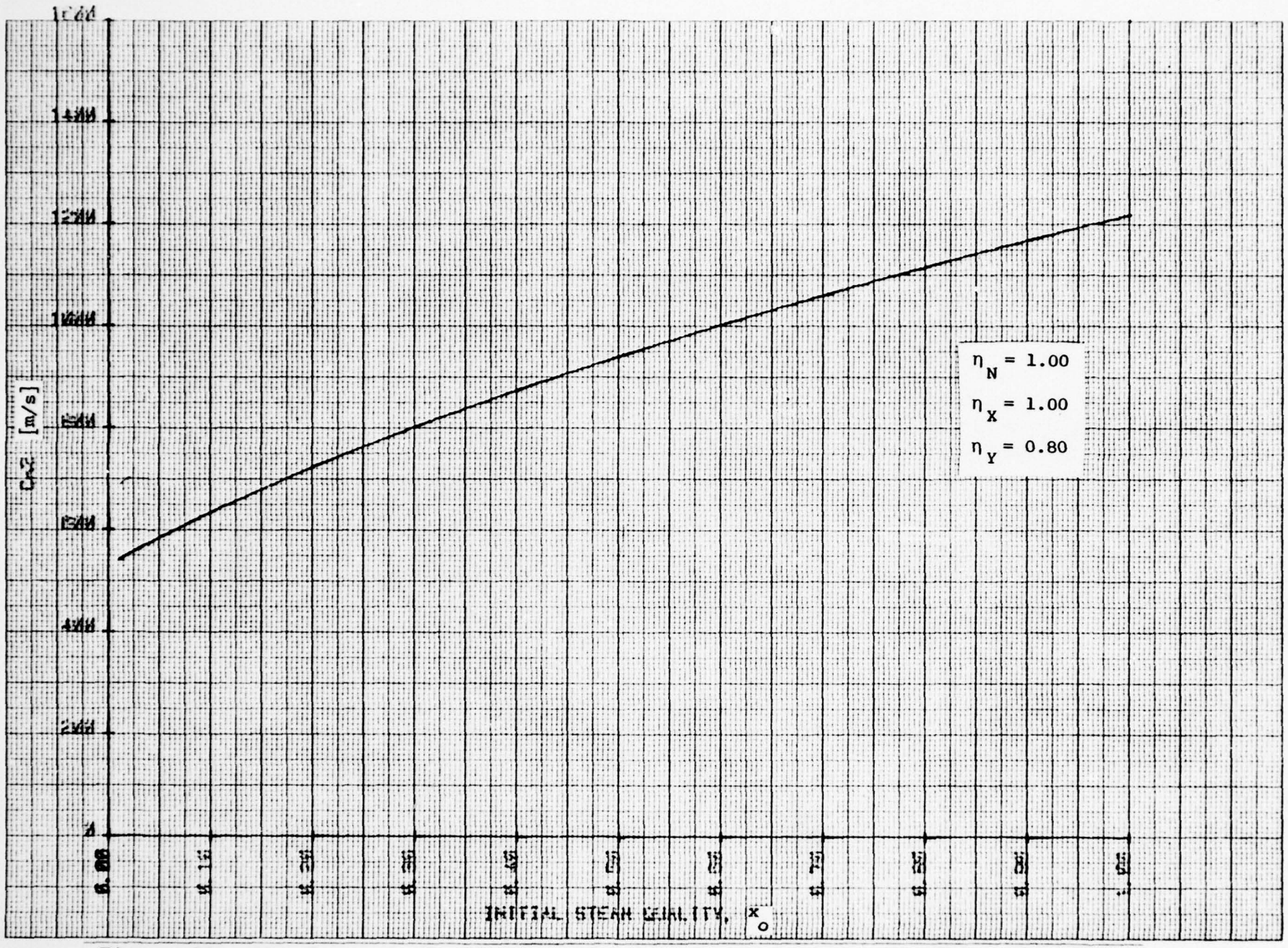

Figure 35. Wet-Steam Cycle Ideal Nozzle Spouting Velocity - One Expansion Stage

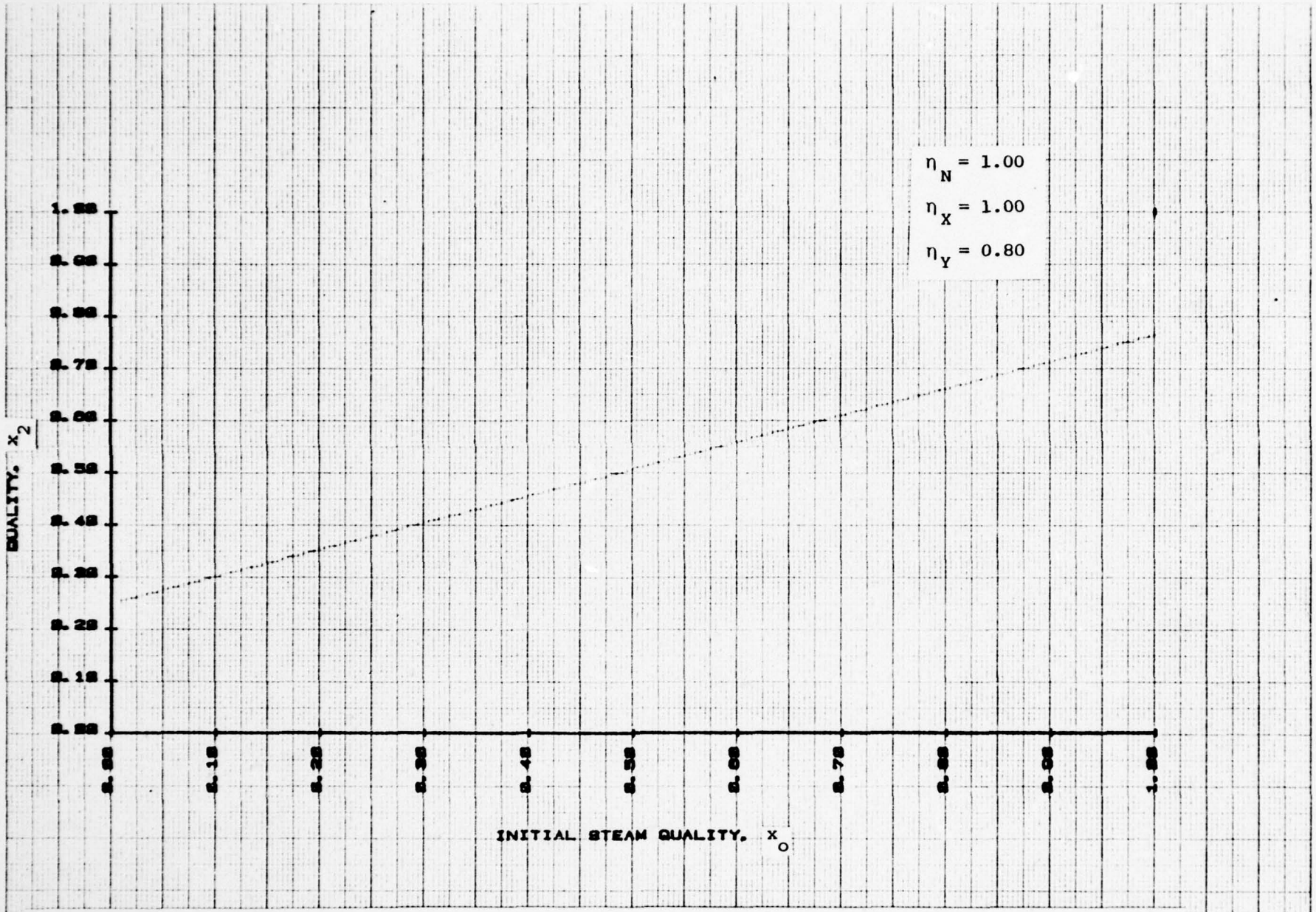

Figure 36. Wet-Steam Cycle Ideal Nozzle Discharge Quality, X2 - One Expansion Stage

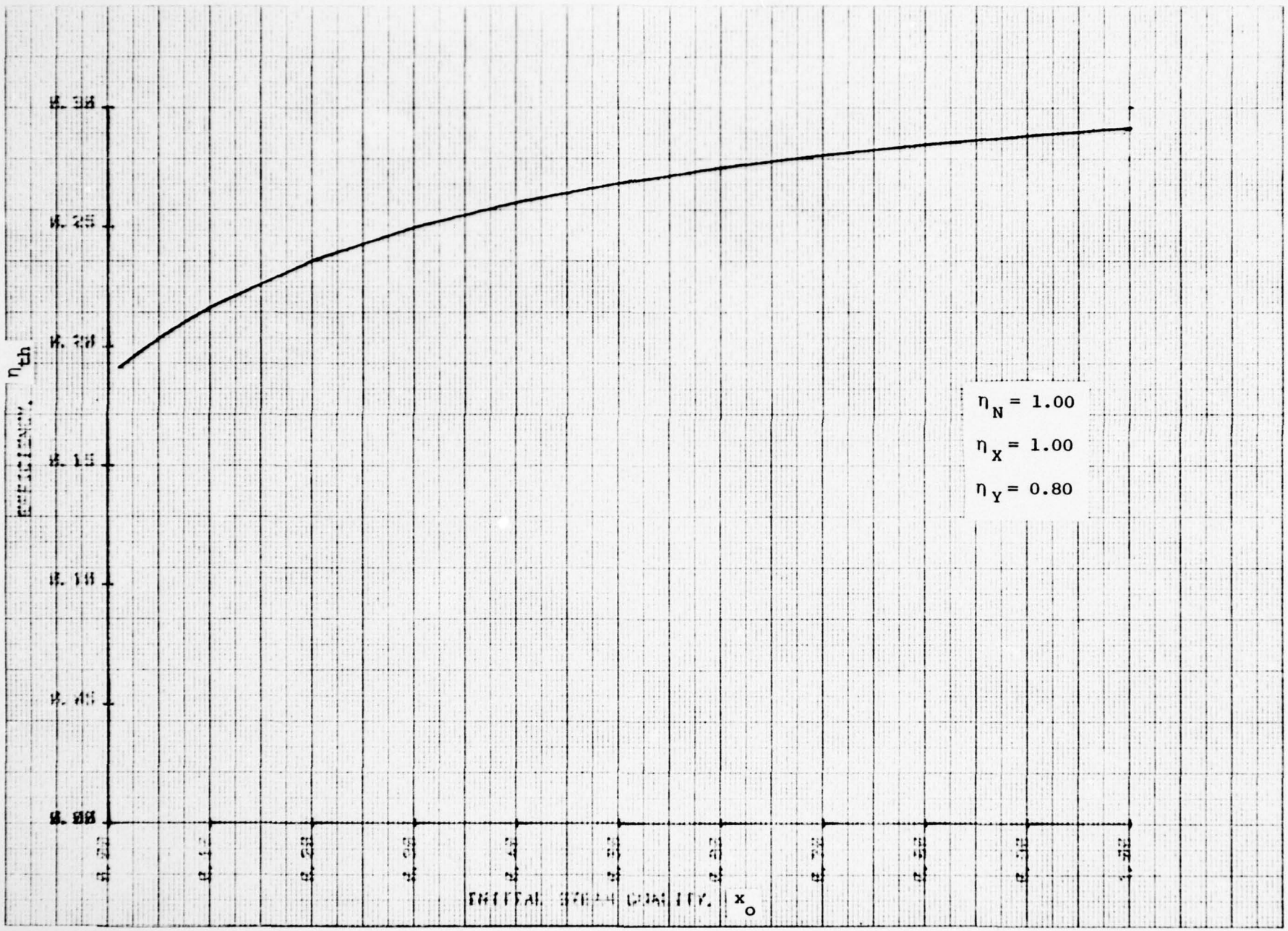

Figure 37. Wet-Steam Cycle Ideal Performance - One Expansion Stage

The initial enthalpy is $i_1 = i' + x_1 r_c$ likewise the initial entropy is $s_1 = s_1' + x_1 r_c/T$. The final quality x_2 follows from $s_1 = s_2' + x_2 r_c/T_2$. The final enthalpy $i_2 = i_2' + x_2 r_c$ is then known and consequently the kinetic energy increase.

For *two stages* with intermediary steam extraction for preheating the feed-water the corresponding results without losses are shown in Figures 38 and 39; for a nozzle efficiency of $\eta_N = 0.85$, a turbine (rotor) efficiency $\eta_x = 0.90$ and 2° subcooling the results are given in Figures 40 and 41.

The mass fraction of steam to be extracted follows from a heat balance and is:

$$y = \frac{1}{1 + \frac{r_c}{\Delta i'}} \quad ,$$

whereas the steam quality of the remaining mixture ready for the second expansion is given by

$$x_{II_1} = \frac{x_{I_2} - y}{1 - y} \quad .$$

Calculated property values* were compared with tabular values and were found to deviate less than about one-fifth of one percent. For preliminary exploration the accuracy was deemed sufficient.

Multistaging with uniform distribution of the temperature drops among the stages was investigated for 5, 8 and 10 stages. The simplification was used that the liquid enthalpy of saturated water would change in proportion to temperature and that therefore the change per stage would be equal.

Results of the analysis are shown in Figures 42 and 43.

*according to Table IX

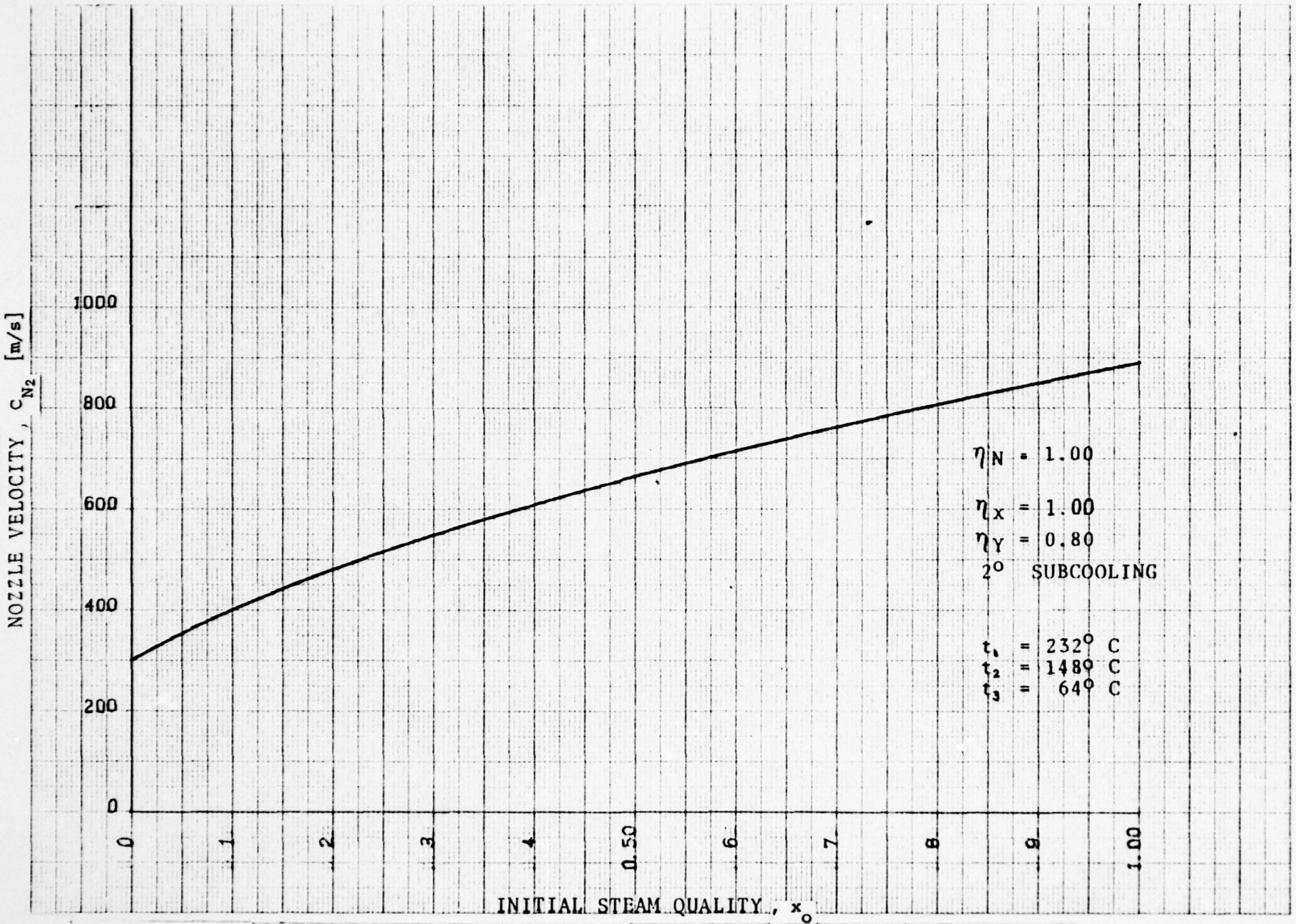

Figure 38. Wet-Steam Cycle Maximum Nozzle Spouting Velocity - Two Expansion Stages, One Extraction Point

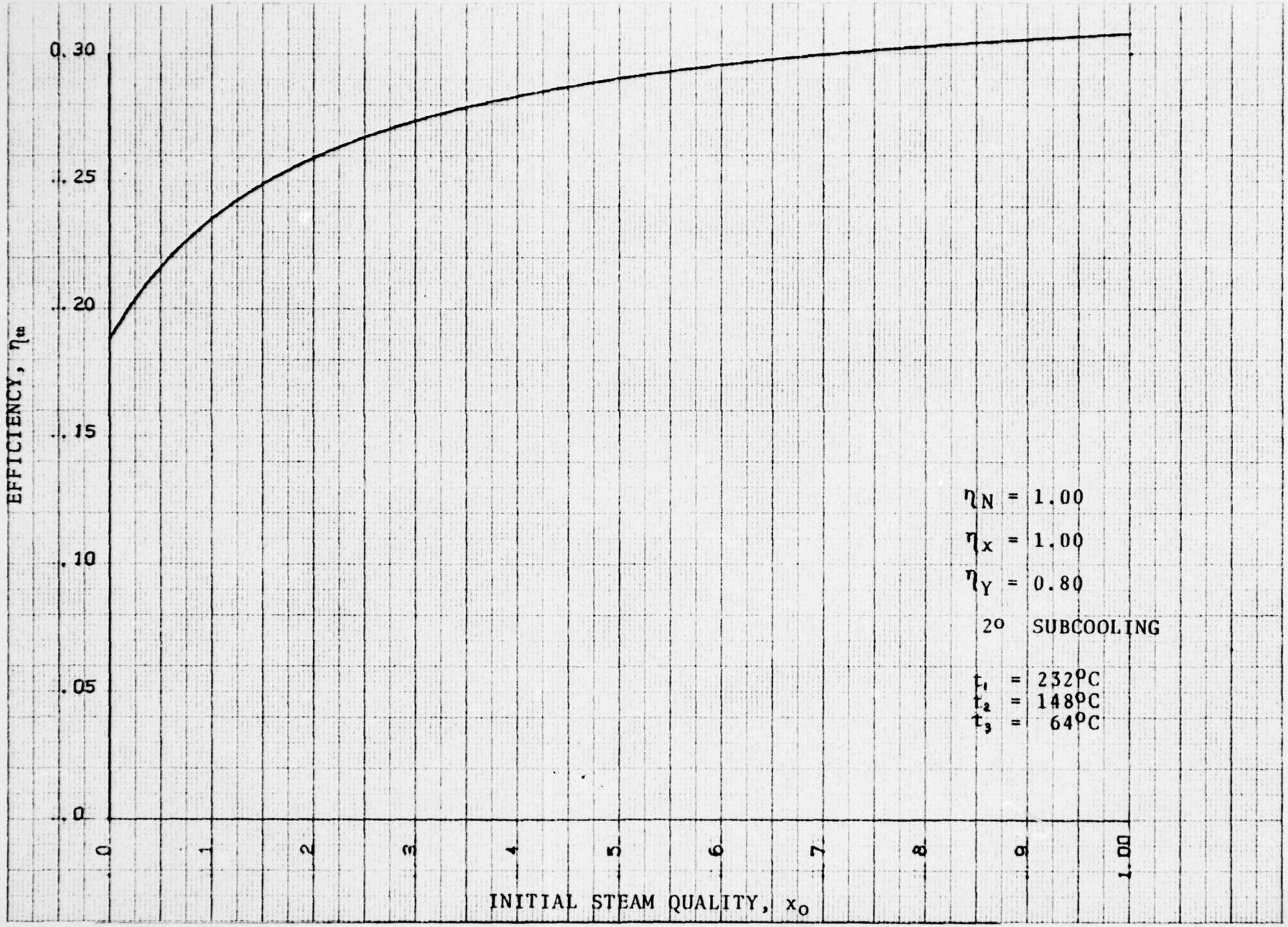

Figure 39. Wet-Steam Cycle Ideal Performance - Two Expansion Stages

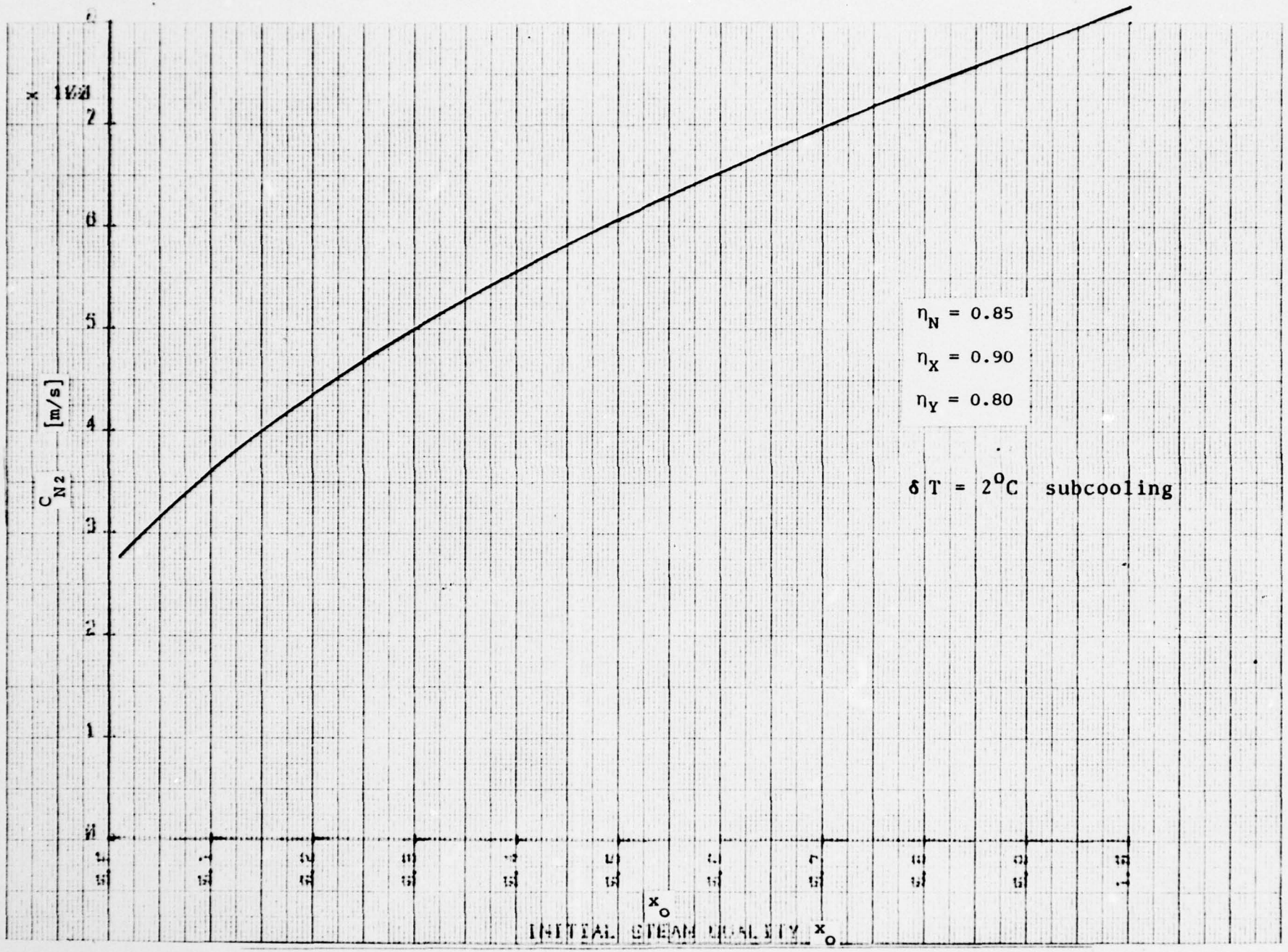

Figure 40. Wet-Steam Cycle Maximum Nozzle Spouting Velocity - Two Expansion Stages, One Extraction Point

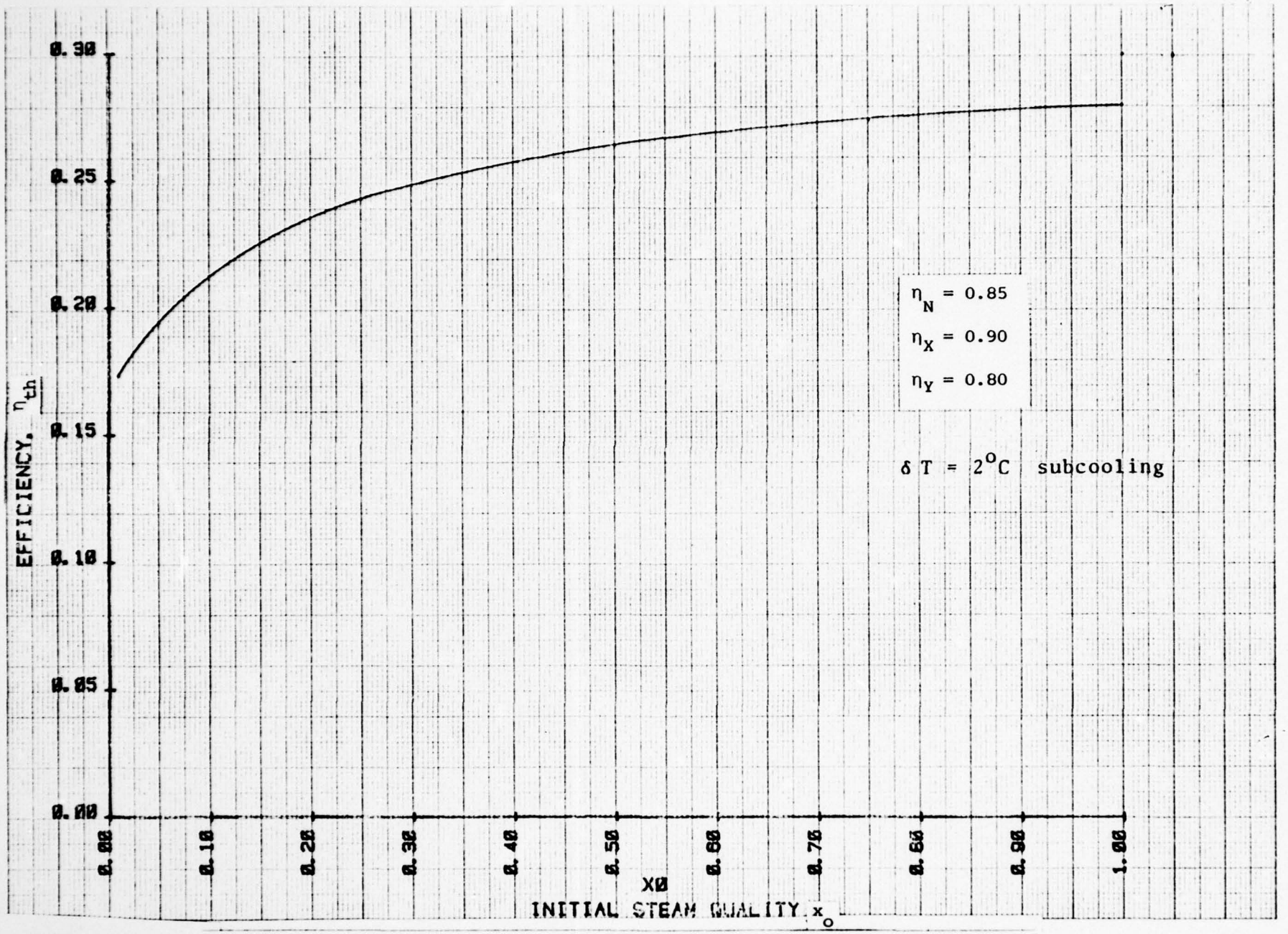

Figure 41. Wet-Steam Cycle Performance - Two Expansion Stages, One Extraction Point

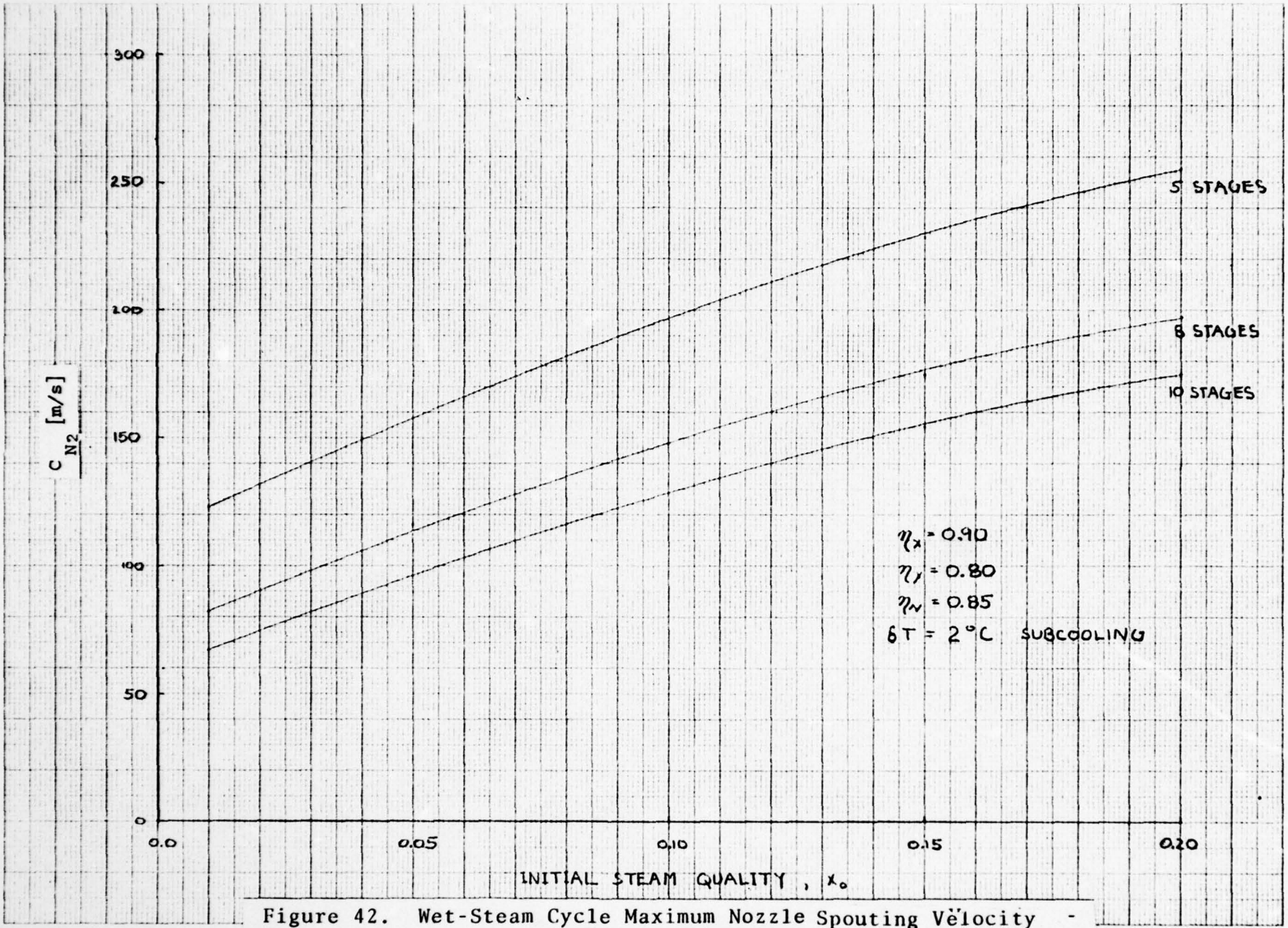

Figure 42. Wet-Steam Cycle Maximum Nozzle Spouting Velocity - Multistage Unit

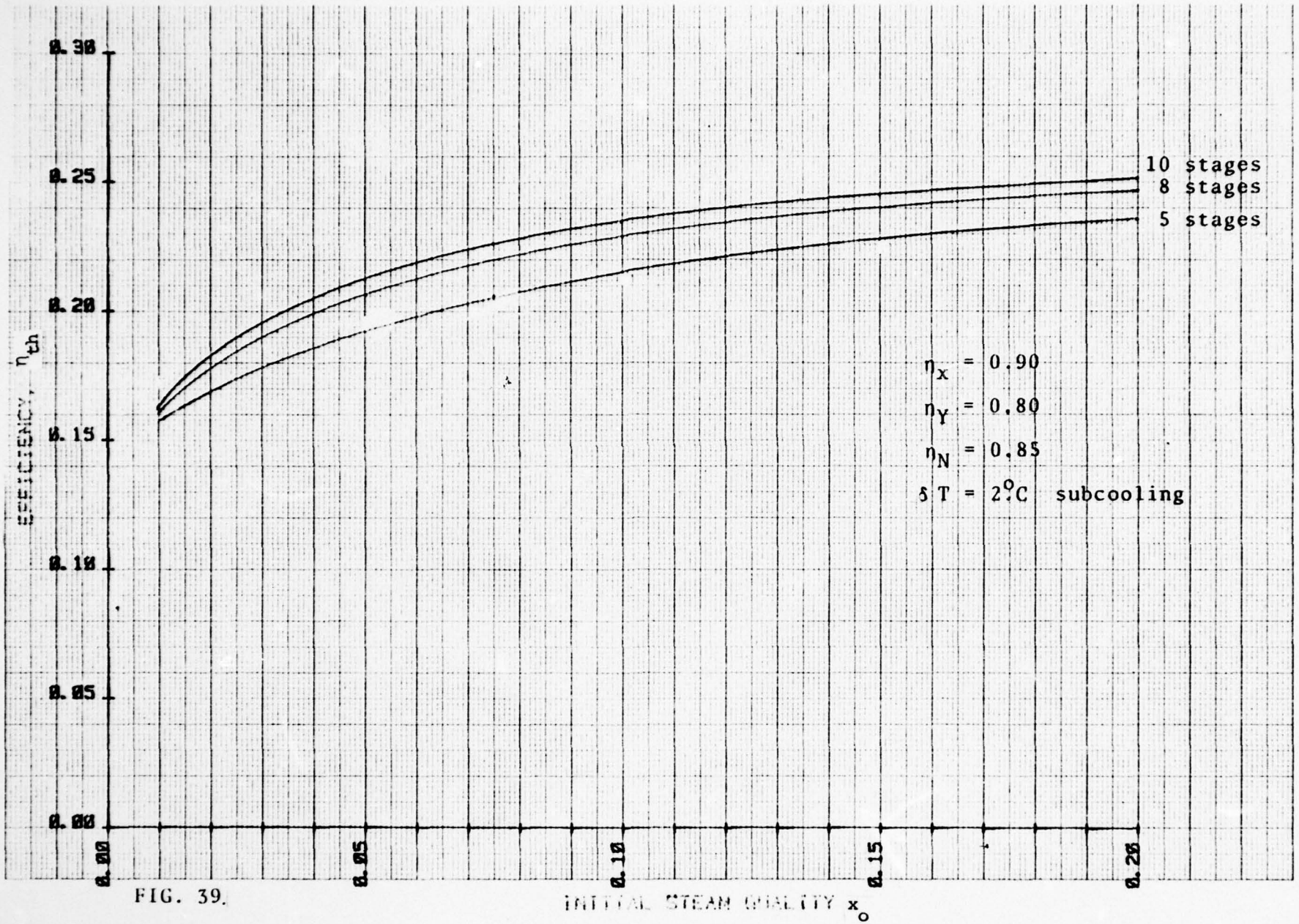

FIG. 39.

Figure 43. Wet-Steam Cycle Performance - Multistage Unit

The transition from one stage to another is simplified in a *radial outflow* (Ljungstrom) *arrangement* with two or three consecutive stages. Since the Euler turbine has an absolute leaving velocity that is always in direction of rotation, an efficient transfer of leaving kinetic energy from a preceding Euler turbine to the succeeding stationary nozzle inlet seems possible without droplet impingement on the nozzle vanes. The flow angle of the emerging droplets may be matched to the inlet of the following stationary nozzle. Such a design involving three high-pressure stages and two low pressure stages has been pursued in more detail. A layout is shown in Figure 44. A listing of conditions is given in Tables X and XI. The installation is shown in Figure 45 and a layout of the heater required in Figure 46.

A more detailed description of the wet-steam turbine and feedwater heater, primary heater and water pump assembly is given in Appendix A.

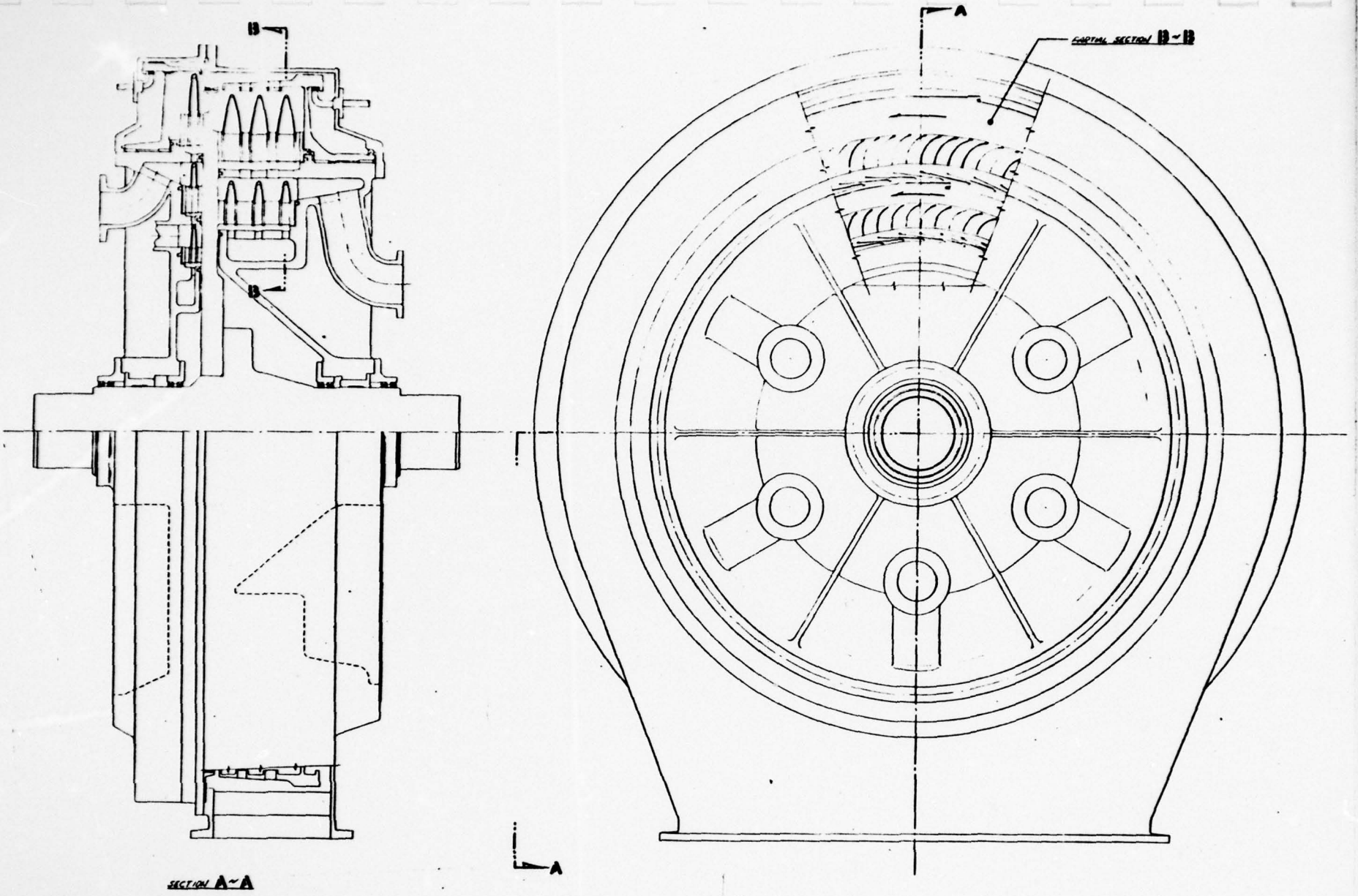

Figure 44.

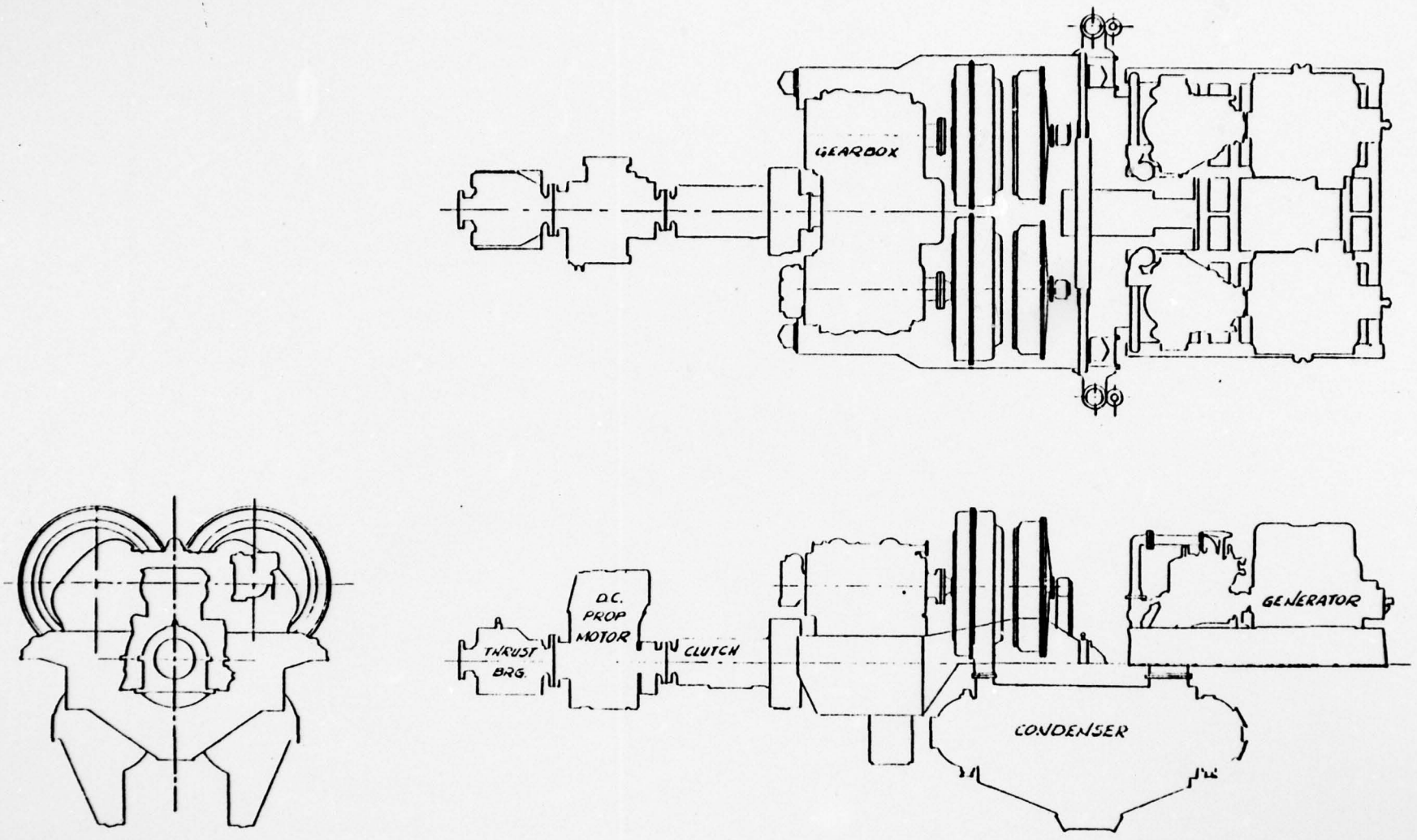

Figure 45. Wet-Steam Marine Propulsion Engine Installation

AD-A061 748 BIPHASE ENERGY SYSTEMS SANTA MONICA CA F/G 13/10.1
DESIGN STUDY OF A TWO-PHASE TURBINE ENGINE FOR SUBMARINE PROPUL--ETC(U)
AUG 78 E RITZI, L HAYS N00014-77-C-0545
UNCLASSIFIED 106-F NL

2 OF 2
ADA
061748

END
DATE
FILMED
2 -79
DDC

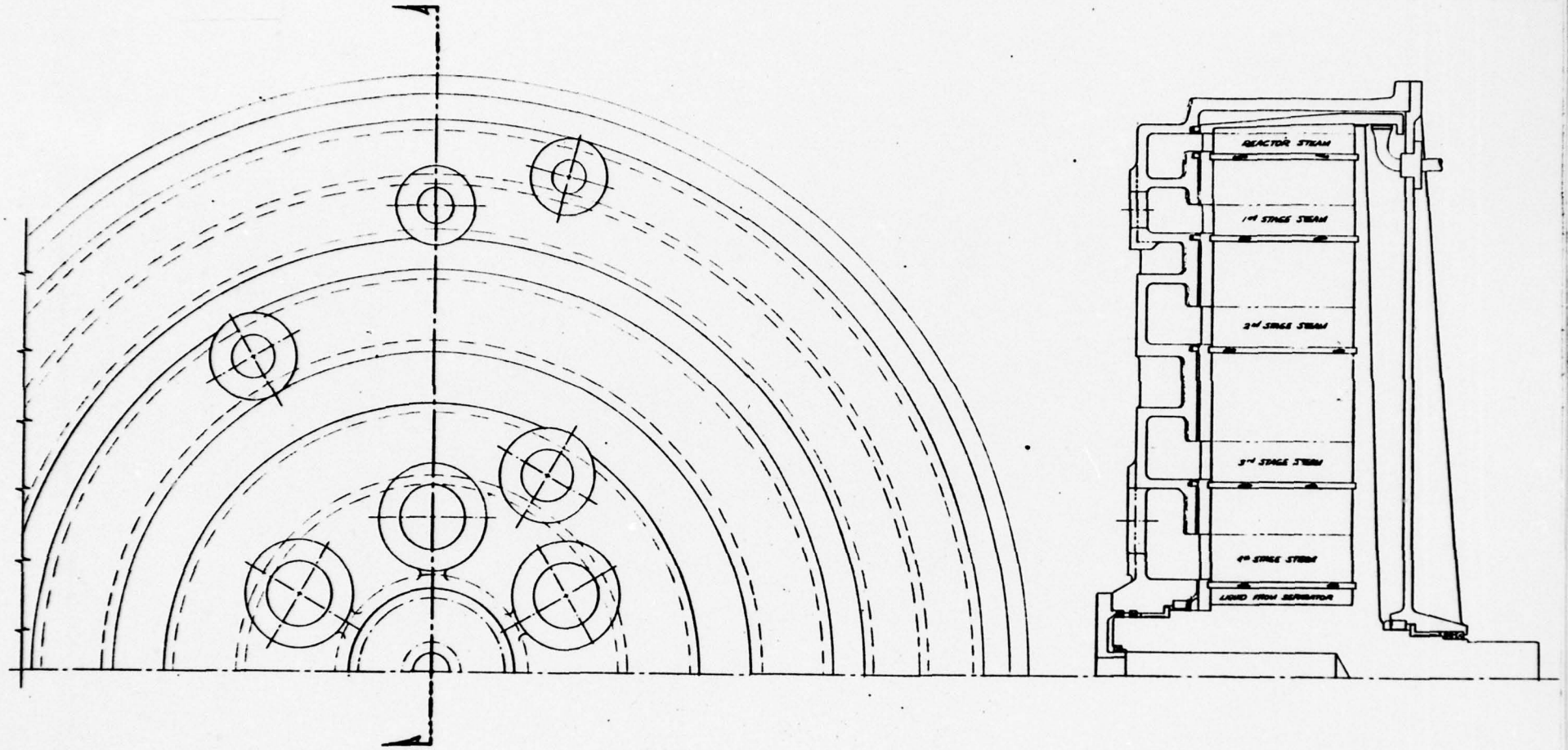
REACTOR STEAM
1st STAGE STEAM
2nd STAGE STEAM
3rd STAGE STEAM
4th STAGE STEAM
LIQUID FROM SEPARATOR

Figure 46.

V. ENGINE CHARACTERISTICS FOR THE STEAM-OIL UNIT

The study has shown how improvements in the thermodynamic cycle over the conventional approach coupled with the application of a liquid turbine leads to attractive engine characteristics.

At the *design point* an overall thermal efficiency of 23.4% is predicted for a set of conditions as shown in Table VII. An improvement in cycle efficiency can be translated into an increased output for given boiler and condenser sizes.

At *part load* (cruise conditions) the performance level achieved at the design point can be sustained as follows. Cruise speeds are about one half of design speeds. The propeller similarity law calls accordingly for $(1/2)^3 = 1/8$ of design power. Extraordinary flexibility is provided by the Biphase engine on account of an additional variable, the liquid to steam mass flow ratio. By its increase the nozzle spouting velocity may be lowered to match the reduced turbine tip speed. It remains to reduce the steamflow by a factor of eight by a reduction of nozzle area. Referring to Figure 29 that objective may be accomplished by blocking the flow to successive sections of the turbine that work in parallel flow for full output. The remainder of the conditions are summarized in the table below.

	Inlet Conditions	Steam Flow	Liquid Flow	Mass-Flow Ratio	Velocities
Design	1	1	1	1	1
Part Load	1	1/8	1/2	4	1/2

The design characteristics are such that the single stage feature allows the design of a turbine of large flow-handling ability with low velocities because of the parallel flow arrangement of the stages and the slowing of the steam by the liquid.

THE DESIGN CONFIGURATION

Figure 29 shows a single stage design. Three such stages are operated in parallel in one unit of 7500 hp. The shaft speed is 16.667 rps = 1000 rpm, at the design point. A speed reduction in the ratio 1000/180 = 5.5 is required. The separator tip speed is 1044 fps = 318 m/s. The mass-flow ratio is r_m = 17.0. The tip-speed ratio is 0.37 which is the ratio of U-tube to separator tip speed. The nozzle exit diameter is 2.03 m. The separator tip speed is high.

A raising of the mass-flow ratio will lower that speed. It should be realized that the set of numbers presented applies to the constraint of no additional pump being used for returning the oil to the nozzle. Part load and starting considerations indicate that a separate boost pump is desirable which would then also allow a higher mass-flow ratio and therefore lower tip speed. An example of a five-stage design with approximately half the stress level was developed for the single component, wet-steam system, Figure 44. It could, however, also be applied to a steam-oil system.

Whether a single stage or a multistage design is used the fact remains that the axial length required for the turbine is much reduced compared to a conventional steam turbine. Thus the parallel arrangement mentioned above becomes feasible. Consequently, a large steam volume can be handled at low steam velocities and low exit losses.

The installation drawing, Figure 31, shows the dual turbines with gears, together with the required heat exchanger sizes. More work is required in that area. Also, an estimation of weights is bound to be subject to wide variations at this stage of the study. Nevertheless the weight of the turbine was estimated to be 22,180 lb. See Table VIII for the weights of the other components.

VI. ENGINE CHARACTERISTICS FOR THE SINGLE COMPONENT WET-STEAM ENGINE

The basic approach toward the Single Component Engine tries to preserve the thermodynamic advantage of the carnotized cycle and the advantages of the liquid turbine on one hand while it tries to overcome the difficulties posed by the second working fluid, the oil, on the other hand.

A design solution was worked out which is closer to the conventional steam turbine insofar as it uses water and steam only as a working fluid and that it resorts to a multistage turbine. The intent was to reduce the number of novel approaches to a minimum so that efforts could be concentrated on the development of the heart of the two-phase engine, the nozzle or, expressed more generally, the mechanism of transferring steam energy effectively to a liquid that is ultimately to be used in a liquid turbine.

While the issue at this point is not the justification of a most promising development plan, it is well to list some of the engine characteristics that have a bearing on those plans.

Concerning the nozzle design, a detailed study shows that an annular radial outflow nozzle that resembles in many ways a conventional full admission turbine nozzle may well provide a solution to the problem of minimizing the transition loss from nozzle to turbine, of allowing effective utilization of the residual kinetic energy of the steam and, finally, of devising turbines with rapid starting characteristics and of high specific output, that is, of maximum power for a minimum diameter and rotative speed. It will, however, be necessary to show good nozzle performance for scaled down

nozzle sizes and for nozzles of low inlet pressures when stage numbers in the order of five are considered.

An initial concentration on a single component engine (water) allows a postponement of the tasks of finding an oil of high thermal stability, low vapor pressure, compatibility with water and acceptable price; also, there would be no need for building a second fluid system with starting accumulators, storage tanks, control and heating devices.

Appendix A contains a more detailed description of the entire wet-steam engine with turbine, pump and heat exchanger. Conventional shell and tube exchangers could be used, especially in the early stages of a development program; however, in order to show potentials toward more compact designs an integrated feed pump/feed water heater was devised, which was shown in Figure 46.

The thermal efficiency of the five-stage wet-steam engine was calculated to 22.8% for a condenser pressure of 0.239 bar = 3.47 psia and an inlet temperature of 232°C (450°F). The turbine diameter for a 7500 hp unit is 2.67 m.; the turbine length is 0.93 m. The engine shaft speed is 2000 rpm when using the Euler turbine as shown. For a U-tube turbine the speed could be cut to about half.

The max. tip speed at the very tip of the turbine rotor (stage three) is $u = \pi \frac{2000}{60} \times 2.521 \text{ m} = 263 \text{ m/s.} = 865 \text{ fps.}$

The highest peripheral velocity at a free surface of a turbine occurs at the third stage; its magnitude is 205 m/s = 674 fps.

The total flow of saturated steam from the reactor is calculated to about 17 kg/s. The feed-water flow at the heater outlet is 74.2 kg/s.

The estimated weight of the 7500 hp turbine is 11,330 kg = 24,930 lbs, of which the rotor and shaft is 4009 kg = 8820 lbs. The volume of a turbine unit is 5.20 m^3 = 183 ft^3.

A first approach to the weight of the feedwater heater (including the last heating stage and all the pump stages) yields 6239 kg = 13,726 lb. The volume of the heater/pump assembly is 2.80 m^3 (99 ft^3). Refinements in design should result in considerable weight savings on both turbine and heater. The weights of the condenser and other components could be taken over from those given for the steam-oil unit, Table VIII. A tabulation of weights and volumes for the wet-steam system is given in Table XIII.

VII. CONCLUSIONS AND RECOMMENDATIONS

The design analysis of Biphase turbine engines for underwater propulsion identified several significant advantages over the existing steam turbine engine.

1. Thermal Efficiencies of the order of 22 to 24% were predicted at full power and 21% at cruise conditions.
2. The main reduction gear can be eliminated with a large (90,000 lb) weight savings (4a) and reduction in noise.
3. Substantial reductions in volume and weight are possible.

For the steam-oil unit with gears the total estimated weight including the 400 kW ship service turbine/generator set was 126 600 kg (278 000 lbs) and the volume 113 m^3 (3970 ft^3). For a breakdown see Table VIII. The estimated weight of the wet-steam engine was 101 800 kg (243 750 lb) and the box volume 86.4 m^3 (3046 ft^3), including the 4000 kW ship service turbine/generator set. For a breakdown see Table XIII.

These numbers are directly comparable with those for an existing engine as presented in Table III of the "Ground Rules" Reference (4a). Also, the installation drawings of Figure 31 for the oil-steam engine, and Figure 45 for the wet-steam engine are drawn to the same scale as Enclosure (1) of Ref. (4a).

4. An advanced Biphase engine which utilized steam and water had the same performance as the steam-oil unit.

In contrast to conventional engines that require removal of condensed water in the turbine, the Biphase engine utilizes the liquid as its dominant working fluid in the turbine. That feature accounts for the few expansion stages in a compact design and the excellent part load performance due to a matching of the nozzle

discharge velocity to the wheel tip speed by means of a variable liquid to vapor ratio.

A preliminary analysis of the steady state runaway speed of the reaction-type liquid turbine (Euler Turbine) indicated values that are only a fraction of that of conventional steam turbines because of the self-adjusting rotating liquid ring level.

5. Direct contact heat exchangers were designed for both the steam-water and steam-oil engines which offer substantial weight and volume savings over existing technology.

An overall, time-average heat transfer coefficient of 51.2 kW/m^2 C = 9014 Btu/h ft^2 F was predicted for the transfer of heat from condensing steam to liquid droplets of 100 μm (micron) diameter. Brown (Ref. 23) predicted values of 65.9 kW/m^2C = 11600 Btu/h ft^2F for the same particle size. He also demonstrated such performance. While typical heat transfer coefficients inside and outside of conventional condenser tubes are about 2000 Btu/h ft^2F, the overall coefficient U is conservatively taken as 500 Btu/h ft^2F (E. Quandt, NSRDC). While Brown (Ref. 23) demonstrated with a stationary spray-type heater an effective heat transfer area to volume ratio of $A_h/V_c = 6/\phi d \cong 8.0$ m^2/m^3, a rotating unit promises to allow values of at least 273 m^2/m^3 = 83.2 ft^2/ft^3 because of the better controllable droplet paths. Tube bundles with tube pitches of 1.5 and 1.37 diameters d in two directions have areas per unit volume of $A_h/V_c = 1.529/d$. For a tube diameter of 1/2" A_h/V_c = 120.4 m^{-1}, for 3/4" A_h/V_c = 80.2 m^{-1}.

Recommended Development Program

Based on these potential advantages an immediate development program is recommended. Logical steps in the development program would be:

1. Demonstration of 350 HP laboratory prototype engine.
2. Development of 2500 HP engine module.
3. Development of a 15,000 HP land based prototype.
4. Development of a ship rated 15,000 HP engine.

Parallel to this program an extensive research and supporting technology effort should be carried out. Some important Research topics which were identified during the design study are:

1. Two-phase nozzle performance for:
   a. high pressure ratio (over 200)
   b. high pressure gradient
   c. low inlet pressure (a few bars)
   d. deviations from axisymmetric geometries
2. Atomization for two-phase nozzles
3. Characterization of two-phase nozzle flow
4. Loss mechanisms in moving surface separator geometries
5. Performance and design of very high speed inlets ($\sim$250 m/s)
6. Frictional and turning losses in curved ducts with a free surface and/or low blockage
7. Wake closure and wave drag for high Froude and high Reynolds numbers ($Re > 10^5$)
8. Diffuser performance for very high Reynolds numbers ($>10^6$) for both straight and curved geometries

9. Heat transfer in convective and condensing flows with the presence of a second component

10. Heat transfer and pressure drop in one component and two-component direct contact heat exchangers

The field of high energy two-phase flow is a recent one essentially, beginning with the liquid metal MHD work of Elliott[1]. A substantial body of theory and experimental data have been developed for many aspects of this discipline. The very positive results of this design study indicate the need for a vigorous expansion of research and supporting technology. Achievement of this objective will result in the most effective development program for a Biphase turbine for underwater propulsion.

NOMENCLATURE AND TABLES

NOMENCLATURE

Arabic

A_m	Meridional flow area
b_N	Nozzle width
c	Absolute velocity
c_d	Drag coefficient for U-tube turbine (roto-pitot)
c_{pb}	Specific heat
C_d	Drag coefficient for liquid droplets
D	Droplet diameter
D_{N_2}	Diameter at nozzle discharge (mean)
D_s	Separator diameter
Δh_a	Steam work per unit mass = $\int_{p_1}^{p_2} v\,dp$
Δh_b	Liquid work per unit mass = $v_b \Delta p$
i	Enthalpy
k	Ratio of specific heats
k	Thermal conductivity
L	Mixer length
m	Molecular mass (weight)
$\dot{m}$	Mass flow

NOMENCLATURE

$\dot{m}_T$	Total mass flow
n	Polytropic exponent
p	Static pressure
p_{C_2}	Condenser pressure
p_{N_1}	Nozzle inlet pressure
p_{N_2}	Nozzle discharge pressure
p_v	Vapor pressure (a function of saturation temperature)
$\dot{P}$	Power
q	Heat flux per unit mass
r	Mass flow ratio, liquid to steam
r*	Nozzle throat radius
r_b	Latent heat of evaporation
r_N	Minimum distance between nozzle axis and axis of rotation
r_p	p_x/p_o pressure ratio
R	Gas constant
t_{C_2}	Minimum temperature of cycle (°C)
T	Absolute temperature (°K)
T_{N_1}	Nozzle inlet temperature
T_{N_2}	Nozzle discharge temperature

NOMENCLATURE

T_{C_2}	Minimum temperature of cycle (°K)
u	Wheel tip speed
v	Specific volume
v_b	Specific volume of liquid
$\dot{V}$	Volume flow
w	Relative velocity
x	Axial nozzle coordinate
x_{N_2}	Mass ratio, oil vapor to steam

Greek

α	Resulting angle of nozzle axis against the peripheral direction at the separator drum
ε	Recuperator effectiveness
η	Absolute viscosity
η''	Efficiency of relative flow in the turbine
η_D	Diffuser efficiency for liquid
η_N	Nozzle efficiency
η_S	Efficiency of transition from nozzle to separator or turbine
η_{th}	Thermal efficiency
η_X	Turbine efficiency (Rotor alone)

NOMENCLATURE

(Page 4 of 4)

η_{XB}	Efficiency of an after-expansion (boost) stage
η_Y	Water pump efficiency
Θ_o	Initial temperature difference across the recuperator

Subscripts

a	Steam
b	Liquid
B	Boost stage
C	Condenser
D	Diffuser
H	Heater (boiler)
m	Mixture
M	Mixer
N	Nozzle
S	Separator
X	Turbine
Y	Water pump
0	Initial stagnation conditions
1	Inlet
2	Outlet

Table I. Impulse Turbine Efficiency (Page 1 of 7)

A. ADIABATIC EXPANSION

If some reaction is employed in the turbine, and the degree of reaction is defined as

$$r^* = \frac{\Delta i_R}{\Delta i_{1s}}$$

$$= \frac{i_{x_1}^* - i_{x_2}^*}{i_{N_1} - i_{x_2}^*}$$

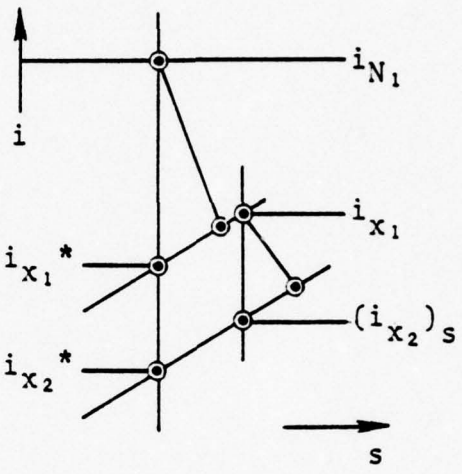

it would then not be possible to factor out the nozzle efficiency η_N in the overall turbine efficiency. See Vavra, Chpt 15.

In order to make the factoring of η_N possible, the reaction be defined as

$$r_R = \frac{i_{x_1} - i_{x_{2s}}}{\frac{c_1^2}{2}} \tag{1}$$

The enthalpy change available for the nozzle follows as

$$i_{N_1} - i_{x_1}^* = (i_{N_1} - i_{x_2}^*) - (i_{x_1}^* - i_{x_2}^*)$$

$$= \frac{c_0^2}{2} - (i_{x_1}^* - i_{x_2}^*) \tag{2}$$

Defining a reheat factor as

$$f = \frac{(i_{x_2})_s}{i_{x_2}^*} - 1 \tag{3}$$

we get

$$i_{x_1} - i_{x_{2s}} = (1 + f)(i_{x_1}^* - i_{x_2}^*) \tag{4}$$

Substitute (4) into (2):

$$i_{N_1} - i_{x_1}^* = \frac{c_0^2}{2} - \frac{(i_{x_1} - i_{x_{2s}})}{(1 + f)}$$

and with (1):

$$= \frac{c_0^2}{2} - \frac{r_R}{(1 + f)} \frac{c_1^2}{2} \tag{5}$$

From the definition of nozzle efficiency

$$\eta_N = \frac{\frac{c_1^2}{2}}{i_{N_1} - i_{x_1}^*} \tag{6}$$

(5) + (6)

$$\frac{1}{\eta_N} \frac{c_1^2}{2} = \frac{c_0^2}{2} - \frac{r_R}{(1 + f)} \frac{c_1^2}{2}$$

$\therefore$

$$\frac{c_0^2}{2} = \left[\frac{1}{\eta_N} + \frac{r_R}{(1 + f)}\right] \frac{c_1^2}{2} \tag{7}$$

B. POLYTROPIC EXPANSION

For the conditions encountered in a biphase nozzle with <u>heat liberated from the liquid droplets</u> the frictionless expansion is polytropic with exponent n.

In place of the isentropic enthalpy changes we have the polytropic heads $\Delta h = \int v dp$: $\Delta h = \Delta h_N + \Delta h_x$

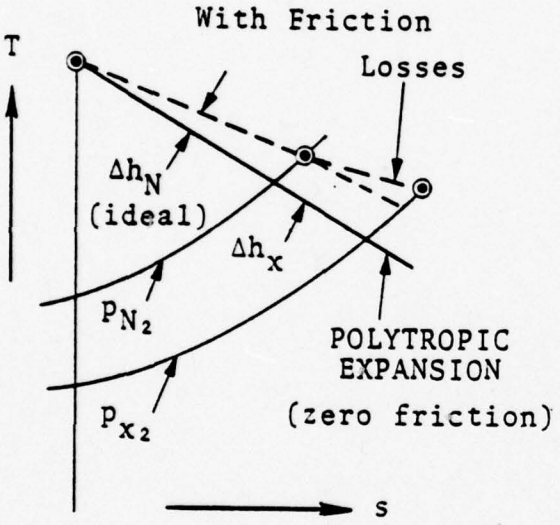

$$\Delta h = \int_{p_1}^{p_2} v dp$$

$$r_R = \frac{\Delta h_x}{\frac{c_1^2}{2}} \qquad (1')$$

$$\Delta h_N = \frac{c_0^2}{2} - \Delta h_x \qquad (2')$$

$$\Delta h_N = \frac{c_0^2}{2} - r_R \frac{c_1^2}{2} \qquad (5')$$

$$\eta_N = \frac{\frac{c_1^2}{2}}{\Delta h_N} \qquad (6')$$

$$\boxed{\frac{c_0^2}{2} = \left(\frac{1}{\eta_N} + r_R\right) \frac{c_1^2}{2}} \qquad (7')$$

when neglecting reheat

C. The theoretically possible *relative* E_{kin} *at the bucket discharge* is

$$\frac{w_2{}^2 th}{2} = \Delta h_x + \phi_R \frac{w_1{}^2}{2} - \frac{u_1{}^2}{2} + \frac{u_2{}^2}{2} \qquad (8)$$

with ϕ_R = carryover coefficient; see Vavra, p. 424.

From (1')

$$\Delta h_x = r_R \frac{c_1{}^2}{2}$$

If we define

$$w_2 = \psi \, w_{2th} \quad . \qquad (9)$$

(8) + (9) + (1'):

$$\frac{w_2{}^2}{2} = \psi^2 \left[r_R \frac{c_1{}^2}{2} + \phi_R \frac{w_1{}^2}{2} - \frac{u_1{}^2}{2} + \frac{u_2{}^2}{2} \right] \qquad (10)$$

From the inlet triangle geometry:

$$\left(\frac{w_1}{c_1}\right)^2 = 1 + \left(\frac{u_1}{c_1}\right)^2 - 2\left(\frac{u_1}{c_1}\right) \cos \alpha_1 \qquad (11)$$

Using $u_2/u_1 = r_2/r_1$ and (10) + (11):

$$\left(\frac{w_2}{c_1}\right)^2 = \psi^2 \left\{ r_R + \phi_R \left[1 + \left(\frac{u_1}{c_1}\right)^2 - 2\left(\frac{u_1}{c_1}\right) \cos \alpha_1 \right] - \left(\frac{u_1}{c_1}\right)^2 \left[1 - \frac{r_2}{r_1} \right)^2 \right] \right\}$$

$$= \psi^2 \left\{ r_R + \phi_R + \left(\frac{u_1}{c_1}\right)^2 \left[\phi_R + \left(\frac{r_2}{r_1}\right)^2 - 1 \right] - 2\phi_R \cos \alpha_1 \left(\frac{u_1}{c_1}\right) \right\} \qquad (12)$$

Now try to arrive at the peripheral component w_{u_2}

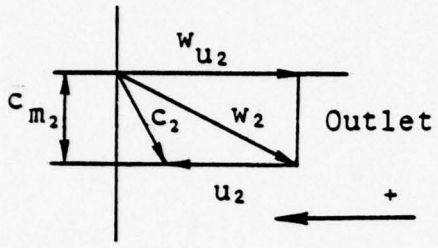

$$\frac{w_{u_2}}{c_1} = -\sqrt{\left(\frac{w}{c_1}\right)^2 - \left(\frac{c_{m_2}}{c_1}\right)^2} \qquad (13)$$

$$\frac{c_{m_2}}{c_1} = \frac{c_{m_1}}{c_1}\left(\frac{c_{m_2}}{c_{m_1}}\right) = \sin\alpha_1\left(\frac{c_{m_2}}{c_{m_1}}\right) \qquad (14)$$

where (c_{m_2}/c_{m_1}) is an input parameter, derived from continuity (blade-height and density ratio).

The peripheral component of the absolute velocity, c_{m_2}, at the outlet follows.

Since w_{u_2} is directed counter to u_2, its sign is taken as negative in (13).

$$c_{u_2} = w_{u_2} + u_2 \qquad \text{(usually negative value)} \qquad (15)$$

$$\frac{c_{u_2}}{c_1} = \frac{w_{u_2}}{c_1} + \frac{r_2}{r_1}\frac{u_1}{c_1} \qquad (15')$$

Now substitute Eq (14) into (13) and in turn into (15'):

$$\frac{c_{u_2}}{c_1} = -\sqrt{\left(\frac{w_2}{c_1}\right)^2 - \sin^2\alpha_1\left(\frac{c_{m_2}}{c_{m_1}}\right)^2} + \frac{r_2}{r_1}\frac{u_1}{c_1} \qquad (16)$$

Substitute Eq (12) into (16)

$$\boxed{\frac{c_{u_2}}{c_1} = \frac{r_2}{r_1}\frac{u_1}{c_1} - \sqrt{\bar{\psi}^2\left\{r_R + \phi_R + \left(\frac{u_1}{c_1}\right)^2\left[\phi_R + \left(\frac{r_2}{r_1}\right)^2 - 1\right] - 2\phi_R\cos\alpha_1\left(\frac{u_1}{c_1}\right)\right\} - \left(\frac{c_{m_2}}{c_{m_1}}\right)^2\sin^2\alpha_1}} \qquad (17)$$

D. An efficiency definition which considers the leaving absolute kinetic energy as lost is

Overall Turbine Efficiency (Static) η_{xs}

$$\eta_{xs} = \frac{2(c_{u_1} u_1 - c_{u_2} u_2)}{c_o^2} \tag{18}$$

E. With recovery of leaving E_{kin}: $\frac{c_E^2}{2} = \phi_E \frac{c_2^2}{2}$

$$\eta_{xT} = \frac{c_{u_1} u_1 - c_{u_2} u_2}{\frac{c_o^2}{2} - \phi_E \frac{c_2^2}{2}} = \frac{\eta_{xs}}{1 - \phi_E \left(\frac{c_2}{c_o}\right)^2} \tag{19}$$

Modifying (17) yields with (7')

$$\eta_{xs} = \frac{2(c_{u_1} u_1 - c_{u_2} u_2)}{\left(\frac{1}{\eta_N} + r\right) c_1^2} = \frac{2}{\left(\frac{1}{\eta_N} + r_R\right)} \left[\frac{c_{u_1}}{c_1} \frac{u_1}{c_1} - \frac{c_{u_2}}{c_1} \frac{u_1}{c_1} \frac{r_2}{r_1}\right]$$

$$\eta_{xs} = \frac{2}{\left(\frac{1}{\eta_N} + r_R\right)} \frac{u_1}{c_1} \left[\cos \alpha_1 - \frac{r_2}{r_1} \frac{c_{u_2}}{c_1}\right] \tag{20}$$

Substitution of Eq (17) into (20) gives an expression for η_{xs} as a function of

$$\eta_{xs} = f\left\{\frac{u_1}{c_1}, \alpha_1, \frac{\bar{c}_{m_2}}{\bar{c}_{m_1}}, \frac{r_2}{r_1}, r_R; \eta_N, \Psi, \phi_R\right\} \tag{20}$$

Herein u_1/c_1 and the degree of reaction r_R are operating parameters; α_1, (r_2/r_1), and for incompressible flow, c_{m_2}/c_{m_1}, are geometric constants. η_N, ψ, ϕ_R express losses (other than the leaving kinetic energy loss) in the nozzle, buckets and in transition between nozzle and buckets.

In the expression (19) for the *total efficiency* the relative leaving kinetic energy is

$$\left(\frac{c_2}{c_o}\right)^2 = \left(\frac{c_2}{c_1}\right)^2\left(\frac{c_1}{c_o}\right)^2 = \left[\left(\frac{c_{u_2}}{c_1}\right)^2 + \left(\frac{c_{m_2}}{c_1}\right)^2\right]\left(\frac{c_1}{c_o}\right)^2 \quad . \tag{21}$$

With Eq (7') and Eq (14):

$$\left(\frac{c_2}{c_o}\right)^2 = \left[\left(\frac{c_{u_2}}{c_1}\right)^2 + \left(\frac{c_{m_2}}{c_{m^1}}\right)^2 \sin^2 \alpha_1\right] \frac{1}{\left(\frac{1}{\eta_N} + r_R\right)} \tag{22}$$

$\frac{c_{u_2}}{c_1}$ is given by Eq (17) .

Table II. Impulse Turbine System Equations (Page 1 of 4)

1. NOZZLE DISCHARGE TEMPERATURE

$$\frac{n}{n-1} = \frac{k}{k-1} + \frac{rc_b}{R_a}$$

$$= \frac{k}{k-1}\left[1 + \frac{rc_b}{(k/k-1)R_a}\right]$$

$$\tau_N = \pi_N^{(n-1)/n}$$

$$T_{N_2} = T_{N_1}/\tau_N$$

2. KINETIC ENERGY INCREASE IN STEAM

$$\Delta h_a = \int_{p_1}^{p_2} v\,dp = \frac{n}{n-1} RT_1\left[1 - \left(\frac{p_2}{p_1}\right)^{(n-1)/n}\right]$$

3. HEAT SUPPLIED BY LIQUID DURING NOZZLE EXPANSION

$$q_{a_N} = -\left[\frac{k/(k-1)}{n/(n-1)} - 1\right]\Delta h_a$$

4. HEAT REJECTION

a. HEAT REJECTION OF STEAM

1. With Recuperator

$$\Theta_o = T_{N_2} - T_{C_2}$$

$$\Delta T_{max} = (\Delta T)_{steam} = (\varepsilon)(\Theta_o)$$

$$T_{C_1} = T_{N_2} - \Delta T_{max}$$

$$i_{C_1} \cong 2T_{C_1} + 1929 \quad (kJ/kg)$$

$$q_a = i_{C_1} - i_{C_2}$$

Table II. Impulse Turbine System Equations (Page 2 of 4)

4. a. HEAT REJECTION OF STEAM

2. Without Recuperator

$$i_{N_2} \cong 2T_{N_2} + 1929 \quad \text{(kJ/kg)}$$

$$i' \cong 4.19\, t_{C_2} = i_{C_2} \quad \text{Enthalpy of saturated liquid (kJ/kg)}$$

$$\frac{q_a}{1+r} = \frac{i_{N_2} - i_{C_2}}{1+r}$$

4. b. HEAT REJECTION DUE TO CONDENSATION OF OIL VAPOR

$$p_v = 10.^{(A' - B'/T_{N_2})} \quad \text{(Pascal)}$$

$$x_{N_2} = \frac{1}{\left(\frac{p_{N_2}}{(p_{v_b})_{N_2}} - 1\right)} \frac{m_b}{m_a}$$

$$x_{C_2} = \frac{1}{\left(\frac{p_{N_2}}{(p_{v_b})_{C_2}} - 1\right)} \frac{m_b}{m_a}$$

$$\frac{q_b}{1+r} = \frac{1}{1+r} (x_{N_2} - x_{C_2})\, r_b$$

4. c. TOTAL HEAT REJECTION

$$\frac{q}{1+r} = \frac{q_a}{1+r} + \frac{q_b}{1+r}$$

5. KINETIC ENERGY INCREASE OF LIQUID

$$\Delta h_b = v_b(p_{N_1} - p_{N_2})$$

Table II. Impulse Turbine System Equations (Page 3 of 4)

6. KINETIC ENERGY INCREASE PER UNIT TOTAL MASS

$$\Delta h_m = \frac{1}{1+r} \Delta h_a + \frac{r}{1+r} \Delta h_b$$

7. KINETIC ENERGY AVAILABLE AT TURBINE INLET

$$\frac{c_{x_1}^2}{2} = \frac{c_{N_2}^2}{2} = \Delta h_m \eta_N$$

8. RELATIVE LEAVING VELOCITY COMPONENT

$$\frac{w_{u_2}}{c_{x_1}} = \sqrt{\psi^2 \left[\left(\cos \alpha - \frac{u_x}{c_{x_1}} \right)^2 + \sin^2 \alpha \right] - \left(\frac{\sin \alpha}{r_{x_2}/r_{x_1}} \right)^2}$$

9. ABSOLUTE LEAVING VELOCITY COMPONENT

$$\frac{c_{u_2}}{c_{x_1}} = \frac{w_{u_2}}{c_{x_1}} - \left(\frac{r_2}{r_1} \right) \left(\frac{u_x}{c_{x_1}} \right)$$

10. COMBINED EFFICIENCY OF NOZZLE AND TURBINE

$$\eta_x = 2 \eta_N \frac{u_x}{c_{x_1}} \left[\cos \alpha + \frac{r_2}{r_1} \left(\frac{w_{u_2}}{c_{x_1}} - \left(\frac{r_2}{r_1} \right) \left(\frac{u_x}{c_{x_1}} \right) \right) \right]$$

11. THERMAL EFFICIENCY

$$\eta_{th} = \left[\frac{(q_a + q_b)/(1+r)}{\eta_x \Delta h_m} + 1 \right]^{-1}$$

12. KINETIC ENERGY AVAILABLE BEFORE SEPARATOR

$$\frac{c_{s_1}^2}{2} = \left(\frac{c_{u_2}}{c_{x_1}} \right)^2 \frac{c_{x_1}^2}{2}$$

Table II. Impulse Turbine System Equations (Page 4 of 4)

13. KINETIC ENERGY OF LIQUID IN SEPARATOR DRUM

$$\frac{c_{s2}^2}{2} = \frac{c_{s1}^2}{2}\left[\frac{1 + \sqrt{1 - \frac{2(p_{N1} - p_{C2})}{r(c_{s1}^2/2)}\frac{v_a}{\eta_Y}}}{2}\right]^2\left(\frac{1}{(1 + c_d/2)}\right)^2$$

14. REQUIRED DIFFUSER EFFICIENCY FOR PRESSURE BALANCE

$$\eta_D = \Delta h_b/(c_{s_2}^2/2)$$

15. NET POWER OUTPUT PER UNIT TOTAL MASS FLOW

$$\frac{\dot{P}}{\dot{m}_T} = \eta_x \Delta h_m$$

16. TOTAL MASS FLOW REQUIRED FOR GIVEN POWER

$$\dot{m}_T = \frac{\dot{P}}{(\dot{P}/\dot{m}_T)}$$

17. SPECIFIC VOLUME OF MIXTURE

$$v_m = \frac{1}{1 + r}\frac{R_a T_{N_2}}{p_{N_2}} + \frac{r}{1 + r} v_b$$

18. TOTAL VOLUME FLOW

$$(\dot{V}_m)_{N_2} = v_m \dot{m}_T$$

19. MERIDIONAL NOZZLE OUTLET AREA

$$A_{m_2} = \frac{\dot{V}_{N_2}}{c_{N_2} \sin \alpha_{N_2}}$$

20. NOZZLE WIDTH

$$b_N = \frac{A_{m_2}}{\pi D_{N_2}}$$

Table III. Impulse Turbine Engine Input Parameters
For Cycle Analysis (Page 1 of 2)

Constants incorporated in program (Cards 14 and 15)

$P = 15{,}000$ hp	Net output
$n = 3\ s^{-1}$	Shaft speed (rps)
$A' = 11.844$	Vapor pressure constant for liquid
$B' = 6450$	Vapor pressure constant for liquid
$v_a/\eta_Y = 1.7 \times 10^{-3}\ m^3/kg$	Water specific volume/efficiency of water pump ($\eta_Y = 0.588$)

Input Cycle Conditions

CARD 14

SUBROUTINE A

$T_1 = 212\ ^oC = 485\ ^oK$	Nozzle inlet temperature
$t_{C_2} = 36\ ^oC$	Subcooled condensate temperature
$P_{N_1} = 19.85 \times 10^5$ Pascals	Nozzle inlet pressure
$P_{N_2} = 0.0836 \times 10^5$ Pascals	Nozzle discharge pressure
$P_{C_2} = 0.082 \times 10^5$ Pascals	Condenser pressure
$v_b = 6.67 \times 10^{-4}\ m^3/kg$	Specific volume of liquid
$r_b = 18.3$ kJ/kg	Heat of evaporation of liquid
$c_b = 1.34$ kJ/kg C	Specific heat of liquid
$(k/k-1)_a = 4.33$	Adiabatic exponent for steam

SUBROUTINE E

$\varepsilon = 0.77$	Recuperator effectiveness

SUBROUTINE C

$m_b/m_a = 6.59$	Ratio of molecular weights

Table III. Impulse Turbine Engine Input Parameters
For Cycle Analysis (Page 2 of 2)

CARD 16

SUBROUTINE A

R_a = 0.462 kJ/kg K	Gas constant for steam

SUBROUTINE B

r_{x_2}/r_{x_1} = 1.188	Turbine radius ratio
η_N = 0.85	Nozzle efficiency
ψ = 0.95	Impulse bucket relative velocity ratio

Table IV. U-Tube Turbine System Equations (Page 1 of 5)

1. NOZZLE DISCHARGE TEMPERATURE

$$\frac{n}{n-1} = \frac{k}{k-1} + \frac{rc_b}{R_a}$$

$$= \frac{k}{k-1}\left[1 + \frac{rc_b}{(k/k-1)R_a}\right]$$

$$\tau_N = \pi_N^{(n-1)/n}$$

$$T_{N_2} = T_{N_1}/\tau_N$$

2. KINETIC ENERGY INCREASE IN STEAM

$$\Delta h_a = \int_{p_1}^{p_2} v\,dp = \frac{n}{n-1} RT_1\left[1 - \left(\frac{p_2}{p_1}\right)^{(n-1)/n}\right]$$

3. HEAT SUPPLIED BY LIQUID DURING NOZZLE EXPANSION

$$q_{a_N} = -\left[\frac{k/(k-1)}{n/(n-1)} - 1\right]\Delta h_a$$

4. HEAT REJECTION

a. HEAT REJECTION OF STEAM

1. With Recuperator

$$\Theta_o = T_{N_2} - T_{C_2}$$

$$\Delta T_{max} = (\Delta T)_{steam} = (\varepsilon)(\Theta_o)$$

$$T_{C_1} = T_{N_2} - \Delta T_{max}$$

$$i_{C_1} \tilde{=} 2T_{C_1} + 1929 \quad (kJ/kg)$$

$$q_a = i_{C_1} - i_{C_2}$$

Table IV. U-Tube Turbine System Equations (Page 2 of 5)

4. a. HEAT REJECTION OF STEAM

2. Without Recuperator

$$i_{N_2} \tilde{=} 2T_{N_2} + 1929 \quad \text{(kJ/kg)}$$

$$i' \tilde{=} 4.19\, t_{C_2} = i_{C_2} \quad \text{Enthalpy of saturated liquid (kJ/kg)}$$

$$\frac{q_a}{1+r} = \frac{i_{N_2} - i_{C_2}}{1+r}$$

4. b. HEAT REJECTION DUE TO CONDENSATION OF OIL VAPOR

$$p_v = 10^{(A' - B'/T_{N_2})} \quad \text{(Pascal)}$$

$$x_{N_2} = \frac{1}{\left(\frac{p_{N_2}}{(p_{v_b})_{N_2}} - 1\right)} \frac{m_b}{m_a}$$

$$x_{C_2} = \frac{1}{\left(\frac{p_{N_2}}{(p_{v_b})_{C_2}} - 1\right)} \frac{m_b}{m_a}$$

$$\frac{q_b}{1+r} = \frac{1}{1+r}\,(x_{N_2} - x_{C_2})\, r_b$$

4. c. TOTAL HEAT REJECTION

$$\frac{q}{1+r} = \frac{q_a}{1+r} + \frac{q_b}{1+r}$$

5. KINETIC ENERGY INCREASE OF LIQUID

$$\Delta h_b = v_b(p_{N_1} - p_{N_2})$$

Table IV. U-Tube Turbine System Equations (Page 3 of 5)

6. KINETIC ENERGY INCREASE PER UNIT TOTAL MASS

$$\Delta h_m = \frac{1}{1+r} \Delta h_a + \frac{r}{1+r} \Delta h_b$$

7. REDUCTION IN MASS FLOW DUE TO SEPARATION AND EVAPORATION

$$\eta_v = (1 - x_{N_2}/r) \frac{r}{1+r}$$

8. TRANSITION EFFICIENCY

$$D_s = D_{N_2} + b_N$$

$$\eta_s = \left[(1 - b_N/D_s) \cos \alpha_{N_2}\right]^2$$

9. KINETIC ENERGY AVAILABLE AT SEPARATOR

$$\frac{c_{s_1}^2}{2} = \eta_N \eta_s \eta_v (\Delta h_m) = \eta_{comb} \Delta h_m$$

10. KINETIC ENERGY AVAILABLE IN SEPARATOR DRUM

$$\frac{c_{s_2}^2}{2} = \frac{c_{s_1}^2}{2} \times \left[\frac{1 + \sqrt{1 + 2 \dot{P}_s / ((c_{s_1}^2/2) \eta_v \dot{m}_b)}}{2}\right]^2$$

POWER ADDITION TO THE SEPARATOR SHAFT

$$\frac{\dot{P}_s}{\dot{m}_b} = \frac{1}{r} \left[(\Delta i_B + \Delta h_m) \eta_{XB} - \frac{v_a \Delta p}{\eta_Y}\right]$$

$$D_{x_1} \approx D_s$$

$$u_{x_1} = \pi D_s n$$

Table IV. U-Tube Turbine System Equations (Page 4 of 5)

11. TURBINE EFFICIENCY CALCULATION

$$\eta_x = 2 \frac{u_{x_1}}{c_{s_2}} \left[1 + \left(\frac{w_{x_2}}{c_{s_2}} \right) \frac{r_{x_2}}{r_{x_1}} - \frac{u_{x_1}}{c_{s_2}} \left(\frac{r_{x_2}}{r_{x_1}} \right)^2 \right]$$

$$\Delta r_s = 0$$

$$\frac{r_{x_2}}{r_{x_1}} = 1$$

$$\frac{w_{x_2}}{c_{s_2}} = \frac{w_{x_1}}{c_{s_2}} \left(\frac{w_{x_2}}{w_{x_1}} \right) = \frac{(1 - u_{x_1}/c_{s_2})}{(1 + c_d/2)} \left(\sqrt{\eta''} \right)$$

12. RESIDUAL KINETIC ENERGY AT TURBINE DISCHARGE

$$\frac{c_{x_2}^2}{2} = \left(\frac{w_{x_2}}{c_{s_2}} - \frac{u_x}{c_{s_2}} \right)^2 \frac{c_{s_2}^2}{2}$$

13. SEPARATOR TIP SPEED (SECOND SEPARATOR)

$$\frac{u_s}{c_{x_2}} = \frac{1}{1 + c_d/2}$$

14. NET POWER OUTPUT PER UNIT TOTAL MASS FLOW

$$\frac{\dot{P}_N}{\dot{m}_T} = \frac{c_{s_2}^2}{2} \cdot \eta_x$$

15. THERMAL EFFICIENCY

$$\eta_{th} = \frac{1}{\left[\frac{q/(1+r)}{\dot{P}_N/\dot{m}_T} + 1 \right]}$$

Table IV. U-Tube Turbine System Equations (Page 5 of 5)

16. REQUIRED DIFFUSER EFFICIENCY FOR PRESSURE BALANCE

$$\eta_D = \Delta h_b / (u_s^2/2)$$

17. SPECIFIC VOLUME OF MIXTURE

$$v_m = \frac{1}{1+r} \frac{R_a T_{N_2}}{p_{N_2}} + \frac{r}{1+r} v_b$$

18. TOTAL MASS FLOW

$$\dot{m}_T = \frac{\dot{P}_N}{(\dot{P}_N/\dot{m}_T)}$$

19. TOTAL VOLUME FLOW

$$(\dot{V}_m)_{N_2} = v_m \dot{m}_T$$

20. MERIDIONAL NOZZLE OUTLET AREA

$$A_{m_2} = \frac{\dot{V}_{N_2}}{c_{N_2} \sin \alpha_{N_2}}$$

21. NOZZLE WIDTH

$$b_N = \frac{A_{m_2}}{\pi D_{N_2}}$$

Table V. U-Tube Turbine Engine Input Parameters
For Cycle Analysis (Page 1 of 2)

Constants incorporated in program (Cards 14 and 15)

$P = 15{,}000$ hp	Net output
$n = 3\ s^{-1}$	Shaft speed (rps)
$A' = 11.844$	Vapor pressure constant for liquid
$B' = 6450$	Vapor pressure constant for liquid
$v_a/\eta_Y = 1.7 \times 10^{-3}\ m^3/kg$	Water specific volume/efficiency of water pump ($\eta_Y = 0.588$)

Input Cycle Conditions

CARD 14

SUBROUTINE A

$T_1 = 212\ ^oC = 485\ ^oK$	Nozzle inlet temperature
$t_{C_2} = 36\ ^oC$	Subcooled condensate temperature
$p_{N_1} = 19.85 \times 10^5$ Pascals	Nozzle inlet pressure
$p_{N_2} = 0.0836 \times 10^5$ Pascals	Nozzle discharge pressure
$p_{C_2} = 0.082 \times 10^5$ Pascals	Condenser pressure
$v_b = 6.67 \times 10^{-4}\ m^3/kg$	Specific volume of liquid
$r_b = 18.3$ kJ/kg	Heat of evaporation of liquid
$c_b = 1.34$ kJ/kg C	Specific heat of liquid
$(k/k-1)_a = 4.33$	Adiabatic exponent for steam

SUBROUTINE E

$\varepsilon = 0.77$	Recuperator effectiveness

SUBROUTINE C

$m_b/m_a = 6.59$	Ratio of molecular weights

Table V. U-Tube Turbine Engine Input Parameters
For Cycle Analysis (Page 2 of 2)

CARD 15

SUBROUTINE a		
$R_a = 0.462$	kJ/kg K	Gas constant for steam
SUBROUTINE B		
$\eta_B = \eta_{XR} = 0.75$		Afterexpansion efficiency
$\Delta i_B = \Delta h_{XR} = 0$		Afterexpansion enthalpy drop
SUBROUTINE C		
$r_{x_2}/r_{x_1} = 1$		U-tube radius ratio
$c_d = 0.15$		U-tube drag coefficient
$\eta'' = 0.85$		U-tube relative flow efficiency

Table VI. Oil-Steam Engine Performance (Page 1 of 2)

Speed n = 3 rps

	U - Tube Turbine T_1 = 505.2°K (450°F)								Impulse Turbine T_1 = 505.2°K (450°F)							
	p_c = 0.086 bar, t_c = 42°C				p_c = 0.2340 bar, t_c = 64°C				p_c = 0.086 bar, t_c = 42°C				p_c = 0.2340 bar, t_c = 64°C			
	η'' = 0.85		η'' = 0.75		η'' = 0.85		η'' = 0.75		ψ = 0.95		ψ = 0.925		ψ = 0.95		ψ = 0.925	
	α_N 15°	α_N 20°	15°	20°	15°	20°	15°	20°	15°	20°	15°	20°	15°	20°	15°	20°
ηth*)	0.230	0.223	0.206	0.203	0.200	0.192	0.182	0.174	0.264	0.254	0.256	0.245	0.227	0.217	0.219	0.209
r	85	85	85	85	85	85	85	85	85	85	85	85	85	85	85	85
D_{N_2} [m]	4.14	4.06	3.58	3.59	3.65	3.53	3.21	3.13	4.89	4.72	4.69	4.51	4.16	4.0	3.97	3.81
b_{N_2} [m]	0.171	0.122	0.226	0.155	0.096	0.070	0.089	0.089	0.081	0.067	0.088	0.073	0.048	0.040	0.053	0.044
ηth*)	0.209	0.209	0.195	0.188	0.193	0.186	0.178	0.172	0.253	0.241	0.244	0.233	0.224	0.214	0.216	0.205
r	100	100	90	95	95	95	88	88	140	146	140	137	100	100	100	100
D_{N_2} [m]	3.25	3.35	3.20	3.01	3.22	3.13	3.07	3.00	3.25	3.00	3.09	3.01	3.64	3.50	3.47	3.31
b_N [m]	0.265	0.172	0.280	0.214	0.120	0.087	0.134	0.096	0.161	0.144	0.178	0.146	0.060	0.05	0.066	0.056
ηth*)	0.200	0.202	0.185	0.186	0.188	0.182	0.176		0.250	0.240	0.242	0.230	0.218	0.209	0.210	0.199
r	103	105	92	96	100	100	90		155	150	150	150	125	119	125	125
D_{N_2} [m]	2.99	3.10	2.93	2.95	3.01	2.95	2.973		2.98	2.93	2.91	2.77	3.00	3.00	2.85	2.71
b_N [m]	0.310	0.198	0.330	0.222	0.135	0.096	0.142		0.187	0.150	0.197	0.167	0.084	0.065	0.093	0.079
	6° SUBCOOLING				6° SUBCOOLING											

*) The residual kinetic energy of the steam at the nozzle exit was considered lost.

Table VI. Oil-Steam Engine Performance (Page 2 of 2)

Speed n = 3 rps

	U-Tube Turbine								Impulse Turbine							
	p_c = 0.086 bar, t_c = 42°C				p_c = 0.2340 bar, t_c = 64°C				p_c = 0.086 bar, t_c = 42°C				p_c = 0.2340 bar, t_c = 64°C			
	η'' = 0.85		η'' = 0.75		η'' = 0.85		η'' = 0.75		ψ = 0.95		ψ = 0.925		ψ = 0.95		ψ = 0.925	
	α 15°	α 20°	α 15°	α 20°	α 15°	α 20°	α 15°	α 20°	α 15°	α 20°	α 15°	α 20°	α 15°	α 20°	α 15°	α 20°
r	85	85	85	85	85	85	85	85	85	85	85	85	85	85	85	85
$\dot{m}_a$ [kg/s] 6 units	15.11	15.74	17.35	17.73	18.4	19.5	20.8	21.9	12.6	13.3	13.1	13.9	15.7	16.6	16.4	17.4
$\dot{m}_b$ [kg/s]	1284	1338	1475	1507	1565	1654	1771	1860	1070	1127	1112	1178	1338	1414	1397	1482
$\dot{V}_m$ [m³/s]	383	399	440	450	173	183	196	205	319	336	332	351	148	156	154	164
r	100	100	90	95	95	95	88	88	140	146	140	137	100	100	100	100
$\dot{m}_a$ [kg/s]	17.06	17.03	18.6	19.5	19.3	20.3	21.3	22.3	13.3	14.2	13.9	14.8	16.0	17.0	16.8	17.9
$\dot{m}_b$ [kg/s]	1706	1703	1674	1851	1833	1925	1874	1960	1859	2072	2101	2029	1603	1697	1678	1786
$\dot{V}_m$ [m³/s]	434	433	472	496	181	191	200	209	340	363	357	379	151	160	158	168
r	103	105	92	96	100	100	90		155	150	150	150	125	119	125	125
$\dot{m}_a$ [kg/s]	18.08	17.74	19.9	19.7	19.9	20.7	21.6		13.5	14.2	14.1	15.1	16.5	17.4	17.4	18.6
$\dot{m}_b$ [kg/s]	1862	1863	1829	1893	1987	2073	1945		2090	2137	2115	2259	2068	2074	2174	2323
$\dot{V}_m$ [m³/s]	461	452	505	501	187	195	203		345	365	361	386	156	165	165	176

Table VII. Computer-Run for Oil/Steam Partial Unit

Speed = 16.6670 rps

Power = 15000/6 hp = 2500 hp

```
****************
U-tube TURBINE

r =        17.0000
n/n-1 =    53.6374
Δha Ha =   1197.4898 kJ/kg
    TN2 =   456.8760 °K
    iN2 =  2842.7521 kJ/kg
    iM1 =  4040.2419 kJ/kg
    TM1 =  2019.6564 °K
    Tc1 =   343.1655 °K
    qa/1+r =
           136.9162 kJ/kg
    XN2 =     0.0002 --
    XO2 =     0.0000 --
    qb/1+r =  0.0002 kJ/kg
    q/1+r = 136.9163 kJ/kg
    qaN =  1100.8197

    Power =
        1864250.0000 W
DN  Dia. D =  2.0340 m
    bn guess= 0.1517 m
    Hb =   1317.9720 J/kg
Δhm Hm =  67771.9622 J/kg
ηcomb Ncomb. =  0.6638 --
    Cs2/Cs1 = 1.0318 --
    Ux/Cs2 =  0.3698 --
ε   Nrecup. = 0.7700 --
    Cd1 =     0.1000 --
    Cd2 =     0.1000 --
η"  N" =      0.8500 --
ηx  Nx =      0.8753 --
    Cx2/Cs2 = 0.1836 --
    P/mt =
          41927.2874 J/kg
ηth Nth* =    0.2244 --
ηD  Nd =      0.9002 --
    ṁt =     44.4639 kg/s
    ṁa =      2.4702 kg/s
    vm =      1.2992 m³/kg
    bn =      0.1516 m
    bn/D =    0.0745 --

****************
```

c_{Nid} = 368.2 m/s

= 1207 fps

c_N = 1112.9 fps

c_u = 1075 fps

*Considers residual steam energy at nozzle exit as lost.

Table VIII. Estimate of Biphase Turbine Engine Weight and Volume: Oil/Steam System

Component	Weight (kg)	Weight (lbs)	Volume (m^3)	Volume (ft^3)
1. Main Propulsion Turbine** (2) (15,000 hp)	20,164	44,360	20.28	714
2. Ship Service Turbine (2) (4000 kW)	1,818	4,000	3.55	125*
3. Oil Heat Exchanger (2)	3,225	7,096*	1.82	64*
4. Water Heat Exchanger (2)	27,775	61,106*	17.65	622*
5. Supports	8,382	18,441*	1.07	37.6*
6. Regenerators (4)	4,043	8,895*	5.05	178*
7. Pumps (6)	454	1,000*	0.23	8*
8. Condenser (2)	27,590	60,697*	54.25	1912*
9. Generator (2)	9,545	21,000*	4.09	144*
10. Clutches (3)	8,182	18,000*	2.54	89.6*
11. Gear	15,455	34,000	2.10	74*
Total	126,607	278,535	112.6	3968

Neutrally Buoyant Volume 129 m^3 (4,561 ft^3)

*Estimate by H. Urbach, NSRDC

**Astern turbines included

Table IX. Saturated Steam Properties

$$\log\left(\frac{p_k}{p}\right) = \frac{\left(1-\frac{T}{T_k}\right)}{T/T_k}\left[\frac{a+bT_k\left(1-\frac{T}{T_k}\right)+dT_k{}^3\left(1-\frac{T}{T_k}\right)^3+eT_k{}^4\left(1-\frac{T}{T_k}\right)^4}{1+f\,T_k\,(1-T/T_k)}\right] = z \qquad (1)$$

$$p/p_k = 10^{-z} \qquad \text{Good up to critical point}$$

$$i = 1996.7\,T - \left[0.075(n+1)\left(\frac{273}{T}\right)^n - v'\right]p + 1.9441 \times 10^6 \quad (\text{J/kg K}) \qquad (7)$$

or

$$i'' = i' + r_c$$

$$r_c = 346.6\sqrt[3]{T_k - T} \quad (\text{kJ/kg}) \qquad \text{Latent heat of evaporation} \qquad (2)$$

$$s' = 10.1796\,\log\left(\frac{T}{273}\right) - 8.6229 \times 10^{-4}(T-273) + 1.8836 \times 10^{-6}(T-273)^2 \quad [\text{kJ/kg K}] \qquad (4)$$

$$q = 4.186\,(t + 2.0 \times 10^{-5}\,t^2 + 3.0 \times 10^{-7}\,t^3) \quad [\text{kJ/kg}] \qquad (3)$$

$$i' = q + v'p = q + p \times 10^{-6} \quad [\text{kJ/kg}] \qquad (5)$$

$$v'' = \frac{RT}{p} - 0.075\left(\frac{273.2}{T}\right)^{10/3} + v' = v_a \qquad (6)$$

Eq (1) By Smith, Keyes & Gerry (1934) (Plank, R.p. 112)

(2) By M. Jakob (1935) (Plank, p. 125)

(3) Regnault Data for Spec. Heat of Liquid (Plank, p. 227)

(4) By integration from (3)

(5) By integration from (3)

(7) From General Eq. of Thermodynamics and Callendar Eq. of State (6)

TABLE X Analysis of Five-Stage Wet-Steam Turbine

N	t_1 °C	Δt °C	Δp bar	i' kJ/kg	$\Delta i'$ kJ/kg	r_c kJ/kg	y	x_1	x_2
1	232.0		8.62	994.2				0.15	0.1815
		18.65							
2	213.35		10.10	911.14		1884.6	0.070	0.1237	0.1766
		32.27			141.91				
3	181.08		7.94	769.23		2003.1	0.1074	0.0775	0.1656
		55.87			241.09				
4	125.21		1.216	528.14		2180.1	0.042	0.1290	0.1596
		22.41			95.46				
5	102.80		0.878	432.68		2243.6	0.068	0.0982	0.1504
		38.80			164.08				
	64.0			268.60		2345.8			

N T	P^{**} kJ/kg	c_{N2} m/s	D_{N2} m	b_N cm	v'' m³/kg	$\dot{m}_s{}^{*}$ kg/s	$\dot{m}_T{}^{\dagger}$ kg/s	$\dot{m}_r{}^{\dagger *}$ kg/s	$\dot{V}$ m³/s	$\dot{P}_Y{}^{\dagger\dagger}$ J/kg
1	10.815	147.1	1.124	1.052	0.1004	5.198	74.25	1.0	0.522	64.0
2	17.221	192.4	1.470	1.041	0.1916	7.416	69.05	0.93	1.421	69.74
3	25.554	248.1	1.895	2.064	0.7686	2.588	61.63	0.83	1.989	48.93
4	12.931	180.3	1.377	7.163	1.5298	4.021	59.04	0.795	6.151	7.179
5	20.392	234.6	1.792	15.727	6.4901		55.03	0.741		4.832
	86.91 kJ/kg									194.69 J/kg

* mass flow of extracted steam
† total mass flow
†* relative mass flow
** net output
†† pumping power

Table XI

EULER TURBINES

7500 hp Unit
n= 2000 rpm = 33.33 rps

		1	2	3	4	5	
$\dot{m}_T$	kg/s	74.25	69.05	61.63	59.04	55.03	Total mass flow
x_2	–	0.1815	0.1766	0.1656	0.1596	0.1504	Quality at nozzle exit
$\dot{m}_b$	kg/s	60.774	56.856	51.424	49.617	46.754	$\dot{m}_b = (1 - x_2)\,\dot{m}_T$
$\dot{V}_b$	m^3/s	0.0608	0.0569	0.0514	0.0496	0.0468	$\dot{V}_b = \dot{m}_b v_b$
r_1/r_2	–	0.8178	0.8157	0.7782	0.8245	0.8023	$v_b = 10^{-3}\ m^3/kg$
w_{u_2}/u_2	–	0.5741	0.5770	0.6264	0.5644	0.5954	$\left\|\frac{w_{u_2}}{u_2}\right\| = \sqrt{\eta''}\,\sqrt{1-(r_1/r_2)^2}\cos\beta_2$ $= \sqrt{0.995}\,\sqrt{1-(r_1/r_2)^2} * 1.0$
D_1	m	1.159	1.503	1.962	1.543	1.856	
D_2	m	1.417	1.842	2.5213	1.726	2.314	
b_N	cm	1.052	1.041	2.064	2.388	5.242	Nozzle width
u_2	m/s	148.4	192.9	214.0	180.8	242.3	$u_2 = \pi D_2 n$ $= (33.33)\,\pi D_2$
w_{u_2}	m/s	85.2	111.3	165.4	102.0	144.3	$w_{u_2} = w_{u_2}/u_2 * u_2$
A	m^2	7.136×10^{-4}	5.108×10^{-4}	3.109×10^{-4}	4.863×10^{-4}	3.2405×10^{-4}	$A = \dot{V}/w_{u_2}$
No.		10	4	2	6	6	Number of rotating nozzles
d	cm	0.953	1.275	1.407	1.016	0.829	Diameter of rotating nozzles
$d/D_2 10^2$	–	0.6725	0.6921	0.5580	0.8938	0.3583	

Table XII. Droplet Heat Conduction (Page 1 of 5)

$\overline{\theta}/\theta_o = f(at/r^2)$ $\qquad$ $\overline{q}d/k\theta_o = f(\overline{\theta}/\theta_o)$

@/@o=	0.7608	@/@o=	0.8756	@/@o=	0.9601
at/r2=	0.0960	at/r2=	0.1610	at/r2=	0.2760
qd/k@o=	5.2837	qd/k@o=	3.6258	qd/k@o=	2.3191
@/@o=	0.7728	@/@o=	0.8817	@/@o=	0.9688
at/r2=	0.1010	at/r2=	0.1660	at/r2=	0.3010
qd/k@o=	5.1011	qd/k@o=	3.5408	qd/k@o=	2.1458
@/@o=	0.7841	@/@o=	0.8874	@/@o=	0.9756
at/r2=	0.1060	at/r2=	0.1710	at/r2=	0.3260
qd/k@o=	4.9316	qd/k@o=	3.4596	qd/k@o=	1.9952
@/@o=	0.7948	@/@o=	0.8928	@/@o=	0.9810
at/r2=	0.1110	at/r2=	0.1760	at/r2=	0.3510
qd/k@o=	4.7737	qd/k@o=	3.3820	qd/k@o=	1.8632
@/@o=	0.8050	@/@o=	0.8980	@/@o=	0.9851
at/r2=	0.1160	at/r2=	0.1810	at/r2=	0.3760
qd/k@o=	4.6262	qd/k@o=	3.3076	qd/k@o=	1.7467
@/@o=	0.8146	@/@o=	0.9029	@/@o=	0.9884
at/r2=	0.1210	at/r2=	0.1860	at/r2=	0.4010
qd/k@o=	4.4879	qd/k@o=	3.2363	qd/k@o=	1.6432
@/@o=	0.8237	@/@o=	0.9076	@/@o=	0.9909
at/r2=	0.1260	at/r2=	0.1910	at/r2=	0.4260
qd/k@o=	4.3579	qd/k@o=	3.1680	qd/k@o=	1.5507
@/@o=	0.8323	@/@o=	0.9121	@/@o=	0.9929
at/r2=	0.1310	at/r2=	0.1960	at/r2=	0.4510
qd/k@o=	4.2355	qd/k@o=	3.1023	qd/k@o=	1.4677
@/@o=	0.8405	@/@o=	0.9163	@/@o=	0.9945
at/r2=	0.1360	at/r2=	0.2010	at/r2=	0.4760
qd/k@o=	4.1199	qd/k@o=	3.0392	qd/k@o=	1.3928
@/@o=	0.8482	@/@o=	0.9204	@/@o=	0.9957
at/r2=	0.1410	at/r2=	0.2060	at/r2=	0.5010
qd/k@o=	4.0106	qd/k@o=	2.9785	qd/k@o=	1.3249
@/@o=	0.8556	@/@o=	0.9242	@/@o=	0.9966
at/r2=	0.1460	at/r2=	0.2110	at/r2=	0.5260
qd/k@o=	3.9070	qd/k@o=	2.9201	qd/k@o=	1.2631
@/@o=	0.8626	@/@o=	0.9279	@/@o=	0.9974
at/r2=	0.1510	at/r2=	0.2160	at/r2=	0.5510
qd/k@o=	3.8086	qd/k@o=	2.8638	qd/k@o=	1.2067
@/@o=	0.8693				
at/r2=	0.1560				
qd/k@o=	3.7150				

Table XII. Droplet Heat Conduction (Page 2 of 5)

@/@o=	0.7608	@/@o=	0.8817	@/@o=	0.9408
at/r2=	0.0960	at/r2=	0.1660	at/r2=	0.2360
ad/k@o=	5.2837	ad/k@o=	3.5408	ad/k@o=	2.6576
	.507				
@/@o=	0.7728	@/@o=	0.8874	@/@o=	0.9436
at/r2=	0.1010	at/r2=	0.1710	at/r2=	0.2410
ad/k@o=	5.1011	ad/k@o=	3.4596	ad/k@o=	2.6104
@/@o=	0.7841	@/@o=	0.8928	@/@o=	0.9464
at/r2=	0.1060	at/r2=	0.1760	at/r2=	0.2460
ad/k@o=	4.9316	ad/k@o=	3.3820	ad/k@o=	2.5647
@/@o=	0.7948	@/@o=	0.8980	@/@o=	0.9489
at/r2=	0.1110	at/r2=	0.1810	at/r2=	0.2510
ad/k@o=	4.7737	ad/k@o=	3.3076	ad/k@o=	2.5204
@/@o=	0.8050	@/@o=	0.9029	@/@o=	0.9514
at/r2=	0.1160	at/r2=	0.1860	at/r2=	0.2560
ad/k@o=	4.6262	ad/k@o=	3.2363	ad/k@o=	2.4776
@/@o=	0.8146	@/@o=	0.9076	@/@o=	0.9537
at/r2=	0.1210	at/r2=	0.1910	at/r2=	0.2610
ad/k@o=	4.4879	ad/k@o=	3.1680	ad/k@o=	2.4361
@/@o=	0.8237	@/@o=	0.9121	@/@o=	0.9560
at/r2=	0.1260	at/r2=	0.1960	at/r2=	0.2660
ad/k@o=	4.3579	ad/k@o=	3.1023	ad/k@o=	2.3959
@/@o=	0.8323	@/@o=	0.9163	@/@o=	0.9581
at/r2=	0.1310	at/r2=	0.2010	at/r2=	0.2710
ad/k@o=	4.2355	ad/k@o=	3.0392	ad/k@o=	2.3569
@/@o=	0.8405	@/@o=	0.9204	@/@o=	0.9601
at/r2=	0.1360	at/r2=	0.2060	at/r2=	0.2760
ad/k@o=	4.1199	ad/k@o=	2.9785	ad/k@o=	2.3191
@/@o=	0.8482	@/@o=	0.9242	@/@o=	0.9620
at/r2=	0.1410	at/r2=	0.2110	at/r2=	0.2810
ad/k@o=	4.0106	ad/k@o=	2.9201	ad/k@o=	2.2824
@/@o=	0.8556	@/@o=	0.9279	@/@o=	0.9639
at/r2=	0.1460	at/r2=	0.2160	at/r2=	0.2860
ad/k@o=	3.9070	ad/k@o=	2.8638	ad/k@o=	2.2468
@/@o=	0.8626	@/@o=	0.9313	@/@o=	0.9656
at/r2=	0.1510	at/r2=	0.2210	at/r2=	0.2910
ad/k@o=	3.8086	ad/k@o=	2.8095	ad/k@o=	2.2121
@/@o=	0.8693	@/@o=	0.9346	@/@o=	0.9673
at/r2=	0.1560	at/r2=	0.2260	at/r2=	0.2960
ad/k@o=	3.7150	ad/k@o=	2.7571	ad/k@o=	2.1785
@/@o=	0.8756	@/@o=	0.9378	@/@o=	0.9688
at/r2=	0.1610	at/r2=	0.2310	at/r2=	0.3010
ad/k@o=	3.6258	ad/k@o=	2.7065	ad/k@o=	2.1456

Table XII. Droplet Heat Conduction (Page 3 of 5)

@/@o=	0.9703	@/@o=	0.9851	@/@o=	0.9926
at/r2=	0.3060	at/r2=	0.3760	at/r2=	0.4460
ad/k@o=	2.1140	ad/k@o=	1.7467	ad/k@o=	1.4836
@/@o=	0.9718	@/@o=	0.9858	@/@o=	0.9929
at/r2=	0.3110	at/r2=	0.3810	at/r2=	0.4510
ad/k@o=	2.0831	ad/k@o=	1.7250	ad/k@o=	1.4677
@/@o=	0.9731	@/@o=	0.9865	@/@o=	0.9933
at/r2=	0.3160	at/r2=	0.3860	at/r2=	0.4560
ad/k@o=	2.0530	ad/k@o=	1.7039	ad/k@o=	1.4521
@/@o=	0.9744	@/@o=	0.9872	@/@o=	0.9936
at/r2=	0.3210	at/r2=	0.3910	at/r2=	0.4610
ad/k@o=	2.0237	ad/k@o=	1.6832	ad/k@o=	1.4368
@/@o=	0.9756	@/@o=	0.9878	@/@o=	0.9939
at/r2=	0.3260	at/r2=	0.3960	at/r2=	0.4660
ad/k@o=	1.9952	ad/k@o=	1.6630	ad/k@o=	1.4219
@/@o=	0.9768	@/@o=	0.9884	@/@o=	0.9942
at/r2=	0.3310	at/r2=	0.4010	at/r2=	0.4710
ad/k@o=	1.9674	ad/k@o=	1.6432	ad/k@o=	1.4072
@/@o=	0.9779	@/@o=	0.9889	@/@o=	0.9945
at/r2=	0.3360	at/r2=	0.4060	at/r2=	0.4760
ad/k@o=	1.9404	ad/k@o=	1.6239	ad/k@o=	1.3928
@/@o=	0.9790	@/@o=	0.9895	@/@o=	0.9947
at/r2=	0.3410	at/r2=	0.4110	at/r2=	0.4810
ad/k@o=	1.9140	ad/k@o=	1.6050	ad/k@o=	1.3787
@/@o=	0.9800	@/@o=	0.9900	@/@o=	0.9950
at/r2=	0.3460	at/r2=	0.4160	at/r2=	0.4860
ad/k@o=	1.8883	ad/k@o=	1.5865	ad/k@o=	1.3649
@/@o=	0.9810	@/@o=	0.9905	@/@o=	0.9952
at/r2=	0.3510	at/r2=	0.4210	at/r2=	0.4910
ad/k@o=	1.8632	ad/k@o=	1.5684	ad/k@o=	1.3513
@/@o=	0.9819	@/@o=	0.9909	@/@o=	0.9955
at/r2=	0.3560	at/r2=	0.4260	at/r2=	0.4960
ad/k@o=	1.8387	ad/k@o=	1.5507	ad/k@o=	1.3380
@/@o=	0.9828	@/@o=	0.9914	@/@o=	0.9957
at/r2=	0.3610	at/r2=	0.4310	at/r2=	0.5010
ad/k@o=	1.8149	ad/k@o=	1.5334	ad/k@o=	1.3249
@/@o=	0.9836	@/@o=	0.9918	@/@o=	0.9959
at/r2=	0.3660	at/r2=	0.4360	at/r2=	0.5060
ad/k@o=	1.7916	ad/k@o=	1.5165	ad/k@o=	1.3121
@/@o=	0.9844	@/@o=	0.9922	@/@o=	0.9961
at/r2=	0.3710	at/r2=	0.4410	at/r2=	0.5110
ad/k@o=	1.7689	ad/k@o=	1.4999	ad/k@o=	1.2995

Table XII. Droplet Heat Conduction (Page 4 of 5)

@/@o=	0.9963	@/@o=	0.9981	@/@o=	0.9991
at/r2=	0.5160	at/r2=	0.5860	at/r2=	0.6560
ad/k@o=	1.2872	ad/k@o=	1.1355	ad/k@o=	1.0153
@/@o=	0.9964	@/@o=	0.9982	@/@o=	0.9991
at/r2=	0.5210	at/r2=	0.5910	at/r2=	0.6610
ad/k@o=	1.2750	ad/k@o=	1.1260	ad/k@o=	1.0077
@/@o=	0.9966	@/@o=	0.9983	@/@o=	0.9992
at/r2=	0.5260	at/r2=	0.5960	at/r2=	0.6660
ad/k@o=	1.2631	ad/k@o=	1.1167	ad/k@o=	1.0002
@/@o=	0.9968	@/@o=	0.9984	@/@o=	0.9992
at/r2=	0.5310	at/r2=	0.6010	at/r2=	0.6710
ad/k@o=	1.2515	ad/k@o=	1.1075	ad/k@o=	0.9927
@/@o=	0.9969	@/@o=	0.9985	@/@o=	0.9992
at/r2=	0.5360	at/r2=	0.6060	at/r2=	0.6760
ad/k@o=	1.2400	ad/k@o=	1.0984	ad/k@o=	0.9854
@/@o=	0.9971	@/@o=	0.9985	@/@o=	0.9993
at/r2=	0.5410	at/r2=	0.6110	at/r2=	0.6810
ad/k@o=	1.2287	ad/k@o=	1.0895	ad/k@o=	0.9782
@/@o=	0.9972	@/@o=	0.9986	@/@o=	0.9993
at/r2=	0.5460	at/r2=	0.6160	at/r2=	0.6860
ad/k@o=	1.2176	ad/k@o=	1.0807	ad/k@o=	0.9711
@/@o=	0.9974	@/@o=	0.9987	@/@o=	0.9993
at/r2=	0.5510	at/r2=	0.6210	at/r2=	0.6910
ad/k@o=	1.2067	ad/k@o=	1.0721	ad/k@o=	0.9641
@/@o=	0.9975	@/@o=	0.9987	@/@o=	0.9994
at/r2=	0.5560	at/r2=	0.6260	at/r2=	0.6960
ad/k@o=	1.1960	ad/k@o=	1.0636	ad/k@o=	0.9572
@/@o=	0.9976	@/@o=	0.9988	@/@o=	0.9994
at/r2=	0.5610	at/r2=	0.6310	at/r2=	0.7010
ad/k@o=	1.1855	ad/k@o=	1.0553	ad/k@o=	0.9505
@/@o=	0.9977	@/@o=	0.9989	@/@o=	0.9994
at/r2=	0.5660	at/r2=	0.6360	at/r2=	0.7060
ad/k@o=	1.1752	ad/k@o=	1.0470	ad/k@o=	0.9437
@/@o=	0.9978	@/@o=	0.9989	@/@o=	0.9995
at/r2=	0.5710	at/r2=	0.6410	at/r2=	0.7110
ad/k@o=	1.1650	ad/k@o=	1.0389	ad/k@o=	0.9371
@/@o=	0.9979	@/@o=	0.9990	@/@o=	0.9995
at/r2=	0.5760	at/r2=	0.6460	at/r2=	0.7160
ad/k@o=	1.1550	ad/k@o=	1.0309	ad/k@o=	0.9306
@/@o=	0.9980	@/@o=	0.9990	@/@o=	0.9995
at/r2=	0.5810	at/r2=	0.6510	at/r2=	0.7210
ad/k@o=	1.1452	ad/k@o=	1.0231	ad/k@o=	0.9242

Table XII. Droplet Heat Conduction (Page 5 of 5)

@/@o=	0.9995	@/@o=	0.9998	@/@o=	0.9999
at/r2=	0.7260	at/r2=	0.7910	at/r2=	0.8560
ad/k@o=	0.9178	ad/k@o=	0.8426	ad/k@o=	0.7787
@/@o=	0.9996	@/@o=	0.9998	@/@o=	0.9999
at/r2=	0.7310	at/r2=	0.7960	at/r2=	0.8610
ad/k@o=	0.9116	ad/k@o=	0.8373	ad/k@o=	0.7742
@/@o=	0.9996	@/@o=	0.9998	@/@o=	0.9999
at/r2=	0.7360	at/r2=	0.8010	at/r2=	0.8660
ad/k@o=	0.9054	ad/k@o=	0.8321	ad/k@o=	0.7697
@/@o=	0.9996	@/@o=	0.9998	@/@o=	0.9999
at/r2=	0.7410	at/r2=	0.8060	at/r2=	0.8710
ad/k@o=	0.8993	ad/k@o=	0.8270	ad/k@o=	0.7653
@/@o=	0.9996	@/@o=	0.9998	@/@o=	0.9999
at/r2=	0.7460	at/r2=	0.8110	at/r2=	0.8760
ad/k@o=	0.8933	ad/k@o=	0.8219	ad/k@o=	0.7610
@/@o=	0.9996	@/@o=	0.9998	@/@o=	0.9999
at/r2=	0.7510	at/r2=	0.8160	at/r2=	0.8810
ad/k@o=	0.8874	ad/k@o=	0.8168	ad/k@o=	0.7560
@/@o=	0.9997	@/@o=	0.9998	@/@o=	0.9999
at/r2=	0.7560	at/r2=	0.8210	at/r2=	0.8860
ad/k@o=	0.8815	ad/k@o=	0.8119	ad/k@o=	0.7524
@/@o=	0.9997	@/@o=	0.9998		
at/r2=	0.7610	at/r2=	0.8260		
ad/k@o=	0.8757	ad/k@o=	0.8070		
@/@o=	0.9997	@/@o=	0.9998		
at/r2=	0.7660	at/r2=	0.8310		
ad/k@o=	0.8700	ad/k@o=	0.8021		
@/@o=	0.9997	@/@o=	0.9998		
at/r2=	0.7710	at/r2=	0.8360		
ad/k@o=	0.8644	ad/k@o=	0.7973		
@/@o=	0.9997	@/@o=	0.9998		
at/r2=	0.7760	at/r2=	0.8410		
ad/k@o=	0.8589	ad/k@o=	0.7926		
@/@o=	0.9997	@/@o=	0.9999		
at/r2=	0.7810	at/r2=	0.8460		
ad/k@o=	0.8534	ad/k@o=	0.7879		
@/@o=	0.9997	@/@o=	0.9999		
at/r2=	0.7860	at/r2=	0.8510		
ad/k@o=	0.8480	ad/k@o=	0.7833		

Table XIII. Estimate of Biphase Turbine Engine Weight
Wet-Steam System

Component	Weight (kg)	Weight (lbs)	Box Volume (m^3)	Box Volume (ft^3)
1. Main Propulsion Turbine** (2) (15,000 hp)	22,660	49,860	10.38	366
2. Hotel Turbine (2) (approx) (4000 kW)	2,045	4,500	3.55	125
3. Heaters and Pumps (Propulsion) (2)	12,478	24,956	5.62	198
4. Heaters and Pumps (Ship Service) (2) (approx)	4,460	9,813	2.84	100
5. Supports	8,382*	18,440	1.07	37.6*
6. Condenser (2)	27,590*	60,700	54.25	1912*
7. Generator (2)	9,545*	21,000	4.09	144*
8. Clutches	8,182*	18,000	2.54	89.6*
9. Gear (2)	15,455	34,000	2.10	74*
Total	101,797	243,754	86,44	3046

*Estimate by H. Urbach, NSRDC

**Drive motor for pump/heater, and astern turbines not included

Table XIV. Heater and Feed Pump Analysis (Sheet 1 of 3)

Stage		4	3	2	1	0
t_a	°C	102.8	125.2	181.1	213.4	233.0
$t_{b\ IN}$	°C	63.0	101.8	124.2	180.1	212.4
$t_{m\ b}$	°C	82.9	113.0	152.2	196.2	222.2
θ_o	C	39.8	23.4	56.9	33.3	20.6
$\bar{\theta}$	C	38.8	22.4	55.9	32.3	19.6
$\varepsilon = \bar{\theta}/\theta_o$	–	0.9749	0.9573	0.9824	0.9700	0.9515
$Fo = \frac{4a_b t}{d^2}$	–	0.3231	0.2691	0.3588	0.3050	0.256
$Nu = \frac{\bar{q}d}{k_b \theta_o} = \frac{2\varepsilon}{3Fo}$	–	2.0116	2.4774	1.8853	2.1202	2.478
$p_a = p_b$	bar	1.117	2.33	10.3	20.4	30.0
Δp_p	bar	0.878	1.216	7.94	10.10	8.62
v_a	m^3/kg	1.530	0.769	0.192	0.100	0.0684
$e_a = \sqrt{pv_a}$	m/s	413.4	423.4	443.6	452.2	396.6
$\lambda_a = \nu_a/e_a$	10^{-8} m	4.477	2.433	0.6609	0.3730	0.2966
v_b	m^3/kg	10^{-3}	10^{-3}	10^{-3}	10^{-3}	10^{-3}
C_{pb}	J/kg C	J/kg C	J/kg C	J/kg C	J/kg C	J/kg C
$\eta_{b\ IN}$	10^{-5} kg/ms					
k_b	W/mC	0.676	0.682	0.683	0.665	0.645
$a_b = \frac{\gamma_b k_b}{C_{pb}}$	10^{-7} m^2/s	1.616	1.629	1.632	1.589	1.541

Table XIV. Heater and Feed Pump Analysis (Sheet 2 of 3)

Stage		4	3	2	1	0
d	μm	100.0	100.0	100.0	100.0	100.0
$t_M = \frac{d^2 Fo}{4a_b}$	ms	5.00	4.13	5.50	4.85	4.15
L	m	0.30	0.30	0.30	0.30	0.30
$\dot{m}_a$ [extracted]	kg/s	4.02	2.59	7.42	5.20	–
$\dot{m}_b$	kg/s	55.03	59.04	61.63	69.05	74.25
$(w_b)_1$	m/s	20.0	20.0	23.2	17.6	15.9
Δp_p	$10^5 \frac{N}{m^2}$	0.878	1.216	7.94	10.10	8.62
$\Delta p_W = w_b^2/2v_b$	$10^5 \frac{N}{m^2}$	2.00	2.00	2.686	1.547	1.257
$\Delta p_f = \frac{32 w_b n}{d^2} \Delta r_R$	$10^5 \frac{N}{m^2}$	0.179	0.179	0.145	0.096	0.082
Δp_T	$10^5 \frac{N}{m^2}$	3.057	3.395	10.771	11.744	9.959
$D_{L1} = (D_{M2})_{n-1}$	m	Pressure rise furnished by stationary diffuser	0.600	0.995	1.560	1.996
u_{L1}	m/s		29.7	49.2	77.3	98.9
$\nu_L = \frac{1}{\sqrt{1 + 2v_b \Delta p_T / u_{L1}^2}}$	–		0.752	0.728	0.847	0.911
$D_{L2} = D_{L1}/\nu_L$	m	0.40	0.798	1.367	1.842	2.190
$D_{M1} = D_{L2} + 2\Delta r_R$	m	0.40	0.798	1.367	1.842	2.190
$U_{M1} = \frac{D_{M1}}{D_{L1}} u_{L1}$	m/s	19.8	39.5	67.7	91.2	98.8

Table XIV. Heater and Feed Pump Analysis (Sheet 3 of 3)

Stage	4	3	2	1	0
$Re\sqrt{C_D} = \frac{u_{M1}}{e}\frac{d}{\lambda_a}\sqrt{\frac{8}{3}\frac{d}{D_{M1}}\left[\frac{v_a}{v_b}-1\right]}$	75.5	194.2	445.2	648.8	760.9
Re from Fig B-2	108.0	225.0	600.0	940.0	1125.0
$w_b)_2 = Re\ (\lambda_a/d)\ e\ \left[\frac{m}{s}\right]$	20.0	23.2	17.6	15.9	13.2
Compare with (w_D),					
$\Delta r_M = w_b \cdot t_M$ [m]	0.039	0.098	0.097	0.077	0.055
$(D_{M2})_n - D_{M1} + 2\Delta r_M = (D_{L1})_{n+1}$ [m]	0.600	0.995	1.560	1.996	2.300
$\phi = \frac{\pi D_{M2}\ L\ w_D}{\dot{w}_b\ v_b}$	205.6	368.0	419.8	432.0	440.8

REFERENCES

[1] Elliott, D.G., *A Two-Fluid Magnetohydradynamic Cycle for Nuclear-Electric Power Conversion,* Technical Report No. 32-116, Jet Propulsion Laboratory, California Institute of Technology, Pasadena, Calif., June 30, 1961.

[2] Ritzi, E.W., *Design Study of A Two-Phase Turbine Engine for Torpedo Propulsion,* Report 105-F, Biphase Energy Systems, Inc., Santa Monica, Calif., June, 1977.

[3] Hays, L., et. al. *Design and Operation of a 1000°C Lithium-Cesium Test System,* Technical Memorandum 33-633, Jet Propulsion Laboratory, Pasadena, Calif., December, 1963.

[4] Contract N---14-77-C-0545, Statement of Work.

[4a] A Statement of the Basic Ground Rules for the Evaluation of Biphase Power Plants for Nuclear Submarines, Memorandum by R.R. Pariseau, Office of Naval Research to Biphase, dated 12 Jan 1978 (Ser 211/009).

[5] Elliott, D.G. and Weinberg, E., *Acceleration of Liquids in Two-Phase Nozzles,* Technical Report 32-987, Jet Propulsion Laboratory, Pasadena, Calif., July, 1968.

[6] Alger, T.W., *The Performance of Two-Phase Nozzles for Total Flow Geothermal Impulse Turbines,* Report 76417 Lawrence Livermore Laboratory, Livermore, Calif., May 28, 1975.

[7] Ibid (3)

[8] Boxer, E., Sterret, J.R. and Wlodarski, J., *Application of Supersonic Impulse Compressor or Turbine-Blade Sections,* NACA RM L 52 B 06, April 1952.

[9] Oswatitsch, K., *Über die Strömung in einem Überschallgitter,* Allgemeine Wärmetechnik, Jahrgang 6, 1955.

[10] Stratford, B.S. and Sansome, G.E., *Theory and Tunnel Tests of Rotor Blades for Supersonic Turbines,* ARC R&M No. 3275, 1962.

[11] Colclough, C.D., "Design of Turbine Blades Suitable for Supersonic Relative Inlet Velocities and the Investigation of Their Performance in Cascades: Part I - Theory and Design", *Journal Mechanical Engineering Science Vol. 8,* No. 1, 1966, p. 110-123, "Part II - Experiments, Results and Discussion", *Journal Mechanical Engineering Science Vol. 8, No. 2,* (1966).

[12] Goldman, L.J. and Scullin, F.J., "Analytical Investigation of Supersonic Turbomachinery Blading", *I - Computer Program for Blading Design,* NASA TN D-4421, March 1968.

[13] Goldman, L.J., "Analytical Investigation of Supersonic Turbomachinery Blading", *II - Analysis of Impulse Turbine-Blade Sections,* NASA TN D-4422, April 1968.

[14] Ackeret, J., "Untersuchung einer nach den Euler'schen Verschlagen (1754) Gebauren Wasserturbine", Schweizerische Bauzeitung, Vol. 123, No. 1, p. 2-4 (1944).

[14a] Euler, L., "Théoric plus complète des machines qui sont mises en inouvement par la réaction de l'eau." Mém. de l'acad. d. sc. de Berlin 1754 (presented 13 Sept. 1753).

[15] VDI-Berichte, Vol. 3, 1955, p.107.

[16] Kotelewskij, G.P., "Bubble Contact Heaters for Power Plants", *Industrial and Engineering Chemistry,* Vol. 48, No. 1, January 1956, 20-25.

[17] Bohm, J., "Vergleichsversuche uber das Anwarmen von Wasser mit Dampf", *Z. VDI, Beih. Verfahrenstechn.,* 1937, 197-201.

[18] Sparrow, E.M. and Gregg, J.L., "A Theory of Rotating Condensation", *Journal of Heat Transfer,* May 1959, 113-120.

[19] Nandapurkar, S.S., and Beatty, K.O., Jr., "Condensation on a Horizontal Rotating Disk", *Am. Inst. of Chem. Engrs., Progress Symposium Series No. 30,* Vol. 56, 1960, 129-137.

[20] Ginwala, K., *Engineering Study of Vapor Cycle Cooling Equipment for Zero-Gravity Environment,* Wadd Technical Report No. TR60-776, Wright Air Development Division, U.S. Air Force, Jan. 1961.

[21]Rice, W., and Crawford, M.E., "Calculated Design Data for the Multiple-Disk Pump Using Incompressible Fluid", *Trans. of the ASME,* July 1974, 274-282.

[22]Millsaps, K. and Pohlhausen, K., "Heat Transfer by Laminar Flow from a Rotating Plate", *Journal of the Aironautical Sciences,* February 1952, 120-126.

[23]Brown, G., "Heat Transmission by Condensation of Steam on a Spray of Water Drops", *Proceedings of the General Discussion on Heat Transfer,* London, 1951.

[24]Carslaw, H.S. and Jaeger, J.C., *Conduction of Heat in Solids,* 1st Edition, Clarendon Press, Oxford, 1947.

[25]Walton, W.H. and Prewett, W.C., The Production of Sprays and Mists of Uniform Drop Size by Means of Spinning Disc Type Sprayers, Proceedings of the Physical Society Section B, Vol 62, Part 6, June 1949, 341-350.

APPENDIX A

In the design solution shown in Figure 44 for the five stage wet-steam turbine the three high-pressure stages (comprising a pressure span from 30 bar to 2.33 bar) are combined with the two low pressure stages (2.33 bar to 0.239 bar) in one housing. The 30 bar pressure region is confined to diameters less than 1.1 meters, and the 10.3 bar region to less than 1.5 m.

The 15% quality steam enters at the plenum A and is accelerated through the first nozzle ring B. The nozzle is layed out for full admission; the flow discharge angle α is assumed to be 15°. The total nozzle widths per stage, b_N, together with the nozzle discharge diameters D_{N2} are given in Table X for all stages. Note that the total nozzle width is divided into three parallel "pancakes" in the two low pressure stages. The nozzle widths given are minimum values, actual widths would be increased by a blockage factor. That factor accounts for the space absorbed by the nozzle wall thickness. Since the smallest theoretical nozzle widths are about 1 cm and the largest width about 15.7/3 = 5.2 cm, an increase by 10 to 25% is favorable. Not shown in Figure 44 are provisions for reducing the nozzle area for part-load. In the two low pressure stages individual "pancakes" could be completely shut-off by axially sliding control rings that could be actuated by steam pistons. For best performance all nozzles should have adjustable area. In the high pressure stages movable sidewalls with slots for the vanes could be considered. Since the pressure ratios per stage are small, see Table below, the nozzle design may

Stage No.	Pressure Ratio
1	1.422
2	1.986
3	4.408
4	2.080
5	4.686
TOTAL	121.34

follow more conventional lines. A nozzle program is available for the isentropic, homogeneous equilibrium (I.H.E.) model that allows the calculation of the throat area required as well as the detailed conditions at any intermediate station. From a number of runs that started with saturated water Figure A1 was developed that allows the prediction of the required nozzle area based on the I.H.E. model. For zero initial steam quality the I.H.E. model underpredicts the mass-flow according to test results. However, according to Ref. 1 at 15% initial quality good agreement is shown. See also Ref. 2. So far our own tests have not covered inlet conditions with other than subcooled liquid entry conditions.

Referring back to Figure 44 the two-phase nozzle discharge flow enters the liquid ring of the Euler turbine. Because of the

---

[1] E.S. Starkman, V.E. Schrock, K.F. Neusen and D.J. Maneely, Expansion of a Very Low Quality Two-Phase Fluid Through a Convergent - Divergent Nozzle." Trans. ASME, Journal of Basic Engineering, June 1964, p. 247-256.

[2] L.S. Dzung and G. Gyarmathy: "Critical Mass Flux Density in Two-Phase Flow", Brown Boveri Review, Vol 65, January 1978, Baden, Switzerland, p. 55-61.

distribution of the liquid droplets over the larger area of the liquid ring the radial velocity component will experience a slow-down from the approach conditions to the liquid ring conditions. Comparing that situation with that of a sudden expansion of a continuous flow, some rise in pressure in the liquid ring should be realizable.

For example, in the first stage the volume flow ratio of steam to water as it is emerging from the nozzle is

$$\dot{V}_a/\dot{V}_b = \frac{1}{r_m}\,\frac{v_a}{v_b} \quad .$$

With a steam quality of 16% at the same location,

$$r_m = \frac{1 - x_2}{x_2} = 5.25 \quad , \quad v_a/v_b = 100 \text{ so that } \dot{V}_a/\dot{V}_b = 19.0 \quad .$$

For a single-phase flow with a sudden expansion in cross-sectional area the efficiency of pressure recovery could be estimated with the momentum law (Carnot's formula) to be

$$\eta = 1 - \left(1 - \frac{w_2}{w_1}\right)^2 \Big/ \left[1 - \left(\frac{w_2}{w_1}\right)^2\right] = 0.10 \quad .$$

A nozzle velocity of 147 m/s would give at 15° nozzle angle a pressure recovery of 0.72 bar, which would be available to augment the turbine discharge velocity.

After the mixture of wet steam discharges from the nozzle the steam flow will deflect to both sides of the Euler turbine where it is to give up its residual swirl velocity in reaction blading of a similar type as the backward bent blading for the liquid flow shown in the partial section B-B in Figure 44. In order to

accelerate the steam flow in a tangential direction a small pressure differential is needed across the Euler turbine rotor, which is made possible by the face seals shown in Figure 44. In order to illustrate the magnitude of the reaction pressure the relations of Table I of Section III may be used to determine the degree of reaction r_R required for a certain

$$\left(\frac{w_2}{u_2}\right)^2 = \left(\frac{w_2}{c_1}\right)^2\left(\frac{c_1}{u_1}\right)^2\left(\frac{r_1}{r_2}\right)^2 \quad .$$

$$r_R = \psi^2\left(\frac{w_2}{u_2}\right)^2\left(\frac{u_1}{c_1}\right)^2\left(\frac{r_2}{r_1}\right)^2 - \phi_R - \left(\frac{u_1}{c_1}\right)\left[\phi_R + \left(\frac{r_2}{r_1}\right)^2 - 1\right] + 2\phi_R \cos\alpha, \left(\frac{u_1}{c_1}\right).$$

With $w_2/u_2 = 0.7$, $u_1/c_1 \cong 1$, $\phi_R = 1$, $r_2/r_1 = 1/0.8, \psi = 0.95$ we obtain $r_R = 0.060$. According to the special definition of $r_R = \Delta h_x/c_1^2/2$ we obtain $\Delta h_x = 0.060\ c_1^2/2 \approx v_a\ \Delta p_a$. For stage one $v_a = 0.10\ m^3/kg$; $c_1^2/2 = (147)^2/2 = 10804\ J/kg$.

$$\Delta p_a = \frac{0.060 \times 10804}{0.10} = 6518\ \frac{N}{m^2} = 0.065\ bar \quad .$$

About half of the steam that leaves the turbine will be extracted and used to preheat feedwater of the same pressure but initially lower temperature.

A solution for a <u>feed water heater</u> that utilizes a direct contact mode of heat exchange and at the same time serves as a <u>boiler feed pump</u> is shown in Figure 46. Also included in the same package is the primary heater for converting the saturated steam furnished by the reactor into wet steam of 15% quality. The unit is rotating at approximately 900 rpm and may be electric motor driven.

That has advantages for start-up and part-load operation. The power demand is roughly 250 kW. The outer diameter of the unit is about 2.3 m, and the total volume 1.25 m^3 (44 ft^3).

The unit has been calculated based on the theory of Section III. The basic steps are (1) the control of droplet size, (2) the prediction of the radial drift velocity w_b of the droplets, (3) the calculation of the radial mixing chamber dimensions to allow sufficient dwell time before coalescence. (4) The selection of the axial width of the chamber that determines the closeness of the droplets according to the continuity equation, (5) check the steam porting and velocity. See also Appendix B.

For each of the four feedwater heater stages the calculation included the required radius ratio of a liquid ring preceding the mixing chamber that produces a static pressure rise sufficient for the liquid to meet the steam pressure and to be accelerated through pores of solid separation rings to the velocity w_b against the friction of the pores. The kinetic energy w_b of the droplets was selected such that its loss upon impingement on the succeeding liquid layer will still assure an overall pump efficiency of 80%.

The port sizes required for the steam were checked. A stress check for the porous cylinders was made. A detailed axial thrust analysis has not yet been performed. By proper seal location it is possible to balance the thrust. A leakage analysis is also required. In contrast to the space restrictions imposed on seals in multistage steam turbines the seals of the proposed feed-water heater and the turbine have generous space available so that the losses may be kept very low.

The condensate from the condenser and the water collected at the discharge of the last stage is fed to the center of the heater; after preheating and final heating in the last chamber, the liquid

is collected in the stationary pitot pick-up and ducted to the first stage nozzle of the turbine, where it is joined by additional reactor steam to make up a 15% quality mixture of wet steam.

All the steam (whether extraction steam or steam from the reactor) that is ducted to the unit is completely condensed and mixed with the feed-water. The sizing was determined for a final temperature difference of 1°C between incoming steam and the droplet temperature before mixing in the liquid ring. The effectiveness is therefore high, (95.1%) for the primary heater. The feed-water is preheated to 212°C before exposure to the reactor steam. That number may make possible higher temperatures at the turbine inlet. The total flow of saturated steam from the reactor is calculated to about 17 kg/s. The feed-water flow at the outlet of the heater is 74.2 kg/s.

It should be noted that a first attempt at a rotating heater design was using rotating disk spinoff of droplets since their size could be predicted from the diameter, speed and surface-tension of water. However, the resulting radial drift velocities amounted to over 100 m/s and the dwell time was hard to meet. Reliance on additional heat transfer area for the steam in the form of the walls or additional disks seemed involved and was not explored further. By the use of a porous material for a nozzle plate it was reasoned that a droplet size of 100 μm (microns) could be generated by the additional action of the liquid ring pressure differential. The assumed droplet velocities of around 20 m/s and less are similar to the average values used by Brown.[23]. In his case, however, the initial spouting velocity was about double our value (which requires about four times as much injection pressure) since that velocity could not be sustained over the entire height of the vessel. In the rotating exchanger the spouting velocity was made equal to the drift velocity resulting as a balance of inertia, drag and buoyancy forces.

The ducts that carry extraction steam to the feed-water heater were sized for an average steam velocity that is 40% of the nozzle exit velocity. A table of values follows.

Stage	Mass-Flow of Extracted Steam $\dot{m}$ [kg/s]	Nozzle Velocity c_N m/s	Specific Volume of Steam v_a m^3/kg	Volume Flow Rate $\dot{V}$ m^3/s	Duct Total Area A cm^2	Diameter For One Duct d cm
1	5.20	147.1	0.100	0.522	88.7	10.63
2	7.42	192.4	0.192	1.421	184.6	15.34
3	2.59	248.1	0.769	1.989	200.4	15.98
4	4.02	180.3	1.530	6.151	852.9	32.96
5		243.6	6.490			

It is of course feasible to use stationary feed-water heaters either of the direct contact type or of the tubular type. The rotating unit seems to have the advantage in comparison to the stationary direct contact type that the droplet stream may be packed together more closely without risking coalescence because of the more orderly droplet trajectories. The ϕ values, which represent the ratio of total chamber volume to total droplet volume of liquid, were therefore reduced from the value of around 6000 of Brown's tests (who used twelve spray nozzles with a cone angle of 80 degrees) to about 440 in the primary heater. The spacing between droplets was therefore cut to a bit less than one half. Some experiments should be made to firm up the validity of those assumptions.

Table XIV summarizes the conditions in the four feed-water heaters, the primary heater and the liquid rings.

Performance Summary, See Table X (Wet-Steam System)

With a nozzle inlet temperature of 232°C, an assumed nozzle efficiency of $\eta_N = 0.87$ the total kinetic energy per unit initial mass-flow is 86.91 kJ/kg. With a turbine rotor efficiency of $\eta_x = 0.90$ (which assumes a carry-over efficiency between stages of $\eta_D = 0.85$ and a final liquid pick-up with that efficiency) the output reduces to 78.22 kJ/kg. The ideal pumping power is 0.195 kJ/kg; the actual power rises with a pump efficiency $\eta_Y = 0.80$ to 0.244 kJ/kg. Therefore the net specific output is 78.22 - 0.244 = 77.98 kJ/kg.

The heat rejection without subcooling is $\dot{Q} = 0.7441 \times 0.1504 \times 2345.8 = 261.5$ kJ/kg. With 1°C subcooling that increases by 3.1 kJ/kg. The final thermal efficiency is therefore

$$\eta_{th} = \frac{1}{1 + \frac{\dot{Q}}{\dot{P}}} = \frac{4}{1 + \frac{264.6}{77.98}} = 0.228 \quad .$$

In this figure leakage losses, disk-friction losses, duct transfer losses and mechanical losses (gears, bearings) are not included. An efficiency improvement potential is to be found in the following:

1) Higher turbine inlet temperature (460°F instead of 450°F).
2) Lower condenser pressure (the present value corresponds to a 64°C condenser temperature or p = 0.239 bar = 3.47 psia).
3) Optimization of initial vapor quality vs. number of stages and wheel stresses.
4) Improved carry-over efficiency (0.95 instead of 0.85).
5) Lower diameter and output for the last stage.

Because of the many other systems investigated it was not possible to explore the possibilities further; there is of course also a limit to what may be predicted at this stage without additional experimental results. What is in favor of high turbine rotor total efficiencies is well controlled conditions and very high Reynolds' members.

An *installation drawing* that incorporates the wet-steam turbine and feed-water heater is shown in Figure 45. The condenser is taken over from the conventional design. The gear-box was also left as is, assuming the same gear ratio 10:1 was used before. No astern turbine is included; the switching is assumed to be accomplished with the existing clutch and gear train.

The ship-service generator turbine is shown unchanged; additional savings in space are possible by replacing it by a Biphase turbine, as was shown in the installation drawing for the oil/steam system.

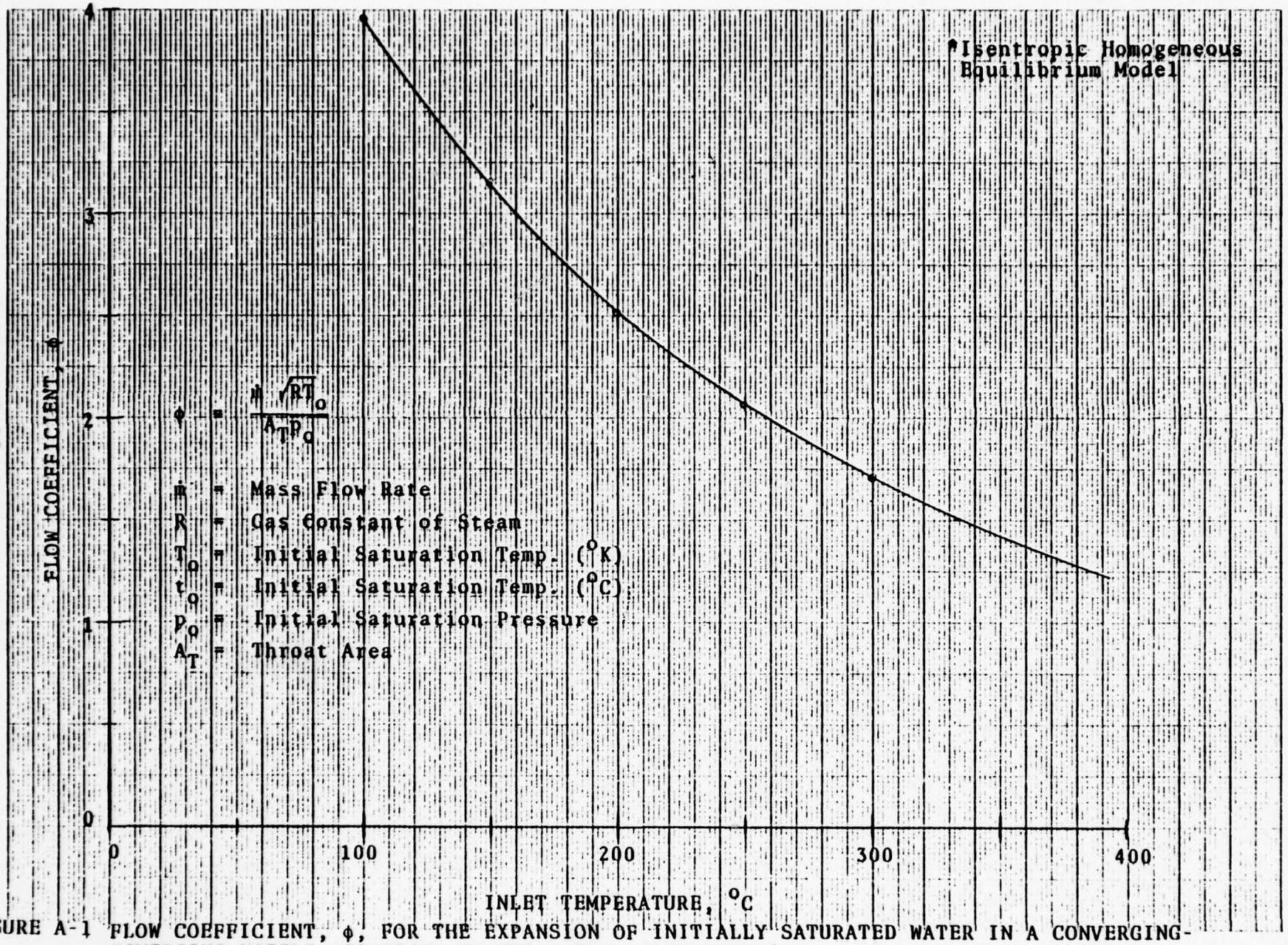

FIGURE A-1 FLOW COEFFICIENT, ϕ, FOR THE EXPANSION OF INITIALLY SATURATED WATER IN A CONVERGING-DIVERGING NOZZLE ACCORDING TO THE I.H.E. FLOW MODEL*

APPENDIX B

DESIGN METHOD FOR THE DIRECT CONTACT HEAT EXCHANGER USING LIQUID SPRAY EXPOSED TO SATURATED STEAM

Assumptions

The droplets are of spherical shape, of constant diameter d and are uniformly distributed.

The heat transfer resistance is solely due to transient conduction in the liquid droplet.

The steam temperature is assumed constant.

Assume the liquid to be heated by the condensing steam. Assume the liquid to be water, or more generally, assume the liquid and the vapor to be of one component, that is of one chemical substance.

Main design criterion

Whether the average liquid velocity, w_b is produced by injection or by centrifuging in a stationary or a rotating exchanger the dwell time criterion has to be met: The conduction of heat into the droplet has to be completed to the desired effectiveness.

Nomenclature

$\dot{m}_a$ = steam mass-flow rate [kg/s]

$\dot{m}_b$ = water mass-flow rate [kg/s]

$\dot{Q}$ = quantity of heat to be transferred per unit time [kW]

= $\dot{m}_a\, r_c$ = heat rate of condensation

= $\dot{m}_b\, c_b\, \bar{\theta}$ = liquid heat absorption

Nomenclature (continued)

$\bar{q}$ = heat flux density (per unit droplet surface area A_h) $\left[\frac{kW}{m^2}\right]$

d = droplet diameter = $2r$ [m]

s = side of cube

A_h = total surface area of all droplets [m^2]

k_b = thermal conductivity of liquid $\left[\frac{W}{mC}\right]$

c_b = specific heat of liquid $\left[\text{for } H_2O : c_b = 4186 \frac{W}{kg\ C}\right]$

v_b = specific volume of liquid $\left[\text{for } H_2O : v_b = 10^{-3} \frac{m^3}{kg}\right]$

a_b = thermal diffusivity of liquid $a_b = v_b\ k_b/c_b$ [m^2/s]

v_a = specific volume of steam [m^3/kg]

r_c = heat of condensation of vapor [kJ/kg]

w_a = average steam velocity [m/s]

w_b = average liquid velocity [m/s]

A_b = cross-sectional area of liquid spray [m^2]

A_a = cross-sectional area of steam flow [m^2]

t = time elapsed between first exposure of droplets to vapor, and coalescence of droplets (impact on liquid layer)

H = linear dimension in direction of w_b, the droplet movement

θ_o = the initial temperature difference between steam and liquid. It is the maximum temperature rise the liquid could be subjected to.

$\bar{\theta}$ = the effective temperature rise of the liquid, where the final temperature is a bulk temperature, that is, it is representative of the heat added to the droplets:

$$\dot{Q} = \dot{m}_b\ c_b\ \bar{\theta} \quad .$$

Nomenclature (continued)

$\varepsilon = \bar{\theta}/\theta_o = \dot{Q}/\dot{m}_b\ c_b\ \theta_o$ effectiveness of heat transfer, $\varepsilon < 1$

V_c = chamber volume of direct contact exchanger (two-phase region only)

$Nu = \frac{\bar{q}\ d}{k_b\ \theta_o}$ NUSSELT NUMBER for average heat flux density

$Fo = \frac{4\ a_o\ t}{d^2}$ FOURIER NUMBER for transient heat exchange

$\phi = \frac{V_c}{V_b}$ ratio of chamber volume and total liquid volume

Steam properties and velocities have the subscript "a"; liquid properties and velocities have the subscript "b".

Relations

1. Relation between total surface area A_h, total liquid volume V_b and droplet diameter d

$$\frac{A_h\ d}{V_b} = 6 \tag{1}$$

2. Relation between total chamber volume V_c and total liquid volume V_b; the continuity equation for the liquid flow

$$\frac{V_c}{V_b} = \phi \tag{2}$$

$$w_b = \phi\ \frac{m_b\ v_b}{A_b} \tag{3}$$

The chamber geometric characteristics

$$V_c = A_b H \tag{4}$$

3. Combination of the above relations

$$\frac{A_h d}{V_c} = \frac{6}{\phi}$$

Eliminate ϕ by means of (3)

$$\frac{A_h d}{V_c} = \frac{6 \dot{m}_b v_b}{w_b A_b}$$

Eliminate A_b by substitution of Eq. (4)

$$\frac{A_h d}{V_c} = \frac{6 \dot{m}_b v_b}{\frac{w_b}{H} V_c} \tag{5}$$

4. The required dwell time is

$$t = \frac{H}{w_b} \tag{6}$$

so that Eq. (5) becomes

$$A_h d = 6 \dot{m}_b v_b t \tag{5'}$$

5. Introduce the Nusselt number $Nu = \bar{q}d/k_b\,\theta_o$ and the Fourier number $Fo = 4a_b\,t/d^2$ into Eq. (5^1) and eliminate A_h and t

$$A_h = \frac{\dot{Q}}{\bar{q}} = \frac{\dot{Q}\,d}{Nu\;k_b\;\theta_o}$$

Eliminate $\dot{Q}$ by means of the effectiveness

$$\varepsilon = \frac{\dot{Q}}{\dot{m}_b\;c_b\;\theta o} = \frac{\bar{\theta}}{\theta_o} \;:\; A_h = \frac{\varepsilon\;\dot{m}_b\;c_b\;\theta_o\;d}{Nu\;k_b\;\theta_o}$$

Per definition

$$t = \frac{Fo\;d^2}{4a_b} = \frac{Fo\;d^2\;c_b}{4\;v_b\;k_b}$$

Substituting the above equations for A_h and t into Eq. (5^1) yields finally

$$\boxed{\frac{\varepsilon}{Nu} = \frac{3}{2}\,Fo} \qquad (6)$$

Equation (6) was already given as equation (24^4) in the main text. Applying Eq. (6) to the values of Table XII, indeed proves the validity of the relationship.

The practical consequences of the relation between the three non-dimensionals ε, Nu and Fo is that we need to design only to meet for example the dwell-time condition and the continuity equation (3); the heat transfer area requirement is then automatically met.

Design procedure

A design procedure consists accordingly of the following steps:

1. Select the desired effectiveness $\varepsilon = \bar{\theta}/\theta_o$ and obtain the corresponding Fourier number $Fo = \frac{4a_b\ t}{d^2}$ from Table XII.

2. Select a suitable liquid velocity w_b and droplet size d. The determination of liquid velocity w_b in case of a rotating heat exchanger is shown in the next section.

3. Calculate the chamber height H from

$$H = w_b\ t = \frac{Fo\ w_b\ d^2}{4\ a_b} \tag{7}$$

It is noted that the required height is proportional to the product $w_b\ d^2$.

4. The continuity equation yields A_b

$$A_b = \phi\ \frac{\dot{m}_b\ v_b}{w_b} \tag{8}$$

A selection of the value $\phi = \frac{V_c}{V_b}$ is required.

While Brown's test (Ref. 23) indicated a value of $\phi \sim 6000$, it seems reasonable to try to lower that value. Especially with rotating sprays it should be possible to avoid coalescence due to colliding droplets, because of the better predictability of droplet paths.

A densiest packing is of course obtained if the droplet spheres touch each other. According to the studies of cristallography, in a closest packing the spheres would assume 74% of the total volume, that is $\phi_{min} = \frac{V_c}{V_b} = \frac{1}{0.74} = 1.35$. In the arrangement where the spheres sit in the centers of cubes with s = d $\phi = \frac{6}{\pi}\left(\frac{s}{d}\right)^3 = 1.910$. The following table shows the relative spacing $s/d = \left(\phi \frac{\pi}{6}\right)^{1/3}$ as a function of ϕ.

ϕ	s/d
100	3.74
1000	8.06
6000	14.64

The continuity equation for the steam is used to check the steam entrance velocity

$$w_a = \frac{\dot{m}_a v_a}{A_a} \frac{1}{1 - \left(\frac{1}{\phi}\right)} \quad . \tag{9}$$

The area A_a may be taken equal to A_b or equal to the side wall area, which is a function of H.

In the rotating heat exchanger the assumed values of w_b and d of step 2 are interconnected with the speed and diameter of the unit.

Rotating Heat Exchanger

Another conceivable configuration for a direct contact heat exchanger is a rotating drum or hollow cylinder, see Figure 46. The configuration shown is representative of a direct contact

feed-water heater using saturated steam. At the same time the unit can be used for pressurizing the feed-water by the required amount so that steam and atomized feed-water are at the same pressure in the mixing chamber of Volume V_c. The radius ratio $\nu_L = D_i/D_a$ across the liquid layer rotating on a solid body in a first chamber (radially inward from the mixing chamber) follows from the required pressure difference between the two successive liquid and mixing chambers: $\Delta p = p_{II} - p_I$.

$$v_b \Delta p = \frac{u_i^2}{2} \left[\frac{1}{\nu_L^2} - 1 \right] \tag{10}$$

Where u_i is the peripheral velocity of the free liquid surface.

The droplet size obtained by flinging a liquid of surface tension σ off a rotating disk of diameter D and tip speed u may be predicted by (Ref. 25) by the relation

$$d = 1.895 \frac{\sqrt{\sigma v_b D}}{u} \quad . \tag{11}$$

The configuration of rotating disks may be approached by annular slots with webs to keep intermediate rings in place. The predicted values for the droplet diameter have been confirmed by experiment, reported in Ref. 25.

The saturated steam enters the mixing chamber from the side with a swirl velocity c that matches the peripheral velocity of the housing that admits the steam. Proper *sealing* of the steam path transition from the stationary housing to the rotating member is required. If the diameter of the seal can be reduced sufficiently, liquid sealing can be considered because of the low speed of the drum.

Because of the matched peripheral velocity c of liquid droplets and steam, drag forces between the two phases occur only insofar as the inertia forces on the droplets are counteracted by the drag to keep the droplets on a swirling path with absolute velocity c as viewed by a stationary observer.

The question was investigated whether the dwell time of the droplets is sufficient for conductive heat transfer into the droplet. The *relative velocity* between droplet and steam in radial direction is designated as w_b and needs to be calculated.

The drag force on the droplet of diameter d is defined by

$$D = C_D \frac{1}{v_a} \frac{w_b^2}{2} \frac{\pi}{4} d^2 \qquad (12)$$

Where v_a is the specific volume of the surrounding medium. The drag coefficient C_D is given as a function of Reynold's number $Re = w_b\, d/v_a$ in Figure B-1 according to a relation given in Ref. 5 which is valid for $0.1 < Re < 20{,}000$:

$$\ln C_D = 3.271 - 0.8893 \ln Re + 0.03417 (\ln Re)^2 + 0.001443 (\ln Re)^3$$

Since the slip velocity w_b is not initially known for the calculation of Re and C_D, the quantity $Re \sqrt{C_D}$ was plotted against Re in Figure B-2, since $Re \sqrt{C_D}$ is expressible in terms of known values as follows.

The inertia force on a spherical droplet of diameter d and specific volume v_b that travels with velocity c on an initially assumed circular path of radius of curvature, r_k, is

$$F = \frac{1}{v_b} \frac{\pi d^3}{6} \frac{c^2}{r_k} \quad . \qquad (13)$$

Corrected for buoyancy B we get

$$F\text{-}B = \frac{1}{v_b} \frac{\pi d^3}{6} \frac{c^2}{r_k} \left(1 - \frac{v_b}{v_a}\right) \tag{14}$$

Equating the two forces of equations (12) and (14) gives

$$\frac{w_b}{c} = \sqrt{\frac{4}{3} \frac{d}{r_k} \frac{1}{C_D} \left[\frac{v_a}{v_b} - 1\right]} \quad . \tag{15}$$

It is convenient to refer velocities to the reference velocity $e = \sqrt{p\, v_a}$ and lengths to the mean free path length $\lambda_a = \frac{v_a\, \eta_a}{e}$. According

$$Re = \frac{w_b}{e} \frac{d}{\lambda_a} \tag{16}$$

and

$$\begin{aligned} Re \sqrt{C_D} &= \frac{w_b}{c} \sqrt{C_D} \frac{c}{e} \frac{d}{\lambda_a} \\ &= \frac{c}{e} \sqrt{\frac{4}{3} \frac{d}{r_k} \left(\frac{d}{\lambda_a}\right)^2 \left[\frac{v_a}{v_b} - 1\right]} \quad . \end{aligned} \tag{17}$$

Therefore, the proof is furnished that the quantity $Re \sqrt{C_D}$ is solely composed of known quantities, namely the droplet diameter d, the vapor property λ_a, the ratio of specific volumes v_a/v_b, the radius of curvature of the path, r_k, and the normalized absolute velocity c/e ($\sim$ Mach number) along the path.

Entering Figure B-2 on the ordinate will yield Re and consequently the desired w/e from (16)

$$\frac{w_b}{e} = \frac{Re}{d/\lambda_a} \tag{18}$$

Rotating Heat Exchanger with droplet diameter determined by Rotating Disk

The following study explored the design possibilities when the droplet size is controlled by Eq. (11). Another approach was finally selected in Section IV; however, the present method is of some interest.

While it is possible to find the slip velocity w_b for a known particle diameter and swirl velocity c according to the above procedure the experience has been that the dwell time criterion was not easily met with small chamber radius ratios. It is undoubtedly a critcal problem with the rotating hollow cylinder chamber that the radius ratio across the chamber should be kept small so that flow losses can be minimized. When using the relation (11) for the particle size it is assumed that the fluid is freely flinging off a rotating disk without blades. If rotating nozzles are provided that can accelerate the liquid in relation to the disk in direction of rotation then the relative velocity with which the droplets meet the outer wall of the chamber may be minimized even for larger chamber radius ratios. With the additional acceleration of the liquid smaller droplets than predicted by Eq. (11) may be expected; as a first step the droplet diameter may be approximated by using the diameter and velocity of the outer chamber wall rather than the values at the inner wall in equation (11).

The question is now what choice exists in the selection of the peripheral chamber velocity u and its diameter D and diameter ratio $\nu = \frac{r_2}{r_1}$.

Substituting Eq. (11) into relation (17) and setting $r_k = D/2$ and $c = u$ we get

$$Re\sqrt{C_D} = \sqrt{\frac{8}{3}}\,(1.895)^{3/2}\,\frac{(\sigma_b\, v_b)^{3/4}}{e_a^{3/2}\,\lambda_a}\sqrt{\frac{v_a}{v_b} - 1}\qquad \frac{D^{1/4}}{\sqrt{\frac{u}{e}}} \tag{19}$$

In order to meet the required dwell time t a radial distance $\Delta r = w_b\, t$ is required, where w_b follows from Eq. (18)

$$w_b = \frac{Re}{d/\lambda_a}\, e \quad ,$$

or, after substitution of Eq. (11)

$$w_b = \frac{Re\ \lambda_a\ u\ e}{1.895\ \sqrt{\sigma v_b\ D}} \quad . \tag{20}$$

From the heat conduction analysis the Fourier Number $Fo = \frac{4\ a_b t}{d^2}$ is a function of the effectiveness $\varepsilon = \frac{\bar{\theta}}{\theta_o}$.

For a given Fo the dwell time follows from Eq. (11)

$$t = \frac{Fo}{4}\,\frac{(1.895)^2}{a_b}\,\frac{\sigma\ v_b\ D}{u^2} \quad . \tag{21}$$

Therefore with Eqs. (20) and (21), and $\Delta r = w_b\, t$

$$\frac{\Delta r}{D} = 1.895 \times \frac{Fo}{4} \frac{\lambda_a}{a_b} \sqrt{\frac{\sigma_b\, v_b}{D}}\ \frac{Re}{(u/e)} \tag{22}$$

After elimination of the diameter between Eq. (19) and (22) we get

$$\left(Re\ \sqrt{C_D}\right)^2 = 34.39\ \frac{Fo}{4}\ \frac{(\sigma\, v_b)^2 \left(\frac{v_a}{v_b} - 1\right)}{\lambda_a\, a_b\, e_a^{\,3}}\ \frac{1}{\left(\frac{\Delta r}{D}\right)\left(\frac{u}{e}\right)^2}\ Re \tag{23}$$

$$\left(Re\ \sqrt{C_D}\right)^2 = B\ \ Re \tag{23a}$$

where B is the constant preceding Re in Eq. (23).

Figure B-3 was prepared from Figure B-1 and is therefore based upon the value of the drag coefficient C_D as a function of Re.

The dwell time criterion is therefore met at the intersection of the drag coefficient curve of Figure B-3 with a straight line inclined at 45° and with the ordinate value B at the origin of the logarithmic plot.

It is seen that high tip speeds and large $\frac{\Delta r}{D}$ values lead to small Reynolds Numbers and small chamber diameters D according to Eq. (19).

The alternate design approach with the droplet size determined by a porous cylindrical ring was already described in Appendix A.

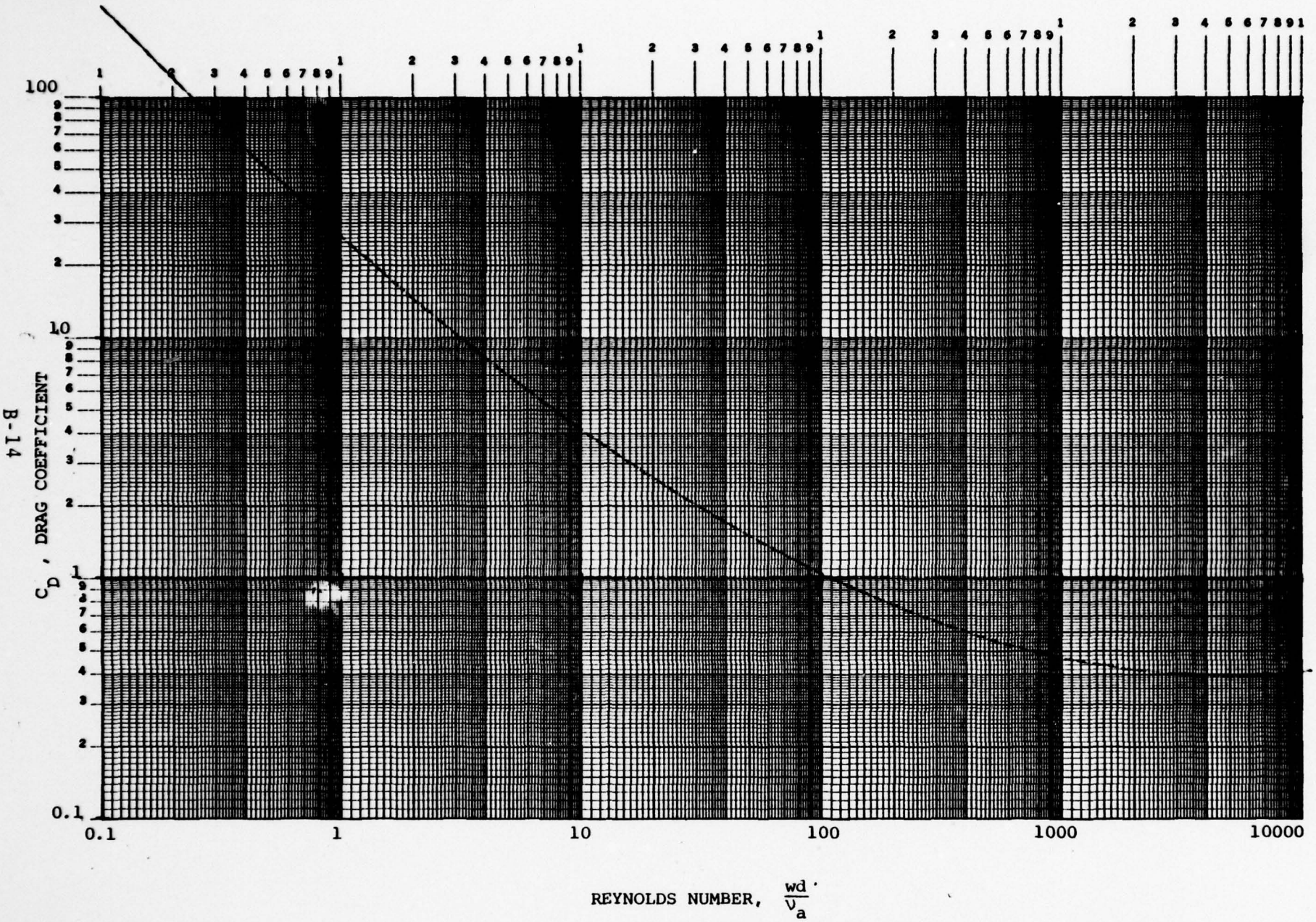

Figure B-1. Drag Coefficient of Spherical Droplets

RYM 7/18/17

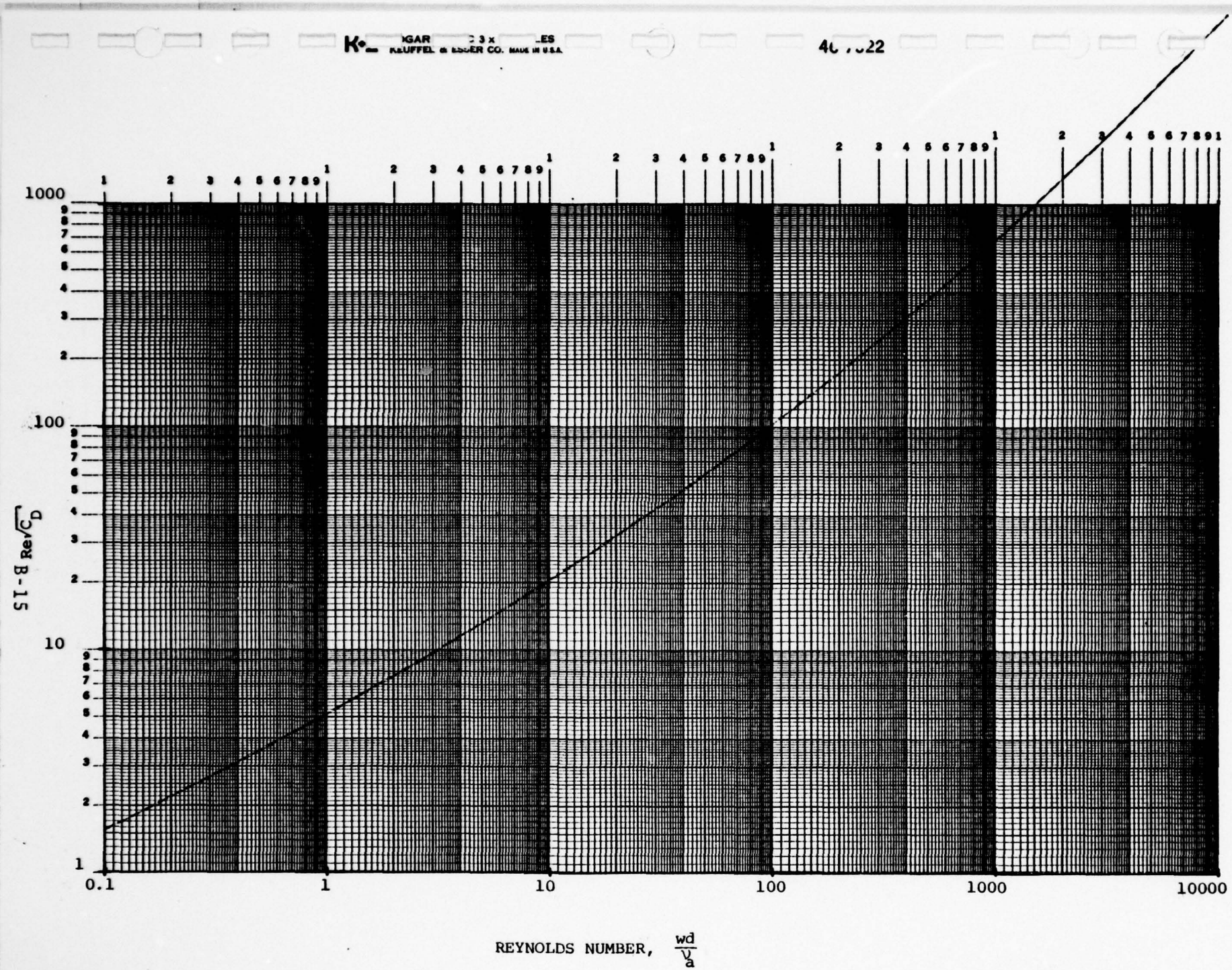

Figure B-2. Working Graph for Determining Slip Velocity of Spherical Droplets for a Given Diameter

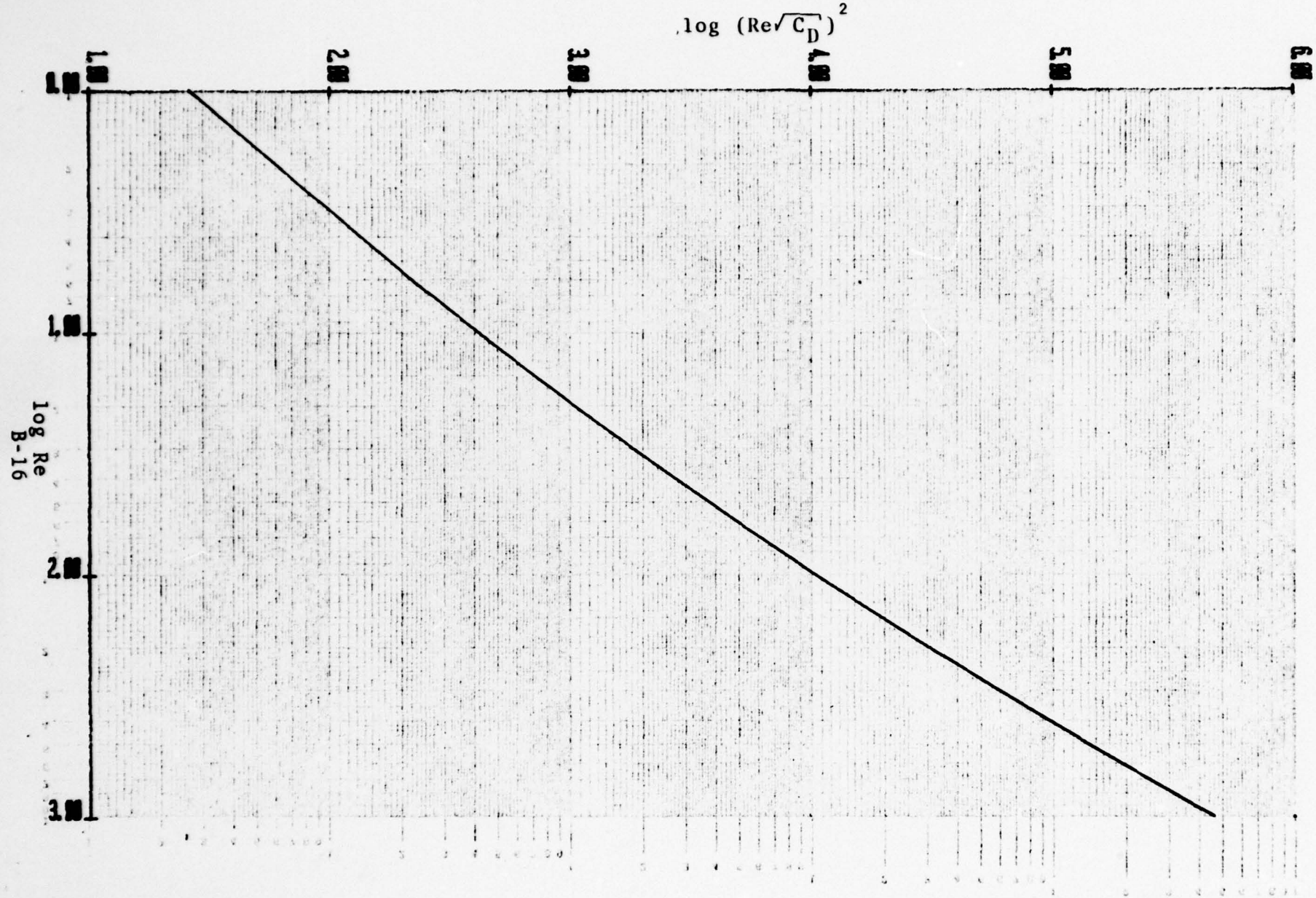

Figure B-3. Dwell Characteristics of Spherical Droplets (Rotating Heat Exchangers)

SECURITY CLASSIFICATION OF THIS PAGE (When Data Entered)

REPORT DOCUMENTATION PAGE

READ INSTRUCTIONS BEFORE COMPLETING FORM

1. REPORT NUMBER: FINAL REPORT	2. GOVT ACCESSION NO.
3. RECIPIENT'S CATALOG NUMBER	
4. TITLE (and Subtitle): Design Study of a Two-Phase Turbine Engine for Submarine Propulsion	5. TYPE OF REPORT & PERIOD COVERED: Final Report 1 July 1977 - 31 May 1978
	6. PERFORMING ORG. REPORT NUMBER
7. AUTHOR(s): Emil Ritzi and Lance Hays	8. CONTRACT OR GRANT NUMBER(s): N-00014-77-C-0545
9. PERFORMING ORGANIZATION NAME AND ADDRESS: Office of Naval Research, Department of Navy, 800 N. Quincy, St., Arlington, VA 02217	10. PROGRAM ELEMENT, PROJECT, TASK AREA & WORK UNIT NUMBERS: 122403, NR 097-422
11. CONTROLLING OFFICE NAME AND ADDRESS: DCASMA-LA, 9920 S. La Cienega Blvd., Inglewood, CA 90301	12. REPORT DATE: August 18, 1978
	13. NUMBER OF PAGES: 177
14. MONITORING AGENCY NAME & ADDRESS (if different from Controlling Office)	15. SECURITY CLASS. (of this report): Unclassified
	15a. DECLASSIFICATION/DOWNGRADING SCHEDULE

16. DISTRIBUTION STATEMENT (of this Report)

See Distribution List

DISTRIBUTION STATEMENT A
Approved for public release
Distribution Unlimited

17. DISTRIBUTION STATEMENT (of the abstract entered in Block 20, if different from Report)

18. SUPPLEMENTARY NOTES

19. KEY WORDS (Continue on reverse side if necessary and identify by block number)

Submarine Propulsion
Steam Engine-Nuclear Propulsion
Two-Phase Engine
Direct Contact Heat Exchanger

20. ABSTRACT (Continue on reverse side if necessary and identify by block number)

A design study of the Biphase turbine engine for underwater propulsion was performed, using a nuclear reactor heat source. A single stage oil/steam turbine without and with gear reduction was designed for 15000 hp at 180 rpm and 1000 rpm respectively. Another Biphase engine which uses steam and water alone was analyzed and designed. Significant performance advantages over conventional steam engines were found, especially at cruise conditions (part load) together with significant weight and space savings. A design method for direct contact heat exchangers of the spray type was developed.

DD FORM 1 JAN 73 1473 EDITION OF 1 NOV 65 IS OBSOLETE

SECURITY CLASSIFICATION OF THIS PAGE (When Data Entered)

DISTRIBUTION LIST

THERMAL ENERGY CONVERSION

	No. Copies
Office of Naval Research 800 N. Quincy Street Arlington, VA 22217 Attn: Power Program, M. Keith Ellingsworth	5
Defense Documentation Center BIdg. 5 Cameron Station Alexandria, VA 22314	12
Naval Research Laboratory 4555 Overlook Avenue Washington, D.C. 20375 Attn: Technical Information Division	6
U.S. Naval Postgraduate School Monterey, CA 93940 Attn: Dept. of Mechanical Engineering	1
U.S. Naval Academy Annapolis, MD 21402 Attn: Dept. of Mechanical Engineering	1
Office of Naval Research Branch Office 1030 East Green Street Pasadena, CA 91106	1
Naval Sea Systems Command Crystal Plaza #6 Washington, D.C. 20360 Attn: Ship Main Propulsion & Energy Branch, Mr. Charles Miller and Mr. Frank Ventriglio	2
Naval Ship Engineering Center National Center Washington, D.C. 20360 Attn: Propulsion Systems, Code 6140B	1
Naval Ship R&D Center Annapolis, MD 21402 Attn: Power Systems Division, Dr. Earl Quandt	2

Department of Energy 1
Washington, D.C. 20545
Attn: Div. of Fossil Fuel Utilization, Mail Stop 412B

Naval Weapons Center 1
China Lake, CA 93555
Attn: Code 3161, Dr. W. Thielbar

University of Miami 1
Clean Energy Research Institute
Coral Gables, Florida
Attn: Prof. T.N. Veziroglu

University of Houston 1
Houston, Texas 77004
Attn: Prof. A.E. Dukler, Director of Engineering

Cornell University 1
Sibley School of Mechanical & Aerospace Engineering
Upson Hall
Ithaca, New York 14853
Attn: Prof. Ed Resler

United Technologies Research Center
Silber Lane
East Hartford, Conn. 06108
Attn: Dr. Simion Kuo